Contract No. 582-23-45978
Work Order No. 6
Tracking No. 2024-13
Task 6.2

Prepared for:

Texas Commission on Environmental Quality
12100 Park 35 Circle MC 164
Austin, TX 78753

Prepared by:

Ramboll
7250 Redwood Blvd., Suite 105
Novato, California 94945

June 27, 2024

Secondary Organic Aerosol (SOA) Update in CAMx

PREPARED UNDER A CONTRACT FROM THE
TEXAS COMMISSION ON ENVIRONMENTAL QUALITY

The preparation of this document was financed through a contract from the State of Texas through the Texas Commission on Environmental Quality.
The content, findings, opinions and conclusions are the work of the author(s) and do not necessarily represent findings, opinions or conclusions of the TCEQ.

Secondary Organic Aerosol (SOA) Update in CAMx

Final Report

Ramboll
7250 Redwood Boulevard
Suite 105
Novato, CA 94945
USA

T +1 415 899 0700
https://ramboll.com

Contents

List of Acronyms and Abbreviations **vii**

Project Summary **1**

Executive Summary **2**

1.0 Introduction **4**

2.0 State of the Science of SOA Formation Literature Review **5**
2.1 Background 5
2.2 SOA models/schemes reviewed 8
2.3 Detailed parameterizations for each SOA model/scheme 11
2.3.1 CAMx 11
2.3.2 CMAQ 13
2.3.3 GEOS-Chem 16
2.3.4 CHIMERE VBS with functionalization/fragmentation processes 17
2.3.5 WRF-Chem MOSAIC 19
2.4 Comparison of first-generation SOA yields 20
2.4.1 Anthropogenic VOC (AVOC) 24
2.4.2 Biogenic VOC (BVOC) 26
2.4.3 Intermediate VOC (IVOC) 27
2.5 Comparison of SOA aging 29
2.5.1 CAMx VBS 35
2.5.2 CMAQ AERO7 37
2.5.3 CMAQ CRACMM 37
2.5.4 CHIMERE VBS 38
2.5.5 WRF-Chem MOSAIC 40
2.6 Effect of NOx on SOA yields 41
2.7 Conclusions and recommendations 41
2.7.1 Major findings 41
2.7.2 Recommendations for CAMx SOA scheme updates 42

3.0 Box Model Tests of CAMx SOA Updates **44**
3.1 Texas box model scenarios 44
3.2 Updated SOA schemes for CAMx 44
3.2.1 SOAP2 scheme in CAMx 44
3.2.2 AERO7 and CRACMM based schemes for CAMx 44
3.2.3 SIMPLE scheme for CAMx 47
3.3 Box model results 49
3.3.1 Base case emissions scenario 49
3.3.2 Scaled emissions scenario 51
3.4 Recommendations for 3-D CAMx testing 59

4.0 CAMx 3-D Simulations with SOA Updates **60**
4.1 CAMx modeling platform 60

4.2 Model performance evaluation (MPE) 60

5.0 Summary and Recommendations 70

6.0 References 72

Table of Figures

Figure 2-1. Illustration of a "two-product" SOA scheme combined with a non-volatile treatment of POA 5

Figure 2-2. Illustration of a volatility basis set (VBS) scheme for SOA and POA with alternative treatments of photochemical OA aging: (a) VBS with no-aging; (b) VBS with stepwise gas-phase OH oxidation causing functionalization; (c) VBS with OH-oxidation causing functionalization and fragmentation; and (d) VBS with condensed-phase OA oligomerization 7

Figure 2-3. Schematic of AERO7 scheme (Murphy et al. 2018) 14

Figure 2-4. First-generation SOA yields for benzene (BENZ), toluene (TOL), and xylene (XYL) under high and low NOx conditions calculated by different models/schemes. 25

Figure 2-5. First-generation SOA yields for isoprene (ISOP), monoterpenes (TERP), and sesquiterpenes (SESQ) under high and low NOx conditions calculated by different models/schemes. 27

Figure 2-6. First-generation SOA yields for IVOC under high and low NOx conditions calculated by different models/schemes. Results for the GEOS-Chem Simple scheme are not shown, and results for CMAQ CRACMM are shown in Figure 2-7. 28

Figure 2-7. First-generation SOA yields for different IVOC types under high and low NOx conditions calculated by CMAQ CRACMM. Our result for aromatic IVOCs disagrees with the value published by Pye et al. (2023) for unknown reasons. 29

Figure 2-8. First-generation and aged SOA yields simulated by different models/schemes for benzene (BENZ), toluene (TOL), and xylene (XYL). For CMAQ CRACMM, results for XYL are averages of 'XYE' and 'XYM'. For WRF-Chem and CHIMERE, results for BENZ and TOL are based on 'ARO1'; results for XYL are based on 'ARO2'. Aged SOA yields are calculated with a 24-hour exposure to OH concentration at 3 x 10^6 molecules/cm^3. 33

Figure 2-9. First-generation and aged SOA yields simulated by different models/schemes for isoprene (ISOP), monoterpenes (TERP), and sesquiterpenes (SESQ). For CHIMERE, results for SESQ are based on humulene. Aged SOA yields are calculated with a 24-hour exposure to OH concentration at 3 x 10^6 molecules/cm^3. 34

Figure 2-10. First-generation and aged SOA yields simulated by different models/schemes for IVOC. For CMAQ, results are presented for alkane IVOC, emitted

oxygenated IVOC, and aromatic IVOC in the smaller plot. Aged SOA yields are calculated with a 24-hour exposure to OH concentration at 3 x 10^6 molecules/cm^3. 35

Figure 2-11. Aging of BENZ, TOL, XYL, and IVOA as a function of accumulated OH exposure under (a) high and (b) low NOx conditions in the CAMx VBS scheme. 37

Figure 2-12. SOA yields from BVOC (left) and aromatics (right) due to oligomerization in the CMAQ AERO7 scheme. 37

Figure 2-13. SOA aging for aromatics and SESQ as a function of OH exposure under high and low NOx conditions in the CMAQ CRACMM scheme. Results for xylene (XYL) are averages of XYM and XYE. 38

Figure 2-14. SOA aging for different IVOC as a function of OH exposure under high and low NOx conditions in the CMAQ CRACMM scheme. 38

Figure 2-15. SOA aging for BVOC and aromatics as a function of OH exposure under (a & c) high and (b & d) low NOx conditions in the CHIMERE VBS scheme. 39

Figure 2-16. SOA aging for IVOC as a function of OH exposure in the CHIMERE VBS scheme. 40

Figure 2-17. SOA aging for IVOC as a function of OH exposure in WRF-Chem MOSAIC scheme. 40

Figure 3-1. SOA yields for terpenes under low and high NOx conditions for the AERO7 and CRACMM schemes (solid lines), and the corresponding fit (dashed lines) for the new schemes implemented in CAMx SOAP2. 46

Figure 3-2. Emission-weighted SOA potential of precursor species under high (left) and low (middle) NOx conditions at DFW, along with the contribution of precursors to the average daily emissions (right). 48

Figure 3-3. Emission-weighted SOA potential of precursor species under high (left) and low (middle) NOx conditions at SAN, along with the contribution of precursors to the average daily emissions (right). 49

Figure 3-4. Emission-weighted SOA potential of precursor species under high (left) and low (middle) NOx conditions at TYL, along with the contribution of precursors to the average daily emissions (right). 49

Figure 3-5. Diurnal profiles of total SOA (μg/m^3) from the 5-day box model base simulations at DFW, SAN, and TYL. 50

Figure 3-6. SOA response surface (24-hr average, μg/m^3) to varying anthropogenic NOx and VOC emissions for DFW for four different SOA schemes. NOx and VOC scaling factors of 1 are the base case simulation. Note that the concentration scale is different for each scheme. 53

Figure 3-7. SOA response surface (24-hr average, μg/m^3) to varying anthropogenic NOx and VOC emissions for SAN for four different SOA schemes. NOx and VOC scaling factors of 1 are the base case simulation. Note that the concentration scale is different for each scheme. 54

Figure 3-8. SOA response surface (24-hr average, μg/m^3) to varying anthropogenic NOx and VOC emissions for TYL for four different SOA schemes. NOx and VOC scaling factors of 1 are the base case simulation. Note that the concentration scale is different for each scheme. 55

Figure 3-9. Ozone response surface (MDA1, ppb) to varying anthropogenic NOx and VOC emissions for DFW, SAN, and TYL for the SOAP2 simulation. NOx and VOC scaling factors of 1 are the base case simulation. Note that the concentration scale is different for each scheme. 56

Figure 4-1. Scatter plots of observed vs modeled organic carbon (OC) for SOAP2 (left), COMPLEX (middle) and SIMPLE (right) at CSN (top) and IMPROVE (bottom) sites. 63

Figure 4-2. Spatial plot showing the normalized mean bias (NMB) metric at CSN sites for OC across the 12 km CONUS2 domain for July, 2016 for SOAP2 (top), COMPLEX (middle), and SIMPLE (bottom). 65

Figure 4-3. Spatial plot showing the normalized mean bias (NMB) metric at IMPROVE sites for OC across the 12 km CONUS domain for July, 2016 for SOAP2 (top), COMPLEX (middle), and SIMPLE (bottom). 66

Figure 4-4. Timeseries of all three model scenarios at CSN sites (482030002 – Karnack and 482011039 – Deer Park) and IMPROVE site (BIBE-Big Bend) in Texas. 67

Figure 4-5. Spatial plot showing the normalized mean bias (NMB) metric at AQS sites for total $PM_{2.5}$ across the 12 km CONUS domain for July, 2016 for SOAP2 (top), COMPLEX (middle), and SIMPLE (bottom). 69

Table of Tables

Table 2-1. Summary of SOA schemes implemented in CTMs reviewed in this work. 9

Table 2-2. SOA mass-based yields from anthropogenic precursors under high (top) and low (bottom) NOx conditions for the CAMx SOAP2 modified two-product scheme (adapted from Table 5-5 of Ramboll, 2022) 11

Table 2-3. SOA mass-based yields from biogenic precursors under high (top) and low (bottom) NOx conditions for the CAMx SOAP2 modified two-product scheme (adapted from Table 5-5 of Ramboll, 2022) 12

Table 2-4. SOA molar-based yields (ppm/ppm) from anthropogenic and biogenic precursors under high (top) and low (bottom) NOx conditions for the CAMx 1.5-D VBS scheme (adapted from CAMx source code). IVOC and monoterpene + NO_3 yields are not NOx-dependent. 13

Table 2-5. SOA molar-based yields from aromatic precursors under high (top) and low (bottom) NOx conditions for the CMAQ AERO7 scheme 14

Table 2-6. SOA molar-based yields from monoterpenes and α-pinene for the CMAQ AERO7 scheme 14

Table 2-7. SOA mass-based yields from isoprene, sesquiterpenes, and IVOC for the CMAQ AERO7 scheme 15

Table 2-8. Aging effect for different precursors in CMAQ AERO7. 15

Table 2-9. SOA mass-based yields[1] from anthropogenic and biogenic precursors under high (top) and low (bottom) NOx conditions for the GOES-Chem complex scheme (adopted from Pye et al. 2010) 17

Table 2-10. SOA mass-based yields[2] from precursors under high (top) and low (bottom) NOx conditions for the CHIMERE VBS scheme (Zhang et al., 2013; CHIMERE, 2023) 19

Table 2-11. SOA mass-based yields from precursors under high (top) and low (bottom) NOx conditions for the WRF-Chem MOSAIC (adopted from Shrivastava et al., 2011). 20

Table 2-12. First-generation SOA yields (g/g) from different precursors simulated by different models/schemes. Temperature is 298K. Ambient OA concentration is assumed to be 10 μg/m^3. Maximum SOA yields are shown in bold and minimum values are underlined. 22

Table 2-13. Ranking of first-generation SOA yield from different precursors by each model/scheme under high and low NOx conditions 23

Table 2-14. SOA yields from different IVOC types implemented in CMAQ CRACMM. The aging effect is calculated with a 24-hour exposure to OH concentration at 3 x 10^6 molecules/cm^3. Temperature is 298K. Ambient OA concentration is assumed to be 10 μg/m^3. 29

Table 2-15. Aged SOA yields (g/g) from different precursors simulated by different models/schemes. The aging effect is calculated with a 24-hour exposure to OH concentration at 3 x 10^6 molecules/cm^3. Temperature is 298K. Ambient OA concentration is assumed to be 10 μg/m^3. Maximum SOA yields are shown in bold, and minimum values are underlined. Shaded values indicate no aging processes implemented. 31

Table 2-16 Ratio of aged SOA yields (Table 2-15) to first-generation SOA yields (Table 2-12) from different precursors simulated by different models/schemes. Maximum ratios are shown in bold, and minimum values are underlined. Shaded values indicate no aging processes implemented. 32

Table 3-1. SOA molar-based yields from anthropogenic precursors under high (top) and low (bottom) NOx conditions for implementation of AERO7 based scheme into CAMx SOAP2 45

Table 3-2. SOA molar-based yields from biogenic precursors under high (top) and low (bottom) NOx conditions for implementation of AERO7 based scheme into CAMx SOAP2 45

Table 3-3. SOA molar-based yields from anthropogenic precursors under high (top) and low (bottom) NOx conditions for implementation of CRACMM based scheme into CAMx SOAP2 46

Table 3-4. SOA molar-based yields from biogenic precursors under high (top) and low (bottom) NOx conditions for implementation of CRACMM based scheme into CAMx SOAP2 46

Table 3-5. SOA molar-based yields from anthropogenic precursors under high (top) and low (bottom) NOx conditions for implementation of the SIMPLE scheme into CAMx SOAP2 47

Table 3-6. SOA molar-based yields from biogenic precursors under high (top) and low (bottom) NOx conditions for implementation of the SIMPLE based scheme into CAMx SOAP2 48

Table 3-7. Secondary organic aerosol (SOA) concentrations (μg/m^3) averaged over days 2 through 5 of base model simulations for each SOA scheme. 51

Table 3-8. Average concentrations (μg/m^3) of secondary organic aerosol (SOA) species over days 2 through 5 for the base and reduced NOx model simulations. 58

Table 4-1. CAMx modeling setup in 2016v3 Modeling Platform. 60

Table 4-2. Model statistical performance metrics and criteria. 61

Table 4-3. Domain wide model performance for organic carbon (OC) at CSN and IMPROVE monitors for July, 2016. 62

Table 4-4. Domain wide model performance for total $PM_{2.5}$ at AQS, CSN and IMPROVE monitors for July, 2016. 68

LIST OF ACRONYMS AND ABBREVIATIONS

ACM2	Asymmetric Convective Model
ALK4	Alkanes $5x10^3$ < kOH <$1x10^4$ (lumped class)
ALK5	Alkanes $1x10^4$ < kOH (lumped class)
AMET	Atmospheric Model Evaluation Tool
APIN	α-pinene (explicit)
AQS	Air Quality System
ARO1	Aromatics kOH <$2x10^4$ (lumped class)
ARO2	Aromatics kOH >$2x10^4$ (lumped class)
ASOA	SOA formed from AVOC
AVOC	Anthropogenic VOC
BC	Boundary conditions
BENZ	Benzene (explicit)
BSOA	SOA formed from BVOC
BVOC	Biogenic VOC
CAMx	Comprehensive Air Quality with Extensions
CB7r1	Carbon Bond version 7, revision 1
CG	Condensable gases
CMAQ	Community Multiscale Air Quality
CONUS	Continental US
CRACMM	Community Regional Atmospheric Chemistry Multiphase Mechanism
CSN	Chemical Speciation Network
DFW	Dallas-Fort Worth
EBI	Euler Backward Iterative
EPA	Environmental Protection Agency
FB	Fractional bias
FE	Fractional error
HUMULE	Humulene (lumped sesquiterpene class)
IMPROVE	Interagency Monitoring of Protected Visual Environments
ISOP	Isoprene (explicit)
IVOC	Intermediate volatility organic compounds
IV-SOA	SOA formed from IVOC
LIMO	Limonene (lumped class)
MDA1	Maximum daily 1-hour average
NMB	Normalized mean bias
NME	Normalized mean error
OA	Organic aerosol
OLE1	Alkenes kOH < $7x10^4$ (lumped class)

OLE2	Alkenes kOH > $7x10^3$ (lumped class)
PBL	Planetary boundary layer
PGM	Photochemical grid model
POA	Primary organic aerosol
$PM_{2.5}$	Particulate matter with a diameter of 2.5 micrometers or less
PPM	Piecewise Parabolic Method
R	Correlation coefficient
SAN	San Antonio
SESQ	Sesquiterpenes (lumped class)
SIP	State Implementation Plan
SOA	Secondary organic aerosol
SOPA	Non-volatile secondary organic aerosol from anthropogenic emissions
SOPB	Non-volatile secondary Organic aerosol from biogenic emissions
SVOC	Semivolatile organic compounds
SV-SOA	SOA formed from SVOC
TERP	Terpenes (lumped class)
TOL	Toluene (lumped class)
TYL	Tyler
VOC	Volatile organic compounds
VBS	Volatility basis set
XYL	Xylenes (lumped class)

PROJECT SUMMARY

Secondary organic aerosol (SOA) contributes a large fraction of particulate air pollution in Texas and treatment of SOA chemistry in air quality models is important to air quality assessments and planning. Ramboll updated the SOA treatment in the Comprehensive Air Quality Model with Extensions (CAMx), which is used by the TCEQ for particulate air pollution modeling. Model tests were performed to determine how SOA concentrations respond to varying emissions, and model results were evaluated against observations to assess model performance. The new SOA schemes will enable the TCEQ to develop more effective strategies to address particulate air pollution in Texas.

EXECUTIVE SUMMARY

The Texas Commission on Environmental Quality (TCEQ) uses the Comprehensive Air Quality Model with Extensions (CAMx) to assess the impact of particulate matter (PM) on air quality. In early 2024, the US Environmental Protection Agency (EPA) announced they were lowering the National Ambient Air Quality Standard (NAAQS) for PM with a diameter of 2.5 micrometers or smaller ($PM_{2.5}$) from 12.0 to 9.0 µg/m^3 (EPA 2024). Because of this change, the TCEQ may be required to perform PM modeling for State Implementation Plan (SIP) purposes.

Secondary organic aerosol (SOA), which is produced from anthropogenic, biogenic and biomass burning sources, is a major component of $PM_{2.5}$ in Texas. Scientific understanding of SOA formation pathways is continuously evolving, and therefore, there is a need to routinely review the state of science on SOA formation and update the CAMx SOA treatment as needed. The choice of model or SOA scheme can significantly influence the predicted SOA concentrations and their evolution over time, which in turn affects air quality forecasts, assessments, and regulations. The purpose of this project was to review and update the CAMx SOA treatment which will enable the TCEQ to develop more effective $PM_{2.5}$ SIP strategies for Texas.

Following a literature review of five widely used chemical transport models (CTMs), which included a comparison of first-generation SOA yields at different OA concentrations as well as aged SOA yields under atmospheric relevant conditions, it was evident that SOA schemes vary widely. Differences include the choice of SOA yield values, the effect of NOx on yields, SOA aging processes, and speciation and treatment of intermediate volatile organic compounds (IVOC) which is an SOA precursor. While there was no compelling reason to change the structure of the current SOA scheme in CAMx (SOAP2), updates to SOA yields that consider more recently published data were recommended. Three updated SOA schemes were developed and implemented into CAMx and tested alongside SOAP2 in box model scenarios for three Texas cities (Dallas-Fort Worth, San Antonio, and Tyler). Two of the new CAMx schemes include updated SOA yield parameters that emulate the AERO7 and CRACMM schemes in the Community Multiscale Air Quality (CMAQ) model, which were developed by the EPA to support air quality planning. The third scheme (referred to as SIMPLE) assumes all SOA is non-volatile with SOA yields that align with multi-model means.

Box model tests included base case simulations and scaled emissions simulations to assess the response of SOA concentrations to varying anthropogenic VOC and NOx emissions. AERO7 and SIMPLE predicted similar SOA concentrations in each of the box model simulations and SOAP2, AERO7, and SIMPLE responded similarly to variations in VOC and NOx emissions. CRACMM predicted a decrease in total SOA when NOx was reduced by 50%, opposite of the other schemes, which is due to the effect of NOx on the monoterpene SOA yield. While most of the schemes reviewed in this work have higher terpene SOA yields under low NOx conditions, the CRACMM trend is reversed. Higher terpene SOA yield under low NOx conditions is also supported by the experimental findings of Sarrafzadeh et al. (2016) and Wildt et al. (2014) and other experiments. Because this behavior is unique to CRACMM and not supported by experimental data, the CRACMM scheme is not recommended for implementation in CAMx.

Further testing of the SIMPLE and AERO7 (re-named to COMPLEX) schemes was performed in 3-D CAMx simulations covering the continental US (CONUS) for the month of July, 2016 using the

EPA's 2016v3 modeling platform (EPA, 2023). Results from three model scenarios (SOAP2, SIMPLE and COMPLEX) were evaluated against observational organic carbon (OC) and $PM_{2.5}$ data from monitoring networks across the CONUS. Model performance was comparable among each of the SOA schemes, including similar bias and error compared to observations, similar spatial trends of statistical metrics across the CONUS, and similar temporal trends of OC concentrations. Although model performance is influenced by uncertainties in model inputs (i.e., anthropogenic and biogenic emission inventories), the reasonable performance of the SIMPLE and COMPLEX SOA schemes, along with the fact that more recent published data was used to develop SOA yield parameters in these schemes, suggests that CAMx SOAP2 should be replaced by SIMPLE and COMPLEX. The SIMPLE scheme has additional practical advantages, including the ability to calculate emission-weighted SOA potential and the potential for efficiency gains with CAMx's source apportionment probing tools by reducing the number of tracer species. The SOA schemes recommended through this work were chosen considering that CAMx SIP models must predict reasonable SOA concentrations and, importantly, that the SOA response to precursor reductions should be traceable to data that is known with some confidence.

In addition to the SOA yield updates evaluated in this project, the following structural updates to CAMx's SOA scheme are also recommended for future implementation and testing:

- Update CAMx's Particulate Source Apportionment Technology (PSAT) probing tool for use with the SIMPLE scheme (i.e., reducing the required number of tracer species), which would allow for more detailed and/or rapid analysis to understand source contributions to $PM_{2.5}$.
- Expand the terpene SOA scheme to differentiate α-pinene from other terpenes in alignment with CB7 species APIN and TERP, respectively (and other oxidant mechanisms).
- Make the SOA yields from NO_3 + terpene reactions different from OH/O_3 + terpene reactions.
- Make the SOA yields from NO_3 + α-pinene reaction near zero which is supported by laboratory data and makes α-pinene different from other terpenes.
- If feasible via minor modifications, improve the treatment of SOA-photolysis to recognize that a large fraction of SOA does not photolyze (the "recalcitrant" fraction; O'Brien and Kroll, 2019) while the remaining fraction does photolyze more rapidly than assumed by SOAP2.

1.0 INTRODUCTION

The TCEQ is preparing for Particulate Matter (PM) modeling that may be required because of the U.S. Environmental Protection Agency (EPA) lowering the National Ambient Air Quality Standard for PM with a diameter of 2.5 micrometers or smaller ($PM_{2.5}$) (EPA 2024). TCEQ is also analyzing contributions of foreign emissions to $PM_{2.5}$ in Texas. Organic aerosol (OA) contributes a large fraction of $PM_{2.5}$ in Texas due to primary OA emissions (POA) and the formation of secondary OA (SOA) from anthropogenic, biogenic, and biomass burning sources (Donahue et al., 2006). SOA precursor emissions include traditional volatile organic compounds (VOC) as well as non-traditional intermediate and semi-volatile VOC (IVOC and SVOC, respectively), as discussed by Murphy et al. (2023) and Huang et al. (2023). Scientific understanding of SOA formation pathways is continuously evolving, and therefore, there is a need to review the state of science on SOA formation and update the Comprehensive Air quality Model with extensions (CAMx) SOA treatment as needed. CAMx is the primary photochemical grid model (PGM) used for PM modeling by TCEQ.

The choice of model or SOA scheme can significantly influence the predicted SOA concentrations and their evolution over time, which in turn affects air quality forecasts, assessments, and regulations. The purpose of this project is to review and update the CAMx SOA treatment which will enable the TCEQ to develop more effective $PM_{2.5}$ SIP strategies for Texas. Updated SOA schemes were developed following a literature review performed by Ramboll on the state of the science of SOA formation and implementation of SOA schemes in photochemical models. These new schemes were implemented into CAMx and compared to the existing SOA scheme in CAMx. Proper implementation was first tested in box model scenarios and scheme recommendations were refined based on box model results. The impact of the updated CAMx SOA schemes on model performance was evaluated in 3-D simulations using a summer modeling period developed from the EPA's modeling platform for the Continental U.S. (CONUS). Model performance was evaluated using ambient monitoring data for speciated and total PM2.5 collected at monitors in urban and rural locations across the CONUS.

2.0 STATE OF THE SCIENCE OF SOA FORMATION LITERATURE REVIEW

2.1 Background

In general, two approaches are implemented in chemical transport models (CTMs) for SOA simulation: the two-product scheme (Figure 2-1) or the volatility basis set (VBS) scheme (with different aging treatments, Figure 2-2). The two-product model is developed based on the gas-particle partitioning theory of Pankow (1994). When SOA precursors are oxidized in the gas phase by the OH radical, ozone (O_3), or NO_3 radical, two gas-phase products (with high and low volatility, respectively) are used to represent all the oxidation products that can potentially condense to form SOA, e.g.:

$$\text{OH + SOA precursor} = (\alpha_1 \times \text{CG1}) + (\alpha_2 \times \text{CG2}) \qquad \text{Eq. 1}$$

where the CG products are condensable gases and α are stoichiometric coefficients. The SOA yield (*Y*) is calculated by combining the gas-particle partitioning theory with α:

$$Y = \frac{\alpha_1}{1 + C_1^*/C_{OA}} + \frac{\alpha_2}{1 + C_2^*/C_{OA}} \qquad \text{Eq. 2}$$

where C_{OA} is the total ambient concentration of organic compounds (i.e., POA + SOA) and α_1, α_2, C_1^*, and C_2^* represent the stoichiometric coefficients and the effective saturation concentrations of the above two products, which can be obtained by fitting the results of laboratory studies. For Eq. 2, yields are defined on a molar basis (mole CG/mole precursor), whereas laboratory studies often report yields in mass units (g/g), and these units can be converted using the molecular weight of the precursor and the CG, although CG molecular weights are usually assumed because the CG represents a mixture of compounds. POA is usually treated as non-volatile in two-product schemes (Strader et al., 1999; Schell et al., 2001).

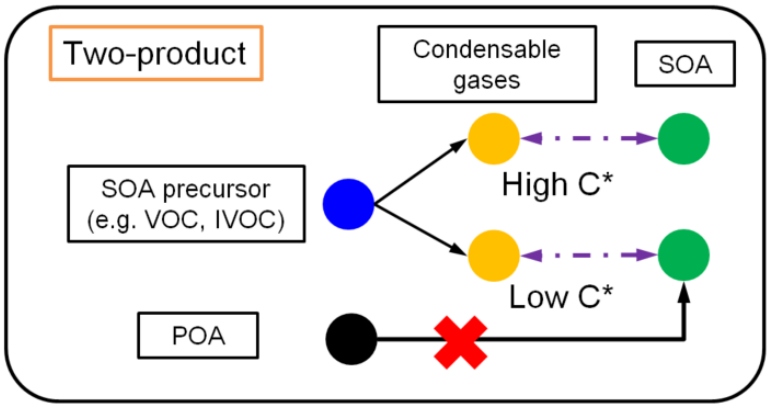

Figure 2-1. Illustration of a "two-product" SOA scheme combined with a non-volatile treatment of POA

The VBS framework (Donahue et al., 2006) expands the two-product model by having more condensable gases that are systematically organized by volatility (i.e., saturation concentration, C^*). Condensable organic compounds are categorized based on their volatility into bins that are typically separated by a factor of 10 in volatility, e.g., four bins with C^* of 1, 10, 100, 1000 μg/m^3.

The yield (α) of condensable gases for each volatility bin can be obtained by fitting the results of laboratory studies. Similar to the two-product model, the VBS framework is based on the absorptive partitioning theory. However, VBS treats POA as semivolatile, dynamically partitioning between the gas and particle phase depending on environmental factors, such as temperature and pre-existing OA concentrations. Figure 2-2 illustrates the "1-dimensional" (1-D) VBS framework where volatility is the coordinate that varies (discretized to volatility bins) and panels a-d have different treatments of SOA aging. In the 2-D VBS introduced by Donahue et al. (2011), both volatility and oxidation state coordinates vary independently. The 1.5-D VBS introduced by Koo et al. (2014) represents volatility and oxidation state by assuming these two coordinates are related.

Figure 2-2a depicts a four-bin VBS framework with no photochemical aging processes of OA after the initial formation of SOA. Initially, SOA precursors (e.g., VOC, IVOC) undergo gas-phase oxidation, leading to the formation of four types of condensable gases, with volatility ranging from 1 μg/m^3 to 1000 μg/m^3. These condensable gases subsequently condense to form SOA without further aging. In this example, the SOA yield is calculated as:

$$\mathrm{Y} = \frac{\alpha_1}{1 + 1/C_{OA}} + \frac{\alpha_2}{1 + 10/C_{OA}} + \frac{\alpha_3}{1 + 100/C_{OA}} + \frac{\alpha_4}{1 + 1000/C_{OA}} \qquad \text{Eq. 3}$$

where α_i is the first-generation oxidation yield, i.e., the yield from the precursor reaction.

Beyond first-generation oxidation of precursors to CGs, multi-generation aging processes can occur and include functionalization and/or fragmentation of gas-phase CGs, oligomerization of condensed-phase SOA, SOA photolysis, and heterogeneous SOA oxidation. Functionalization and oligomerization typically increase SOA mass, whereas fragmentation and photolysis decrease SOA mass. Figure 2-2b depicts a VBS framework incorporating a stepwise OH-oxidation functionalization process as included in many VBS schemes, where CGs undergo gas-phase reactions (usually parameterized as OH-oxidation) that add oxygen-containing functional groups and successively lower volatility. This functionalization increases molecular weight with each oxidation generation, which can be parameterized as a percentage increase (usually 7.5% or 15%) to account for added oxygen.

Gas-phase reactions of CGs can cause molecular fragmentation as well as functionalization. As SOA ages, fragmentation reactions may gain significance. Figure 2-2c shows a VBS framework with both functionalization and fragmentation (e.g., the CHIMERE model VBS scheme, described below). In this scenario, OH-oxidation of the CGs results in products across lower (functionalization) and higher (fragmentation) volatility bins that are often parameterized using predefined fractions.

Particle-phase oligomerization, as illustrated by Figure 2-2d, is another SOA aging process, where condensed SOA molecules join together and are converted to larger SOA molecules with very low effective volatility or non-volatile SOA. Some schemes refer to oligomerization as polymerization. Typically, the rate of the oligomerization process is independent of the gas-phase oxidant level.

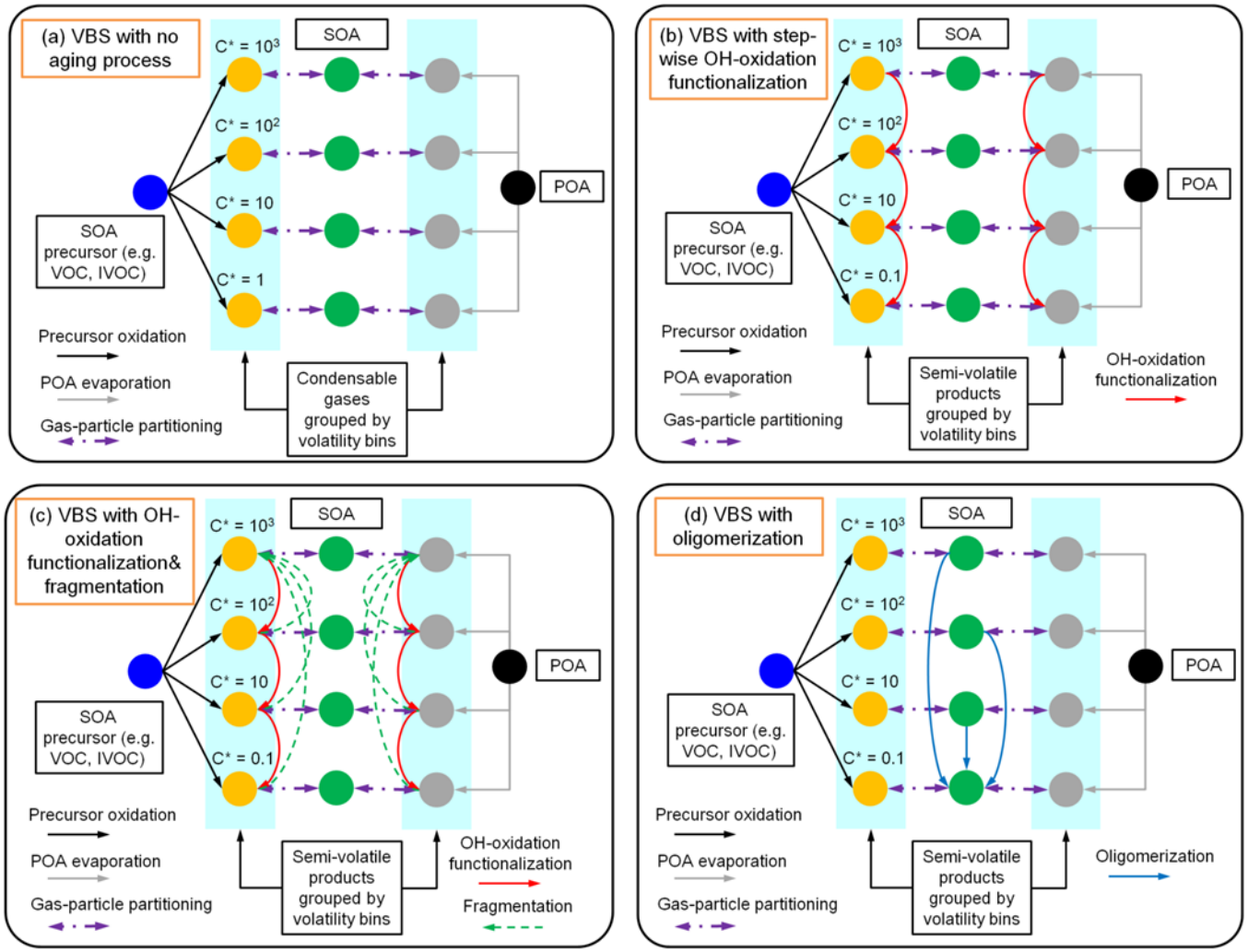

Figure 2-2. Illustration of a volatility basis set (VBS) scheme for SOA and POA with alternative treatments of photochemical OA aging: (a) VBS with no-aging; (b) VBS with stepwise gas-phase OH oxidation causing functionalization; (c) VBS with OH-oxidation causing functionalization and fragmentation; and (d) VBS with condensed-phase OA oligomerization

2.2 SOA models/schemes reviewed

To understand the current state of SOA modelling in chemical transport models (CTMs), we reviewed schemes implemented in several regional models that are used in the U.S., Europe and Asia as well as one global model that provides boundary conditions to regional models. We reviewed a total of eight SOA schemes implemented in five models, namely the Comprehensive Air Quality with Extensions (CAMx, https://www.camx.com/, accessed on Feb 15th, 2024), the Community Multiscale Air Quality (CMAQ, https://github.com/USEPA/CMAQ/, accessed on Feb 15th, 2024), GEOS-Chem (https://geos-chem.readthedocs.io/en/stable/, accessed on Feb 15th, 2024), WRF-Chem (https://ruc.noaa.gov/wrf/wrf-chem/, accessed on Feb 15th, 2024), and CHIMERE (https://www.lmd.polytechnique.fr/chimere/docs/, accessed on Feb 15th, 2024). For each of the models/schemes, we reviewed the official documentation (e.g., user's guide), peer-reviewed publications, and, in some cases, the model source code to understand each SOA parameterization and gather current parameter data.

Most schemes consider SOA formation from anthropogenic VOC (AVOC), intermediate volatility VOC (IVOC), and biogenic VOC (BVOC). Some schemes also account for the impact of sunlight exposure and atmospheric oxidations on SOA formation/destruction, which is generally referred to as "SOA aging". Table 2-1 provides the general information for each SOA model/scheme with more detailed information given in Section 2.3. For each model/scheme, we present important details using the same units as the model developer (e.g., SOA yields provided in either mass-based or molar yields) for traceability. In Section 2.4, we show SOA yields computed under standardized conditions with each model/scheme to obtain direct comparisons. We compare the yields of non-aged (i.e., first-generation) SOA from typical precursors simulated by each model/scheme. Furthermore, we discuss how SOA aging is treated by different models/schemes in Section 2.5 and how NOx conditions impact SOA yields in Section 2.6.

Table 2-1. Summary of SOA schemes implemented in CTMs reviewed in this work.

Model name/ version	SOA scheme	SOA precursors[1]	Aging treatment	POA treatment	SOA photolysis	References
CAMx Version 7.20	SOAP2	BENZ/TOL/XYL ISOP/TERP/SESQ IVOC	No aging effect	Non-volatile, no further reactions	J_{SOA} = 0.1% J_{NO2}	Ramboll (2022)
	1.5D VBS		Stepwise OH oxidation aging for SOA formation from AVOC and IVOC	Semivolatile; gas-phase undergoes further oxidation		Ramboll (2022); Koo et al. (2014)
CMAQ Version 5.4	AERO7	BENZ/TOL/XYL ISOP/TERP/SESQ IVOC	Particle-phase of semivolatile products forms oligomers; products generated by TERP + NO_3 undergo hydrolysis to form low-volatile products.	Semivolatile; gas-phase undergoes further oxidation	Not considered	CMAQ source code (https://github.com/USEPA/CMAQ)
	CRACMM	BENZ/TOL/XYM/XYE APIN/LIM/SESQ IEPOX IVOC, etc. Oxygenated IVOC (i.e., volatile chemical products)	OH oxidation aging resulting in functionalization and fragmentation based on modified 2-D VBS framework	Semivolatile; gas-phase undergoes further oxidation	Not considered	Pye et al. (2023)
GEOS-Chem Version 14.3.0	Simple	ISOP/TERP/SESQ For anthropogenic sources, SOA precursors are scaled based on CO emissions	No aging effect	Non-volatile; 50% of POA is directly emitted; 50% is formed with a lifetime of 1.15 days, without dependence on local oxidation levels.	Described in literature but not found in source code	Pai et al. (2020) Hodzic and Jimenez (2011)
	Complex	BENZ/TOL/XYL ISOP/MTPO/LIMO/SESQ IVOC	No aging effect	Semivolatile; gas-phase undergoes further oxidation with OH to form oxidized POA with lower volatility.		Pai et al. (2020) Pye et al. (2010) GEOS-Chem source code (https://geos-chem.readthedocs.io/en/stable/)
CHIMERE Version 2023	VBS	TERP/HUMULE/ISOP ARO1/ARO2 ALK4/ALK5 OLE1/OLE2 IVOC	OH oxidation aging with both functionalization and fragmentation; the aerosol phase undergoes oligomerization to form non-volatile products.	Semivolatile; gas-phase undergoes further oxidation.	Not considered	Zhang et al. (2013); Shrivastava et al. (2015); Couvidat et al. (2018); CHIMERE (2023)

Model name/ version	SOA scheme	SOA precursors[1]	Aging treatment	POA treatment	SOA photolysis	References
WRF-Chem Version 4.4	MOSAIC	ISOP/TERP/SESQ ALK4/ALK5 ARO1/ARO2 OLE1/OLE2 IVOC	No aging for ASOA and BSOA; Stepwise OH oxidation of IVOC with 15% of mass added for each generation; no fragmentation.	Semivolatile; gas-phase undergoes further oxidation	Described in literature (Zawadowicz et al. 2020) but turned off in source code	Shrivastava et al. 2011

2.3 Detailed parameterizations for each SOA model/scheme

2.3.1 CAMx

The Comprehensive Air quality Model with Extensions (CAMx) is the primary photochemical grid model used for PM modeling by TCEQ. The latest CAMx version v7.20 was released on May 2nd, 2022 (https://www.camx.com/, accessed on Feb 15th, 2024). CAMx provides two options to simulate SOA chemistry/partitioning: a "two-product" semivolatile equilibrium scheme called SOAP (Strader et al., 1999) and a hybrid 1.5-dimension volatility basis set (1.5-D VBS) approach (Koo et al., 2014). The former is compatible with advanced probing tools, including the Particulate Source Apportionment Technology (PSAT) and the decoupled direct method (DDM), while the latter is not. For both schemes, a photolysis rate of 0.1% x J_{NO2} (NO_2 photolysis rate) is applied to account for in-particle SOA removal via photolysis.

2.3.1.1 CAMx SOAP2

In the CAMx SOAP scheme (hereafter SOAP2), the primary organic aerosol (POA) is treated as non-volatile and does not chemically evolve. SOA formation is represented by a modified "two product" model, described above (see Figure 2-1), where gas-phase VOC/IVOC are oxidized to CGs that can condense to SOA. SOAP2 modifies the two-product scheme by adding a third product, which is considered non-volatile and always condenses to SOA. The CG products from anthropogenic (benzene, toluene, xylene) and biogenic (isoprene, monoterpene, sesquiterpene) precursors have different volatilities in SOAP2. Thus, SOAP2 includes 6 product species overall, as shown in Table 2-2 and Table 2-3. Note that the C* is given at 300K. The SOA mass yields do not differentiate between different oxidants (i.e., OH, O_3, and NO_3) in SOAP2. It should also be pointed out that the SOA mass yield coefficients are fitted to aged SOA yields, and therefore no further SOA aging (e.g., oligomerization) is included in SOAP2. Aqueous-phase formation of non-volatile SOA from glyoxal and methylglyoxal is also included with SOAP2.

Table 2-2. SOA mass-based yields from anthropogenic precursors under high (top) and low (bottom) NOx conditions for the CAMx SOAP2 modified two-product scheme (adapted from Table 5-5 of Ramboll, 2022)

C* [μg/m^3] @ 300K	0	0.31	14
CG/SOA MW [g/mol]	220	150	160
ΔH_{vap} [kJ/mol]	-	147	116
Benzene	0	0.391	0.248
	0	0.167	0.487
Toluene	0.044	0.293	0.304
	0.262	0.345	0.663
Xylene	0.025	0.049	0.084
	0.294	0.306	0.291
IVOC	0.129	0.225	012
	0.277	0.275	0.0

Table 2-3. SOA mass-based yields from biogenic precursors under high (top) and low (bottom) NOx conditions for the CAMx SOAP2 modified two-product scheme (adapted from Table 5-5 of Ramboll, 2022)

C* [μg/m^3] @ 300K	0	0.45	26
CG/SOA MW [g/mol]	220	180	180
ΔH_{vap} [kJ/mol]	-	123	118
Isoprene	0	0.023	0.076
	0.011	0.029	0.156
Monoterpene	0.070	0.045	0.075
	0.070	0.090	0.150
Sesquiterpene	0.175	0.328	0.092
	0.270	0.400	0.136

2.3.1.2 CAMx VBS

The CAMx hybrid VBS approach, called 1.5-D VBS, combines the simplicity of 1-D VBS (Donahue et al. 2006; Robinson et al. 2007) with the ability to describe the evolution of OA in both dimensions of oxidation state and volatility (Koo et al. 2014). Unlike SOAP2, CAMx 1.5-D VBS treats POA as semivolatile, and uses two basis sets with five volatility bins (C* ranging from 10^{-1} to 10^3 μg/m^3) to describe SOA formation from anthropogenic and biogenic precursors. Gas-phase oxidation products in different volatility bins are continuously oxidized by OH (with an OH rate constant of 2×10^{-11} cm^3/molecule/s) that move mass from higher volatility bins to the next lower volatility bin in a step-wise manner (for example, from C*=1000 μg/m^3 to C*=100 μg/m^3 and from C*=100 μg/m^3 to C*=10 μg/m^3). For biogenic SOA, this stepwise aging effect is disabled. Table 2-4 shows the SOA parameters used for the CAMx 1.5-D VBS scheme. The SOA yields from monoterpenes + NO_3 reaction are different from monoterpenes + OH reaction, and the SOA yields for monoterpenes and IVOC are not NOx-dependent. CAMx 1.5-D VBS differentiates IVOC from gasoline engines (IVOG), diesel engines (IVOD), biomass burning (IVOB), and other anthropogenic sources (IVOA). Aqueous-phase formation of non-volatile SOA from glyoxal and methylglyoxal is included with the CAMx 1.5D VBS.

Table 2-4. SOA molar-based yields (ppm/ppm) from anthropogenic and biogenic precursors under high (top) and low (bottom) NOx conditions for the CAMx 1.5-D VBS scheme (adapted from CAMx source code). IVOC and monoterpene + NO_3 yields are not NOx-dependent.

C* [μg/m^3] @ 298K	0	1	10	100	1000
CG/SOA MW [g/mol]	172	167	163	158	153
ΔH_{vap} [kJ/mol]	35	35	35	35	35
Benzene	0	0.001	0.079	0.148	0.222
	0	0.035	0.108	0.185	0.268
Toluene	0	0.006	0.145	0.281	0.432
	0	0.006	0.145	0.437	0.281
Xylene	0	0.001	0.127	0.201	0.301
	0	0.048	0.195	0.252	0.364
Isoprene	0	0	0.009	0.006	0
	0	0.004	0.013	0.006	0
Monoterpenes (OH oxidation)	0	0.01	0.101	0.173	0.451
	0	0.087	0.077	0.309	0.54
Monoterpenes (NO_3 oxidation)[1]	0.314	0.029	0	0.862	0
Sesquiterpenes	0	0.092	0.188	0.968	0.679
	0	0.092	0.188	0.968	0.679
IVOG[1]	0.022	0.098	0.373	0.699	0
IVOD[1]	0.081	0.135	0.800	0.604	0
IVOA[1]	0.081	0.135	0.800	0.604	0
IVOB[1]	0.081	0.135	0.800	0.604	0

[1]Yields are not NOx-dependent

2.3.2 CMAQ

The Community Multiscale Air Quality (CMAQ) model is developed and distributed by the U.S. Environmental Protection Agency (EPA) with continuous updates since its first release over 20 years ago. The recent version CMAQ v5.4 was released in October 2022. CMAQ offers three SOA options: AERO7 inherited from earlier versions (Appel et al. 2021), CRACMM (Pye et al. 2023) introduced in v5.4 for the first time, and the 2D-VBS developed by Tsinghua University (https://github.com/USEPA/CMAQ/tree/2DVBS). We reviewed the first two schemes because both were developed by the EPA to support air quality planning in the U.S. and elsewhere.

2.3.2.1 CMAQ AERO7

The CMAQ AERO7 introduced in version 5.3 (Appel et al. 2021) tracks SOA formation from anthropogenic VOC (benzene, alkanes, aromatics, PAHs), biogenic VOC (isoprene, α-pinene, monoterpenes, and sesquiterpenes), and IVOC (Figure 2-3). Additionally, AERO7 accounts for in-cloud SOA formation from glyoxal and methylglyoxal and aqueous formation from IEPOX. The model employs VBS to represent SOA yields from different precursors, with varying volatility ranges for each precursor type.

Table 2-5 through Table 2-7 lists the SOA yields used in AERO7 for precursors considered in this project. Specifically, AERO7 uses a VBS approach with four bins (volatility ranging from 0.01 μg/m^3 to 100 μg/m^3 at 298K, Table 2-5) to represent SOA yields from anthropogenic VOC precursors (e.g., benzene, long alkanes, PAHs) and seven bins (volatility ranging from 0.01 to 107

μg/m^3 at 298K, Table 2-6) for α-pinene and monoterpenes. Isoprene and sesquiterpenes oxidation products are parameterized with two and one semivolatile products, respectively (Table 2-7). IVOC in CMAQ is represented by pcVOC, which oxidizes with OH to form a low-volatility condensable vapor (pcSOG, C*=10^{-5} μg/m^3) with a molar yield of 1 (Murphy et al. 2017, Table 2-7).

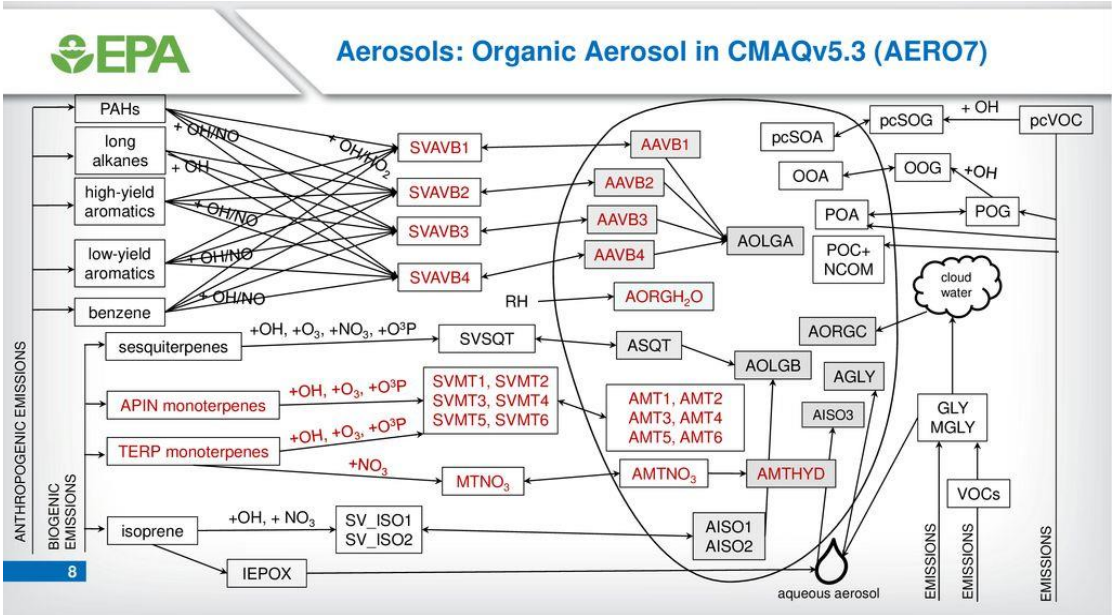

Figure 2-3. Schematic of AERO7 scheme (Murphy et al. 2018)

Table 2-5. SOA molar-based yields from aromatic precursors under high (top) and low (bottom) NOx conditions for the CMAQ AERO7 scheme

C* [μg/m^3] @ 298K	0.01	1	10	100
CG/SOA MW [g/mol]	198	179	169	158
ΔHvap [kJ/mol]	18	18	18	18
Benzene	0	0.034	0	0.392
	0.146	0	0	0
Toluene	0	0.016	0.051	0.047
	0.14	0	0	0
Xylene	0	0.015	0.023	0.06
	0.193	0	0	0

Table 2-6. SOA molar-based yields from monoterpenes and α-pinene for the CMAQ AERO7 scheme

C* [μg/m^3] @ 298K	0.01	0.1	1	10	100	1000	10000
CG/SOA MW [g/mol]	300	200	186	184	170	168	/
ΔHvap [kJ/mol]	102	91	80	69	58	47	36
Monoterpenes; α-pinene	0.04	0.032	0.032	0.103	0.143	0.285	0.16

Table 2-7. SOA mass-based yields from isoprene, sesquiterpenes, and IVOC for the CMAQ AERO7 scheme

C* [μg/m^3] @ 298K	0.617	116.01	24.984	1E-05
CG/SOA MW [g/mol]	132	133	273	170
ΔHvap [kJ/mol]	40	40	40	40
Isoprene	0.0288	0.232	-	-
Sesquiterpenes	-	-	1.537	-
IVOC	-	-	-	1.176

AERO7 incorporates different aging treatments for SOA formed from different precursors as detailed in Table 2-8. The SOA formed from AVOC, isoprene, and sesquiterpenes, undergo oligomerization processes in the particle phase to form non-volatile products with a rate of 9.49 x 10^{-6} s^{-1} (equivalent to a lifetime of 20.5 hr). In contrast, for monoterpene + OH oxidation, no additional oligomerization occurs, while for monoterpene + NO_3 oxidation, hydrolysis of particle-phase products results in non-volatile product with a rate of 9.25 x 10^{-5} s^{-1} (equivalent to a lifetime of ~3 hr). SOA photolysis is currently not considered in AERO7.

Table 2-8. Aging effect for different precursors in CMAQ AERO7.

SOA precursors	Aging effect treatment
Aromatics	Under high-NOx conditions, oxidation products form non-volatile oligomers (AOLGA) at a rate of 9.49E-6 s^{-1}; under low-NOx conditions, oxidation products do not form oligomers, i.e., no aging effect.
Isoprene/Sesquiterpene	Aging is NOx-independent; oxidation products form non-volatile oligomers (AOLGB) at a rate of 9.49E-6 s^{-1}
Monoterpenes	There is no aging effect for OH and O_3 oxidation products; NO_3 oxidation products undergo hydrolysis to form a non-volatile product (AMTHYD) at a rate of 9.26E-5 s^{-1}
IVOC	No aging effect

2.3.2.2 CMAQ CRACMM

The Community Regional Atmospheric Chemistry Multiphase Mechanism (CRACMM) was a new chemical mechanism introduced in CMAQv5.4 (Pye et al., 2023). Unlike conventional SOA schemes, CRACMM partially integrates CG formation and CG aging with oxidant formation in the gas-phase chemical mechanism which means that SOA yield parameters are too complex to be tabulated for CRACMM as for the other schemes. CRACMM SOA formation considers a comprehensive range of reactive organic carbon (ROC) emissions, including alkane-like ROC, aromatics, furans, isoprene, monoterpenes, sesquiterpenes, glyoxal and methylglyoxal. Furthermore, CRACMM categorizes IVOC based on functional groups, including aromatic IVOC, oxygenated IVOC (e.g., volatile chemical products (VCP)), and alkane IVOC. Aqueous SOA formation from IEPOX, glyoxal, and methylglyoxal follow CMAQ AERO7.

The gas-phase oxidation of various SOA precursors results in diverse SOA products with fixed molar yields, generating secondary oxygenated species like LVOC, SVOC, and IVOC with varying

volatilities and/or empirical SOA species (e.g., highly oxygenated molecules (HOM)) that usually are non-volatile. Eq. 4 through Eq. 8 illustrate relevant SOA products generated from benzene (BEN) in CRACMM:

BEN + OH → 0.470 BENP + 0.530 PHEN + … Eq. 4

BENP + NO → 0.001 VROCP4OXY2 + 0.001 VROCN1OXY6 Eq. 5

+ 0.499 FURANONE + …

BENP + HO2 → 0.398 VROCN1OXY6 + … Eq. 6

FURANONE + OH → 0.040 ASOATJ + … Eq. 7

PHEN + OH → 0.152 ASOATJ + … Eq. 8

The non-volatile products (e.g., ASOATJ in the benzene example) always form SOA, while the gas-phase of oxygenated L/S/IVOC products (e.g. VROCP4OXY2, VROCN1OXY6 in the benzene example) undergo further reactions with OH within a modified 2-D VBS framework. This process leads to additional functionalization and fragmentation. The SOA yield from benzene oxidation can be computed by multiplying together the stoichiometric coefficients that connect Eq. 4 to each subsequently formed SOA product, i.e., applying linear algebra. Our calculated SOA yields for CRACMM SOA precursors (see Section 2.4) are consistent with the values published by Pye et al. (2023) except for aromatic IVOCs where our result disagrees with the published value for unknown reasons. As shown in Section 2.5, the SOA aging process in CMAQ CRACMM can either increase or decrease SOA mass. SOA photolysis is currently not considered in CRACCM.

2.3.3 GEOS-Chem

GEOS-Chem is a global chemical transport model driven by meteorological input from the Goddard Earth Observing System (GEOS) of the NASA Global Modeling and Assimilation Office (https://zenodo.org/records/10640536, accessed on March 1st, 2024). GEOS-Chem is widely used for studying air quality, atmospheric chemistry, and climate change, and it has been applied to understand the sources and transport of pollutants, as well as their impact on human health and ecosystems. Within GEOS-Chem, two OA schemes are available: a simple scheme and a complex scheme (hereafter GEOS-Chem Simple and GEOS-Chem Complex) as described by Pai et al. (2020). The former aims to provide computationally efficient estimates of OA concentrations without explicit thermodynamic partitioning and does not track the fate and formation of different aerosol species (Hodzic and Jimenez, 2011). The latter builds upon the VBS framework with more detailed representation and has been recently updated.

2.3.3.1 GEOS-Chem Simple scheme

The GEOS-Chem Simple scheme converts a single lumped ASOA precursor (named SOAP) to non-volatile SOA with a fixed lifetime of 1 day and a fixed yield of 100%. For BVOC, the Simple scheme assume formation of non-volatile BSOA with fixed yields of 3% for isoprene and 10% for monoterpenes and sesquiterpenes. 50% of the BSOA are formed promptly while 50% are formed with a fixed lifetime of 1.15 days. The ASOA precursor emissions (i.e., model species SOAP) for

combustion sources are estimated using CO emissions as a proxy, with scaling factors of 1.3% and 6.9% for fire/biofuel and fossil fuel sources respectively. SOA formation from IVOC is not explicitly considered in the GOES-Chem simple scheme. The Simple scheme has no treatment of SOA aging or photolysis.

2.3.3.2 GEOS-Chem Complex scheme

The GEOS-Chem complex scheme incorporates SOA formation from anthropogenic and biogenic precursors based on a VBS scheme. The SOA yields from OH and O_3 oxidation are listed in Table 2-9 (Pye et al. 2010). The resulting products undergo further dynamic partitioning between the aerosol and gas phases based on their saturation vapor pressure and ambient aerosol concentration. This scheme does not include further aging processes and our review of the source code found no treatment of SOA photolysis. SOA formation from IVOC is simulated using naphthalene as a proxy. Additionally, irreversible SOA formation occurs from the aqueous-phase reactive uptake of isoprene (Marais et al. 2016) which is outside the primary focus of the current study.

Table 2-9. SOA mass-based yields[1] from anthropogenic and biogenic precursors under high (top) and low (bottom) NOx conditions for the GOES-Chem complex scheme (adopted from Pye et al. 2010)

C* [µg/m3] @ 298K	Non-volatile	0.1	1	10	100
ΔH_{vap} [kJ/mol]	42	42	42	42	42
ISOP[2]	0	0	0.0306	0.0000	0.0945
MTPA[3]	0	0.04	0.0095	0.0900	0.0150
	0	0.08	0.0190	0.1800	0.0300
LIMO	0	0	0.4743	0.1174	1.4190
	0	0	0.3661	0.3214	0.8168
SESQ	0	0	0.0005	1.1463	2.9807
	0	0	0.0000	0.5738	1.4893
BENZ	0	0	0.0778	0.0000	0.7932
	0.37	0	0.0000	0.0000	0.0000
TOL	0	0	0.0315	0.0944	0.0800
	0.30	0	0	0.0000	0.0000
XYL	0	0	0.0250	0.0360	0.0899
	0.36	0	0	0.0000	0.0000
IVOC[4]	0	0	0.0390	0.2960	0.2350
	0.73	0	0	0.0000	0.0000

[1] SOA yield for OH and O_3 oxidation. Yields for NO_3 oxidation of isoprene and terpenes are not presented here.
[2] Yields are not NOx-dependent
[3] α-pinene and similar monoterpenes
[4] Naphthalene used as a proxy

2.3.4 CHIMERE VBS with functionalization/fragmentation processes

The CHIMERE model is a Eulerian chemistry-transport model widely used for operational regional air quality forecasts (Honore et al. 2008) and simulations in Europe (Beekmann and Vautard, 2010; Sciare et al. 2010) as well as other regions of the world (Zhang et al. 2012; Hodzic et al. 2009, 2010). The latest version, v2023r1, was released in December 2023. Within CHIMERE, three SOA formation schemes are available: single-step oxidation, the Hydrophilic/Hydrophobic Organics (H_2O) mechanism (Couvidat et al. 2018), and a VBS scheme (Zhang et al. 2013; Cholakian et al.

2018). The VBS scheme includes two subsets: one involving only functionalization and the other involving functionalization, fragmentation and oligomerization (Zhang et al. 2013; Shrivastava et al. 2015).

We reviewed the CHIMERE VBS scheme with functionalization/fragmentation/oligomerization processes, referred to as CHIMERE VBS. This scheme models SOA formation from SOA precursors based on the VOC lumping scheme of the SAPRC99 mechanism and utilizing four volatility bins (C* ranging 1 to 1000 μg/m^3 at 300K) with corresponding SOA mass yields listed in Table 2-10 (Zhang et al. 2013; CHIMERE, 2023). For AVOC, the first two generations of gas-phase products undergo functionalization reactions with a 7.5% mass gain to account for oxygen:

$$ASOA_n(g) + OH \rightarrow 1.075*ASOA_{n-1}(g) \qquad \text{Eq. 9}$$

Subsequent generations undergo both functionalization (15% yield plus oxygen mass gain) and fragmentation (75%):

$$ASOA_n(g) + OH \rightarrow 0.16125*SOA_{n-1}(g) + 0.75*SOA_4(g) \qquad \text{Eq. 10}$$

Implicitly, Eq. 10 assumes a 10% yield of volatile products such as CO or CO_2. For BVOC, the fragmentation process occurs from the first generation:

$$BSOA_n(g) + OH \rightarrow 0.16125*BSOA_{n-1}(g) + 0.75*SOA_4(g) \qquad \text{Eq. 11}$$

In the CHIMERE VBS scheme, both functionalization and fragmentation occur with an OH rate constant of $1x10^{-11}$ cm^3 molecule^{-1} s^{-1}. Non-volatile SOA is formed by oligomerization with a reaction constant corresponding to a lifetime of 1 hour (Eq. 12 and Eq. 13, i.e., k = $3x10^{-4}$ s^{-1}).

$$ASOA_n(p) \rightarrow ANVSOA \qquad \text{Eq. 12}$$

$$BSOA_n(p) \rightarrow BNVSOA \qquad \text{Eq. 13}$$

CHIMERE represents IVOC using three high volatility bins of the POA VBS (POA7 to POA9, corresponding to C* from 10^4 to 10^6 μg/m^3). The IVOC mass fraction assigned to each bin is 24%, 29%, and 47% (Zhang et al. 2013). The gas-phase fraction of each volatility bin undergoes oxidation by OH radical to form oxidized POA (OPOA) with lower and/or higher volatility. Similar to ASOA formation, the first two generations of IV-SOA (SOA formed from IVOC) undergo only functionalization reactions (Eq. 14), while subsequent generations are assumed to undergo both functionalization and fragmentation (Eq. 15):

$$POA_n\ (g) + OH \rightarrow 1.075\ OPOA_{n-1}\ (g) \qquad \text{Eq. 14}$$

$$POA_n\ (g) + OH \rightarrow 0.75\ OPOA_{n+1}\ (g) + 0.16125\ OPOA_{n-1}\ (g) \qquad \text{Eq. 15}$$

Table 2-10. SOA mass-based yields[2] from precursors under high (top) and low (bottom) NOx conditions for the CHIMERE VBS scheme (Zhang et al., 2013; CHIMERE, 2023)

C* [µg/m3] @ 300K ΔH_{vap} [kJ/mol]	1 30	10 30	100 30	1000 30	CG/SOA MW [g/mol]
ISOP	0.0003 0.009	0.0225 0.03	0.015 0.015	0 0	180
TERP[1]	0.012 0.1073	0.1215 0.0918	0.201 0.3587	0.507 0.6075	180
HUMULE	0.075 0.075	0.15 0.15	0.75 0.75	0.9 0.9	180
ARO1	0.003 0.075	0.165 0.225	0.3 0.375	0.435 0.525	150
ARO2	0.0015 0.075	0.195 0.3	0.3 0.375	0.435 0.525	150
ALK4	0 0	0.0375 0.075	0 0	0 0	120
ALK5	0 0	0.15 0.3	0 0	0 0	150
OLE1	0.0008 0.0045	0.0045 0.009	0.0375 0.06	0.15 0.225	120
OLE2	0.003 0.0225	0.0225 0.0435	0.0825 0.129	0.27 0.375	120

[1] Same mass yields are used for APINEN, BPINEN, OCIMEN, and LIMONE. TERP used to represent all monoterpene species.
[2] Mass yields for OH and O_3 oxidation are the same for BVOC.

2.3.5 WRF-Chem MOSAIC

WRF-Chem is a numerical model that adds chemistry modules to the Weather Research and Forecasting (WRF) meteorological model to simulate interactions between meteorology and atmospheric chemistry. The latest version, v4.4, was released in April 2022. Within WRF-Chem, users can select from five aerosol schemes (WRF-Chem, 2022): 1) Modal Aerosol Dynamics Model for Europe (MADE/SORGAM, Schell et al. 2001), 2) Modal Aerosol Dynamics Model for Europe with the VBS (MADE/VBS), 3) Modal Aerosol Module (MAM), 4) Model for Simulating Aerosol Interactions and Chemistry (MOSAIC) sectional model aerosol parametrization, and 5) bulk aerosol module from GOCART.

We reviewed the MOSAIC scheme as another example of a VBS scheme with functionalization and fragmentation. In the MOSAIC scheme (Shrivastava et al. 2011), SOA formation from OH-oxidation is considered and reactions with O_3 and NO_3 radicals are not included. The formation of SOA from both AVOC and BVOC is modeled using 4-bin VBS (C* ranging from 0.1 to 100 µg/m^3 at 298K) with fixed yields (Table 2-11). No additional aging processes are considered for the condensable gases. SOA photolysis is included in the source code but turned off by default.

Table 2-11. SOA mass-based yields from precursors under high (top) and low (bottom) NOx conditions for the WRF-Chem MOSAIC (adopted from Shrivastava et al., 2011).

C* (μg/m^3) @ 298K	1	10	100	1000	MW [g/mol]
ISOP	0.001	0.023	0.015	0	250
	0.009	0.03	0.15	0	
TERP	0.012	0.122	0.201	0.5	250
	0.107	0.092	0.359	0.6	
SESQ	0.075	0.15	0.75	0.9	250
	0.075	0.15	0.75	0.9	
ARO1	0.01	0.24	0.45	0.7	250
	0.01	0.24	0.7	0.7	
ARO2	0.01	0.24	0.45	0.7	250
	0.01	0.24	0.7	0.7	
ALK4	0	0.38	0	0	250
	0	0.075	0	0	
ALK5	0	0.15	0	0	250
	0	0.3	0	0	
OLE1	0.001	0.005	0.038	0.15	250
	0.005	0.009	0.06	0.225	
OLE2	0.003	0.026	0.083	0.27	250
	0.023	0.044	0.129	0.375	

In WRF-Chem, IVOC is represented by three bins, with volatility ranging from 10^4 to 10^6 μg/m^3. The formation of SOA from IVOC involves OH-oxidation of both the non-oxygen (with subscript c) and oxygen parts (with subscript o), with a first-order rate constant of $4x10^{-11}$ cm^3 molecule^{-1} s^{-1}. For the non-oxygen part, oxidation results in formation of non-oxygen and oxygen parts (with 15% mass added) with lower volatility (Eq. 16 and Eq. 18). At the same time, the oxygen parts oxidize with OH and move to lower volatility bin (Eq. 17 and Eq. 19). Therefore, at any time, both non-oxygen and oxygen parts move to successively lower volatility bins. The lower volatility species (C* equal to 0.01 μg/m^3) are assumed to be inert and with no fragmentation reactions.

$$\text{IVOC (g)}_{n,\,c} + \text{OH} \rightarrow \text{SOA}_{n-1,c}(g) + 0.15*\text{SOA}_{n-1,o}(g) \qquad \text{Eq. 16}$$

$$\text{IVOC (g)}_{n,\,o} + \text{OH} \rightarrow \text{SOA}_{n-1,o}(g) \qquad \text{Eq. 17}$$

$$\text{SOA (g)}_{n,\,c} + \text{OH} \rightarrow \text{SOA}_{n-1,c}(g) + 0.15*\text{SOA}_{n-1,o}(g) \qquad \text{Eq. 18}$$

$$\text{SOA (g)}_{n,\,o} + \text{OH} \rightarrow \text{SOA}_{n-1,o}(g) \qquad \text{Eq. 19}$$

2.4 Comparison of first-generation SOA yields

We conducted a comprehensive comparison of the first-generation SOA mass yields from several SOA precursors considered by the eight SOA models/schemes evaluated. First-generation means the SOA yield before adding any additional SOA aging and/or photolysis effects considered by each model/scheme. Most models/schemes use the same SOA yield calculation for reactions initiated by OH, O_3 and NO_3. Utilizing either Eq. 2 or Eq. 3, the SOA yields were determined at 298 K and total

OA concentrations ranging from 0.1 μg/m^3 to 50 μg/m^3. Our analysis included calculations for anthropogenic precursors (benzene, toluene, xylene), IVOC and biogenic precursors (isoprene, monoterpene, and sesquiterpenes). Table 2-12 compares the simulated SOA mass yields at an OA concentration (C_{OA}) of 10 μg/m^3, which is relevant to ambient air quality and often used as a reference C_{OA} for comparison. Table 2-13 shows the ranking of different SOA precursors to first generation products and highlights the differences between the schemes.

Table 2-12. First-generation SOA yields (g/g) from different precursors simulated by different models/schemes. Temperature is 298K. Ambient OA concentration is assumed to be 10 μg/m³. Maximum SOA yields are shown in bold and minimum values are underlined.

Precursor	NOx condition	CAMx		CMAQ		GEOS- Chem		CHIMERE	WRF-Chem	Multi-model averages[5]	Ratio of. Max./Min
		SOAP2	VBS	AERO7	CRACMM	Simple	Complex	VBS	MOSAIC		
Benzene[1] (BENZ)	high	0.505	0.116	0.143	0.231	**1.000**	0.143	0.192	0.177	0.215	8.6
	low	0.403	0.220	0.370	0.657	**1.000**	0.370	0.358	0.200	0.368	5.0
Toluene[2] (TOL)	high	0.481	0.189	0.082	0.106	**1.000**	0.083	0.192	0.177	0.187	12.1
	low	0.926	0.211	0.301	0.549	**1.000**	0.300	0.358	0.200	0.406	5.0
Xylene[3] (XYL)	high	0.114	0.130	0.049	0.092	**1.000**	0.049	0.172	0.177	0.112	20.4
	low	0.737	0.258	0.360	0.915	**1.000**	0.360	0.336	0.200	0.452	5.0
IVOC	high	0.355	0.511	**1.000**	0.209[6]	/	0.205	2.69E-04	2.69E-04	0.345	3715
	low	0.546	0.511	**1.000**	0.183[6]	/	0.730	2.69E-04	2.69E-04	0.465	3715
Isoprene (ISOP)	high	**0.048**	0.012	0.046	/	0.030	0.037	0.035	0.014	0.032	4.0
	low	**0.093**	0.026	0.046	/	0.030	0.037	0.067	0.025	0.046	3.8
Monoterpenes (TERP)	high	0.139	0.095	0.168	**0.368**	0.100	0.095	0.131	0.095	0.149	3.9
	low	0.209	0.182	0.168	0.046	0.100	0.189	**0.247**	0.182	0.165	5.4
Sesquiterpenes[4] (SESQ)	high	0.524	0.217	0.439	0.122	0.100	**0.844**	0.202	0.220	0.334	8.4
	low	0.704	0.217	0.439	**1.080**	0.100	0.422	0.202	0.220	0.423	10.8

[1] For WRF-Chem and CHIMERE, results for BENZ are based on 'ARO1'
[2] For WRF-Chem and CHIMERE, results for TOL are based on 'ARO1'.
[3] For WRF-Chem and CHIMERE, results for XYL are based on 'ARO2'. For CMAQ CRACMM, results for XYL are averages of 'XYE' and 'XYM'.
[4] For CHIMERE, results for SESQ are based on humulene.
[5] Excluding CRACMM and GOES-Chem Simple for IVOC calculation; excluding CRACMM for isoprene calculation.
[6] Average of alkane and oxygenated IVOCs. See details in Table 2-14.

Table 2-13. Ranking of first-generation SOA yield from different precursors by each model/scheme under high and low NOx conditions

Ranking (from low to high)	CAMx SOAP2	CAMx VBS	CMAQ AERO7	CMAQ CRAMM	GOES-Chem Simple	GEOS-Chem Complex	CHIMERE VBS	WRF-Chem MOSAIC
				High NOx conditions				
1	ISOP	ISOP	ISOP	Xylene	ISOP	ISOP	IVOC	IVOC
2	Xylene	TERP	Xylene	Toluene	TERP	Xylene	ISOP	ISOP
3	TERP	Benzene	Toluene	SESQ	SESQ	Toluene	TERP	TERP
4	IVOC	Xylene	Benzene	Benzene	Benzene	TERP	Xylene	Benzene
5	Toluene	Toluene	TERP	TERP	Toluene	Benzene	Benzene	Toluene
6	Benzene	SESQ	SESQ		Xylene	IVOC	Toluene	Xylene
7	SESQ	IVOC	IVOC			SESQ	SESQ	SESQ
				Low NOx conditions				
1	ISOP	ISOP	ISOP	TERP	ISOP	ISOP	IVOC	IVOC
2	TERP	TERP	TERP	Toluene	TERP	TERP	ISOP	ISOP
3	Benzene	Toluene	Toluene	Benzene	SESQ	Toluene	SESQ	TERP
4	IVOC	SESQ	Xylene	Xylene	Benzene	Xylene	TERP	Benzene
5	SESQ	Benzene	Benzene	SESQ	Toluene	Benzene	Xylene	Toluene
6	Xylene	Xylene	SESQ		Xylene	SESQ	Benzene	Xylene
7	Toluene	IVOC	IVOC			IVOC	Toluene	SESQ

2.4.1 Anthropogenic VOC (AVOC)

Figure 2-4 shows the SOA mass yields (in g/g) as a function of the ambient OA concentrations resulting from three ASOA precursors (benzene (BENZ), toluene (TOL), and xylene (XYL)) predicted by each model/scheme. For WRF-Chem and CHIMERE, 'ARO1' is used to represent BENZ and TOL and 'ARO2' is used to represent XYL. For the GOES-Chem Simple scheme, the SOA yield is 100%.

Under high NOx conditions, the results indicated an increase in SOA yields with higher OA concentrations across all models/schemes, except for CMAQ CRACMM, where changes were minimal due to the allocation of almost 100% of SOA to non-volatile products. CAMx SOAP2 predicts the highest SOA yields for BENZ and TOL under high NOx conditions and shows a different trend than the other models/schemes. The SOA yield in CAMx SOAP2 increases more steadily over the range of OA concentrations compared to the more rapid SOA yield increase at higher OA that is observed in most other models/schemes. WRF-Chem and CHIMERE showed the highest XYL SOA when OA concentration exceeded 5 $\mu g/m^3$. Overall, CAMx-VBS, CHIMERE VBS, and WRF-Chem MOSAIC predicted similar SOA yields, with results from CMAQ AERO7 and GEOS-Chem Complex schemes being almost identical. In the GEOS-Chem Simple scheme, a constant SOA yield of 1.0 g/g is observed regardless of the AVOC precursor or NOx conditions. At an OA concentration of 10 $\mu g/m^3$, the averaged SOA yield from BENZ, TOL, and XYL was 0.313 g/g (ranging from 0.116 g/g in CAMx VBS to 1.0 g/g in GOES-Chem Simple), 0.289 g/g (ranging from 0.082 g/g in CMAQ AERO7 to 1.0 g/g in GOES-Chem Simple), and 0.223 g/g (ranging from 0.049 g/g in CMAQ AERO7/GOES-Chem Complex to 1.0 g/g in GOES-Chem Simple), respectively.

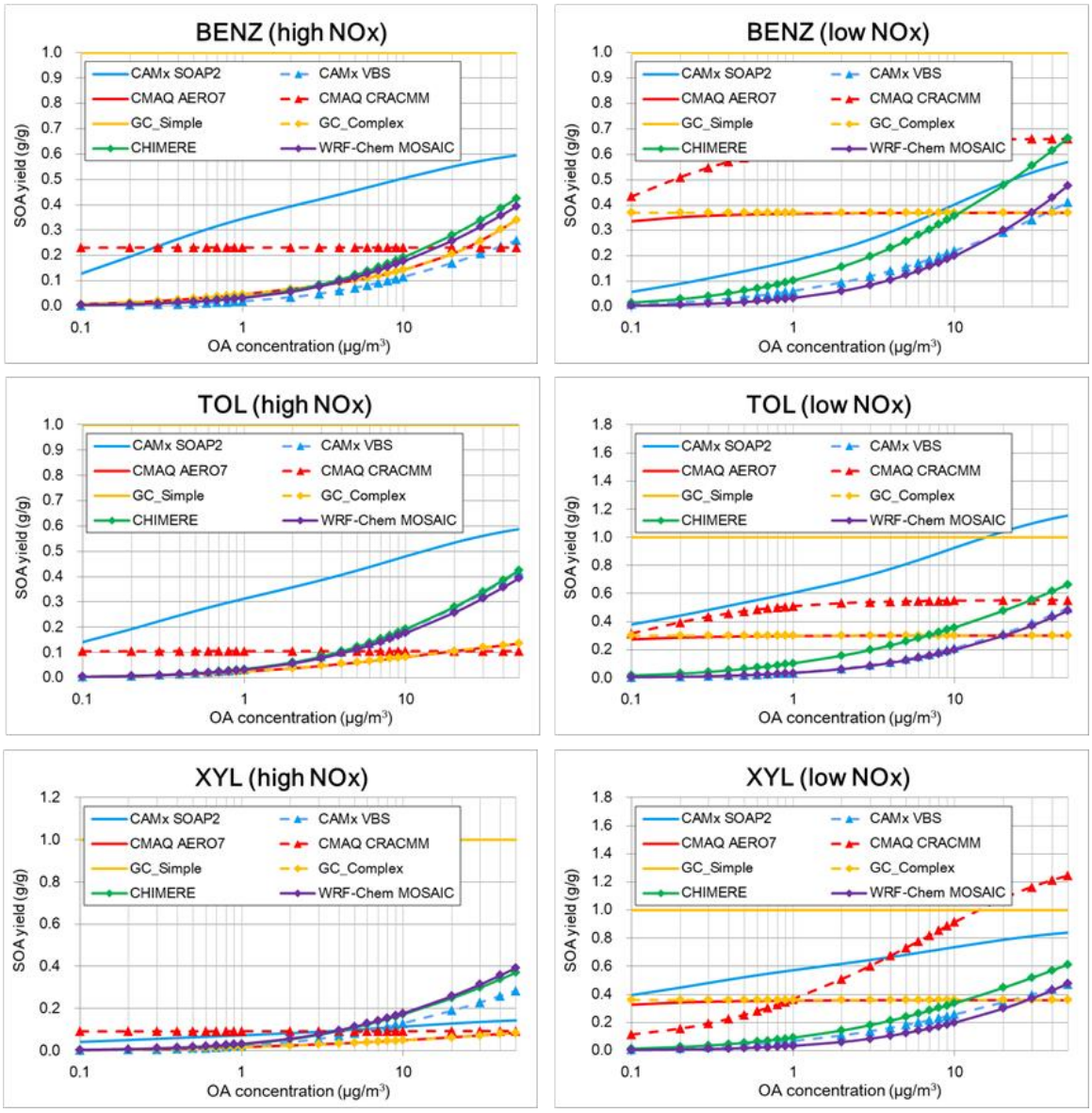

Figure 2-4. First-generation SOA yields for benzene (BENZ), toluene (TOL), and xylene (XYL) under high and low NOx conditions calculated by different models/schemes.

Under low NOx conditions, the CMAQ AERO7 and GEOS-Chem Complex schemes are almost identical and exhibit negligible increases in SOA yields with OA concentrations. WRF-Chem MOSAIC and CAMx VBS predict comparable, lower SOA yields for all three aromatics compared to CHIMERE. CMAQ CRACMM predicted the highest SOA yield for BENZ, while TOL SOA was highest with CAMx SOAP2. Compared to high NOx conditions CMAQ CRACMM scheme SOA yields are higher in the low NOx conditions for all precursors. At an OA concentration of 10 µg/m^3, the averaged SOA yield from BENZ, TOL, and XYL was 0.447 g/g (ranging from 0.200 g/g in WRF-Chem MOSAIC to 1.0 g/g in GOES-Chem Simple), 0.481 g/g (ranging from 0.200 g/g in WRF-Chem MOSAIC to 1.0 g/g in GOES-Chem Simple), and 0.521 g/g (ranging from 0.200 g/g in WRF-Chem MOSAIC to 1.0 g/g in GOES-Chem Simple), respectively.

2.4.2 Biogenic VOC (BVOC)

Figure 2-5 shows the first-generation SOA mass yields (in g/g) calculated by each model/scheme as a function of ambient OA concentrations for three BSOA precursors, namely isoprene (ISOP), monoterpenes (TERP), and sesquiterpenes (SESQ). For CMAQ CRACMM, SOA yields from isoprene were not provided due to the unique requirement for aqueous SOA formation from isoprene epoxydiols (for instance, particle pH, liquid water, and sulfate are required for calculation) which makes it incomparable to other models/schemes.

For isoprene SOA, all models/schemes (excluding GEOS-Chem Simple) demonstrated increased SOA yields with higher OA concentrations. CAMx SOAP2, CAMx VBS, WRF-Chem, and CHIMERE VBS predicted higher SOA yields under low NOx conditions compared to high NOx conditions. In contrast, CMAQ AERO7 and GEOS-Chem schemes show NOx-independent SOA yields. WRF-Chem MOSAIC and CAMx VBS exhibited nearly identical and the lowest SOA yields among the models/schemes evaluated. Under high NOx conditions, CMAQ AERO7 and CAMx SOAP2 showed similar SOA yields when the OA concentrations were below 20 μg/m^3. These yields were the highest predicted values when OA concentrations were above 2 μg/m^3. Conversely, the GEOS-Chem Simple scheme employs a constant yield (0.3 g/g) regardless of OA concentrations, resulting in higher SOA yields at low OA concentrations (C_{OA} < 2 μg/m^3) and being surpassed by other models/schemes (except WRF-Chem MOSAIC and CAMx VBS) at high OA concentrations. For an ambient OA concentration of 10 μg/m^3, the averaged SOA yield from isoprene under high NOx conditions is 0.032 g/g (ranging from 0.012 g/g in CAMx VBS to 0.048 g/g in CAMx SOAP2). The corresponding value under low NOx conditions is 0.046 g/g (ranging from 0.025 g/g in WRF-Chem MOSAIC to 0.093 in CAMx SOAP2).

Regarding TERP, SOA yields predicted by the CMAQ CRACMM and GEOS-Chem Simple scheme exhibit minimal variation across different OA concentrations, whereas other models/schemes predict higher SOA yields with increased OA concentrations. CMAQ CRACMM predicted a TERP SOA yield of approximately 0.35 g/g under high NOx conditions, significantly surpassing other models/schemes. In contrast, under low NOx conditions, the SOA yield predicted by CMAQ CRACMM was lowest at around 0.05 g/g. CAMx VBS and WRF-Chem MOSAIC predicted identical SOA yields for TERP, while CHIMERE predicted similar but slightly higher SOA yields. CAMx SOAP2, CMAQ AERO7, and GEOS-Chem Complex Scheme simulated a slower increase in SOA yield as OA concentration increased compared to the aforementioned models/schemes. With an ambient OA concentration of 10 μg/m^3, the averaged SOA yield from TERP under high NOx conditions is 0.149 g/g (ranging from 0.095 g/g in CAMx VBS and WRF-Chem MOSAIC to 0.368 g/g in CMAQ CRACMM), whereas under low NOx conditions, it is 0.165 g/g (0.046 g/g in CMAQ CRACMM to 0.247 g/g in CHIMERE VBS).

For SESQ, the GEOS-Chem Complex scheme and CMAQ CRACMM predicted the highest SOA yield under high and low NOx conditions, respectively. Results from CHIMERE VBS and WRF-Chem MOSAIC aligned closely in the middle range, while the GEOS-Chem Simple scheme, with a constant value of 0.1 g/g, predicted the lowest SOA yield from SESQ at most OA concentrations. The SOA yields predicted by CAMx SOAP2 were highest at low OA concentrations but in the middle range at high OA concentrations. CMAQ AERO7 yields were similar to GEOS-Chem Complex at low NOx but only about half of GEOS-Chem Complex at high NOx. With an ambient OA concentration

of 10 μg/m^3, the averaged SOA yield from SESQ under high NOx conditions is 0.334 g/g (ranging from 0.1 g/g in GEOS-Chem Simple and GEOS-Chem Complex to 0.844 g/g in CMAQ CRACMM), whereas under low NOx conditions is 0.423 g/g (ranging from 0.1 g/g in GEOS-Chem Simple to 1.080 g/g in CMAQ CRACMM).

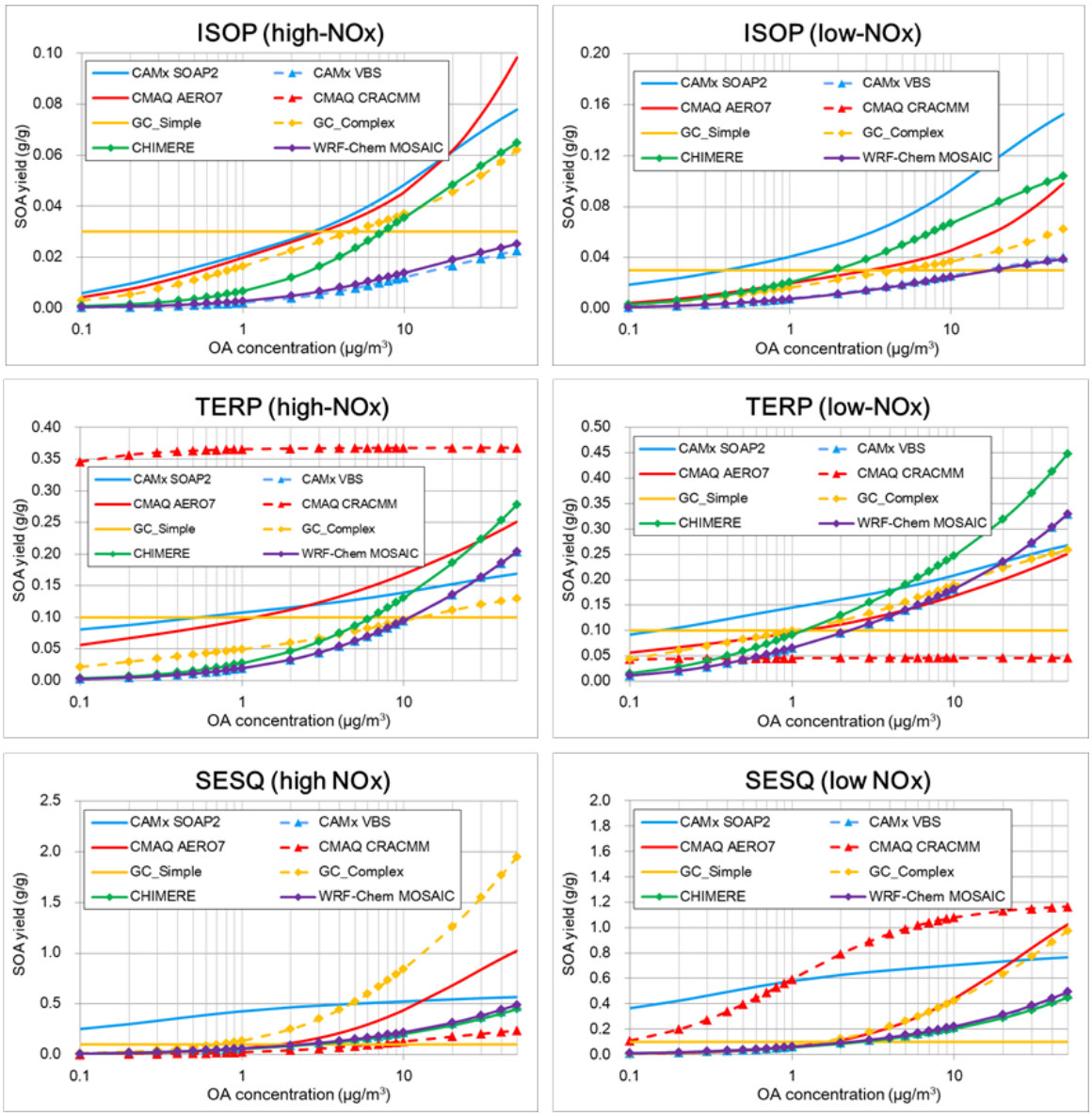

Figure 2-5. First-generation SOA yields for isoprene (ISOP), monoterpenes (TERP), and sesquiterpenes (SESQ) under high and low NOx conditions calculated by different models/schemes.

2.4.3 Intermediate VOC (IVOC)

IVOC emissions play an important role in anthropogenic SOA formation (Robinson et al., 2016; Ma et al., 2016; Zhao et al., 2014). The SOA yields from IVOC, referred to as IV-SOA, predicted by each model/scheme are shown in Figure 2-6. The GOES-Chem Simple scheme is omitted since it does not explicitly account for IVOC. Additionally, the results for CMAQ CRACMM are displayed separately in Figure 2-7 due to the distinct treatment of several IVOC types by CRACMM.

In the CMAQ AERO7 scheme, a constant IV-SOA yield of 1.0 g/g is observed regardless of NOx conditions, surpassing the values simulated by other models/schemes. Under high NOx conditions, the CAMx VBS and GEOS-Chem Complex scheme exhibit similar trends in SOA yields, demonstrating higher values at increased OA concentration. CAMx VBS predicts higher SOA yields than GEOS-Chem Complex at all OA concentrations. Under low NOx conditions, the GEOS-Chem Complex scheme predicts a constant SOA yield at 0.73 g/g, which exceeds CAMx VBS when OA concentrations are below 20 μg/m^3. The first-generation IV-SOA yields simulated by CHIMERE VBS and WRF-Chem MOSAIC are deemed negligible at both high and low NOx.

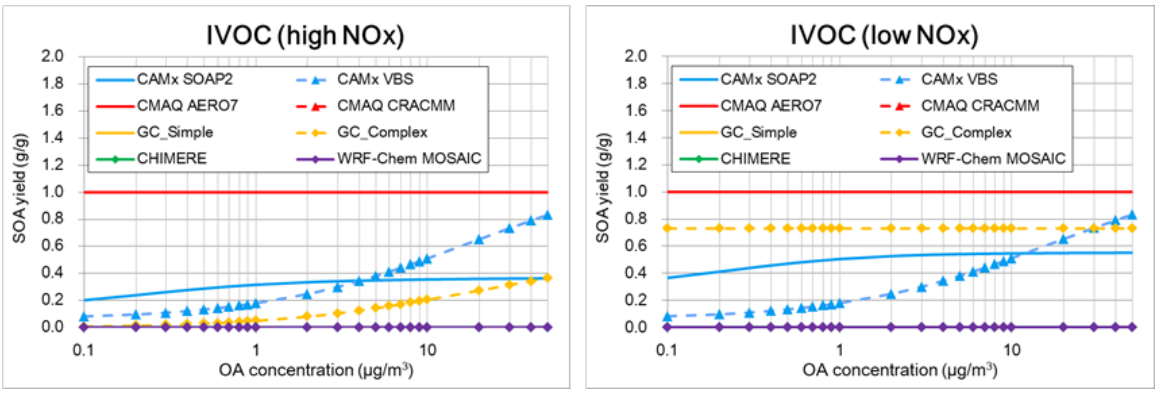

Figure 2-6. First-generation SOA yields for IVOC under high and low NOx conditions calculated by different models/schemes. Results for the GEOS-Chem Simple scheme are not shown, and results for CMAQ CRACMM are shown in Figure 2-7.

In contrast to other models/schemes, CRACMM distinguishes IVOC based on functional groups: alkane IVOC, aromatic IVOC, and oxygenated IVOC. As shown by Figure 2-7, SOA yields from alkane IVOC increase with higher OA concentrations, and high NOx conditions lead to higher SOA yields than low NOx conditions. For directly emitted oxygenated IVOC, a constant SOA yield of 0.12 g/g is simulated. Aromatic IVOC, however, exhibits considerably lower SOA yields with minimal variations based on the OA concentrations. As mentioned in Section 3.2.2, our calculated SOA yields for alkane IVOC and oxygenated IVOC are consistent with the values published by Pye et al. (2023) but for aromatic IVOCs our result disagrees with the published value for unknown reasons. On average, CRACMM predicted a SOA yield of 0.209 g/g from alkane and oxygenated IVOC under high NOx conditions and of 0.183 g/g under low NOx conditions.

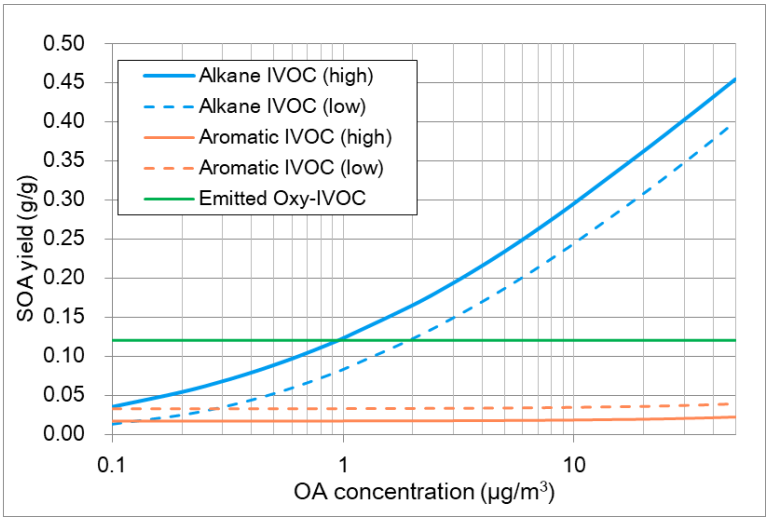

Figure 2-7. First-generation SOA yields for different IVOC types under high and low NOx conditions calculated by CMAQ CRACMM. Our result for aromatic IVOCs disagrees with the value published by Pye et al. (2023) for unknown reasons.

Table 2-14. SOA yields from different IVOC types implemented in CMAQ CRACMM. The aging effect is calculated with a 24-hour exposure to OH concentration at 3 x 10^6 molecules/cm^3. Temperature is 298K. Ambient OA concentration is assumed to be 10 μg/m^3.

SOA yield (g/g)	NOx condition	Alkane IVOC	Emitted Oxy-IVOC	Aromatic IVOC[1]	Average[2]
First-generation	High	0.296	0.121	0.019	0.209
	Low	0.245	0.121	0.035	0.183
Aged	High	0.077	0.121	0.015	0.099
	Low	0.039	0.121	0.190	0.080

[1] Our result for aromatic IVOCs disagrees with the value published by Pye et al. (2023) for unknown reasons.
[2] Arithmetic average of SOA yield from alkane and oxygenated IVOC types. Aromatic IVOCs are excluded due to disagreement with Pye et al. (2023) values.

2.5 Comparison of SOA aging

Among the eight models/schemes that we evaluated, the CAMx SOAP2, GEOS-Chem Simple, and GEOS-Chem Complex schemes do not consider SOA aging processes. For the other models/schemes, the treatment of SOA aging differs. Generally, there are three ways to represent SOA aging: OH-oxidation in the gas-phase, condensed phase oligomerization and/or hydrolysis. OH-oxidation aging is usually parameterized as gas-phase OH reaction forming products with lower volatility (i.e., functionalization) and/or products with higher volatility (i.e., fragmentation). The functionalization process usually decreases volatility and increases SOA mass, while the fragmentation process increases volatility and decreases SOA mass. This OH-oxidation aging is adopted by CAMx VBS (for ASOA and IV-SOA), WRF-Chem MOSAIC, CHIMERE, and CMAQ CRACMM, with implementation being specific to each scheme. The oligomerization aging is characterized as a first-order particle-phase reaction (usually with a lifetime of 20 hr) forming non-volatile products without dependence on oxidant level. CMAQ AERO7 applies this oligomerization process for SOA formed from all precursors except monoterpenes. For SOA formed from

monoterpenes + NO_3, AERO7 applies aerosol hydrolysis to form non-volatile products with a lifetime of ~3 hr.

The aging effects for the models/schemes are shown below. Table 2-15 summarizes the aged SOA yields at 298 K with a total OA concentration of 10 μg/m^3 simulated by different models/schemes. Table 2-16 shows the ratio of aged SOA yields to first-generation SOA yields simulated by different models/schemes. A 24-hour exposure to OH concentration at 3 x 10^6 molecules/cm^3 was used to calculate the aged SOA yields. This equals an accumulated OH exposure of 2.59 x 10^{11} molecules s/cm^3. Figure 2-8 through Figure 2-10 compares the first-generation and aged SOA yields simulated by different models/schemes for various SOA precursors.

Table 2-15. Aged SOA yields (g/g) from different precursors simulated by different models/schemes. The aging effect is calculated with a 24-hour exposure to OH concentration at 3 x 10^6 molecules/cm^3. Temperature is 298K. Ambient OA concentration is assumed to be 10 µg/m^3. Maximum SOA yields are shown in bold, and minimum values are underlined. Shaded values indicate no aging processes implemented.

Precursor	NOx condition	CAMx		CMAQ		GEOS- Chem		CHIMERE	WRF-Chem	Multi-model averages[5]	Ratio of Max./Min.
		SOAP2	VBS	AERO7	CRACMM	Simple	Complex	VBS	MOSAIC		
Benzene[1] (BENZ)	high	0.505	0.802	0.224	0.232	**1.000**	0.143	0.787	0.177	0.484	7.0
	low	0.403	1.073	0.370	0.612	1.000	0.370	**1.114**	0.200	0.643	5.6
Toluene[2] (TOL)	high	0.481	**1.305**	0.124	0.106	1.000	0.083	0.787	0.177	0.508	15.7
	low	0.926	**1.332**	0.301	0.502	1.000	0.300	1.114	0.200	0.709	6.7
Xylene[3] (XYL)	high	0.114	0.828	0.072	0.093	**1.000**	0.049	0.665	0.177	0.375	20.4
	low	0.737	**1.143**	0.360	0.510	1.000	0.360	0.983	0.200	0.662	5.7
IVOC	high	0.355	1.148	1.000	0.099[6]	/	0.205	0.016	**1.517**	0.707	93.4
	low	0.546	1.148	1.000	0.080[6]	/	0.730	0.016	**1.517**	0.826	93.4
Isoprene (ISOP)	high	0.048	0.012	0.058	/	0.030	0.037	**0.082**	0.014	0.040	6.8
	low	0.093	0.026	0.058	/	0.030	0.037	**0.124**	0.025	0.056	5.0
Monoterpenes	high	0.139	0.095	0.168	0.368	0.100	0.095	**0.540**	0.095	0.200	5.7
(TERP)	low	0.209	0.182	0.168	0.046	0.100	0.189	**0.803**	0.182	0.235	17.5
Sesquiterpenes[4]	high	0.524	0.217	0.784	0.533	0.100	0.844	**0.857**	0.220	0.510	8.6
(SESQ)	low	0.704	0.217	0.784	**1.043**	0.100	0.422	0.857	0.220	0.544	10.4

[1] For WRF-Chem and CHIMERE, results for BENZ are based on 'ARO1'
[2] For WRF-Chem and CHIMERE, results for TOL are based on 'ARO1'. For CMAQ CRACMM, results for XYL are averages of 'XYE' and 'XYM'.
[3] For WRF-Chem and CHIMERE, results for TOL are based on 'ARO2'.
[4] For CHIMERE, results for SESQ are based on humulene.
[5] Excluding CRACMM and GOES-Chem Simple for IVOC calculation; excluding CRACMM for isoprene calculation.
[6] Average of alkane and oxygenated IVOCs. See details in Table 2-14.

Table 2-16 Ratio of aged SOA yields (Table 2-15) to first-generation SOA yields (Table 2-12) from different precursors simulated by different models/schemes. Maximum ratios are shown in bold, and minimum values are underlined. Shaded values indicate no aging processes implemented.

Precursor	NOx condition	CAMx		CMAQ		GEOS- Chem		CHIMERE	WRF-Chem	Multi-model averages[5]
		SOAP2	VBS	AERO7	CRACMM	Simple	Complex	VBS	MOSAIC	
Benzene[1] (BENZ)	high	1.00	**6.92**	1.57	1.00	1.00	1.00	4.09	1.00	1.54
	low	1.00	**4.88**	1.00	0.93	1.00	1.00	3.11	1.00	1.44
Toluene[2] (TOL)	high	1.00	**6.90**	1.50	1.00	1.00	1.00	4.09	1.00	1.76
	low	1.00	**6.31**	1.00	0.91	1.00	1.00	3.11	1.00	1.48
Xylene[3] (XYL)	high	1.00	**6.35**	1.46	1.00	1.00	1.00	3.86	1.00	1.68
	low	1.00	**4.44**	1.00	0.56	1.00	1.00	2.92	1.00	1.27
IVOC	high	1.00	2.25	1.00	0.47	/	1.00	60	**5635**	1.95
	low	1.00	2.25	1.00	0.44	/	1.00	60	**5635**	1.74
Isoprene (ISOP)	high	1.00	1.00	1.27	/	1.00	1.00	**2.32**	1.00	1.27
	low	1.00	1.00	1.27	/	1.00	1.00	**1.85**	1.00	1.21
Monoterpenes (TERP)	high	1.00	1.00	1.00	1.00	1.00	1.00	**4.13**	1.00	1.34
	low	1.00	1.00	1.00	1.00	1.00	1.00	**3.25**	1.00	1.42
Sesquiterpenes[4] (SESQ)	high	1.00	1.00	1.79	4.12	1.00	1.00	**4.24**	1.00	1.52
	low	1.00	1.00	1.79	0.97	1.00	1.00	**4.24**	1.00	1.28

[1] For WRF-Chem and CHIMERE, results for BENZ are based on 'ARO1'
[2] For WRF-Chem and CHIMERE, results for TOL are based on 'ARO1'. For CMAQ CRACMM, results for XYL are averages of 'XYE' and 'XYM'.
[3] For WRF-Chem and CHIMERE, results for TOL are based on 'ARO2'.
[4] For CHIMERE, results for SESQ are based on humulene.
[5] Excluding CRACMM and GOES-Chem Simple for IVOC calculation; excluding CRACMM for isoprene calculation.

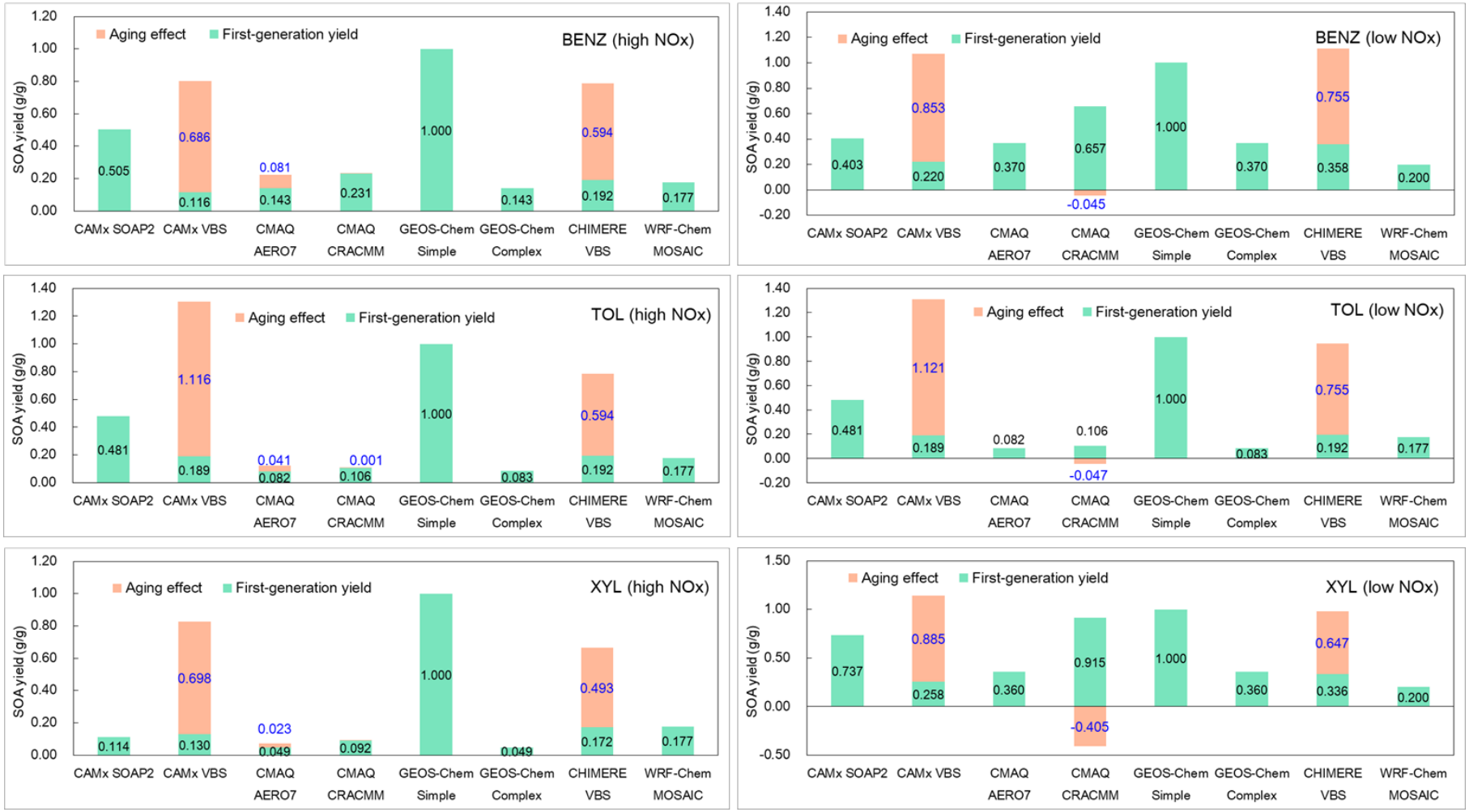

Figure 2-8. First-generation and aged SOA yields simulated by different models/schemes for benzene (BENZ), toluene (TOL), and xylene (XYL). For CMAQ CRACMM, results for XYL are averages of 'XYE' and 'XYM'. For WRF-Chem and CHIMERE, results for BENZ and TOL are based on 'ARO1'; results for XYL are based on 'ARO2'. Aged SOA yields are calculated with a 24-hour exposure to OH concentration at 3 x 10^6 molecules/cm^3.

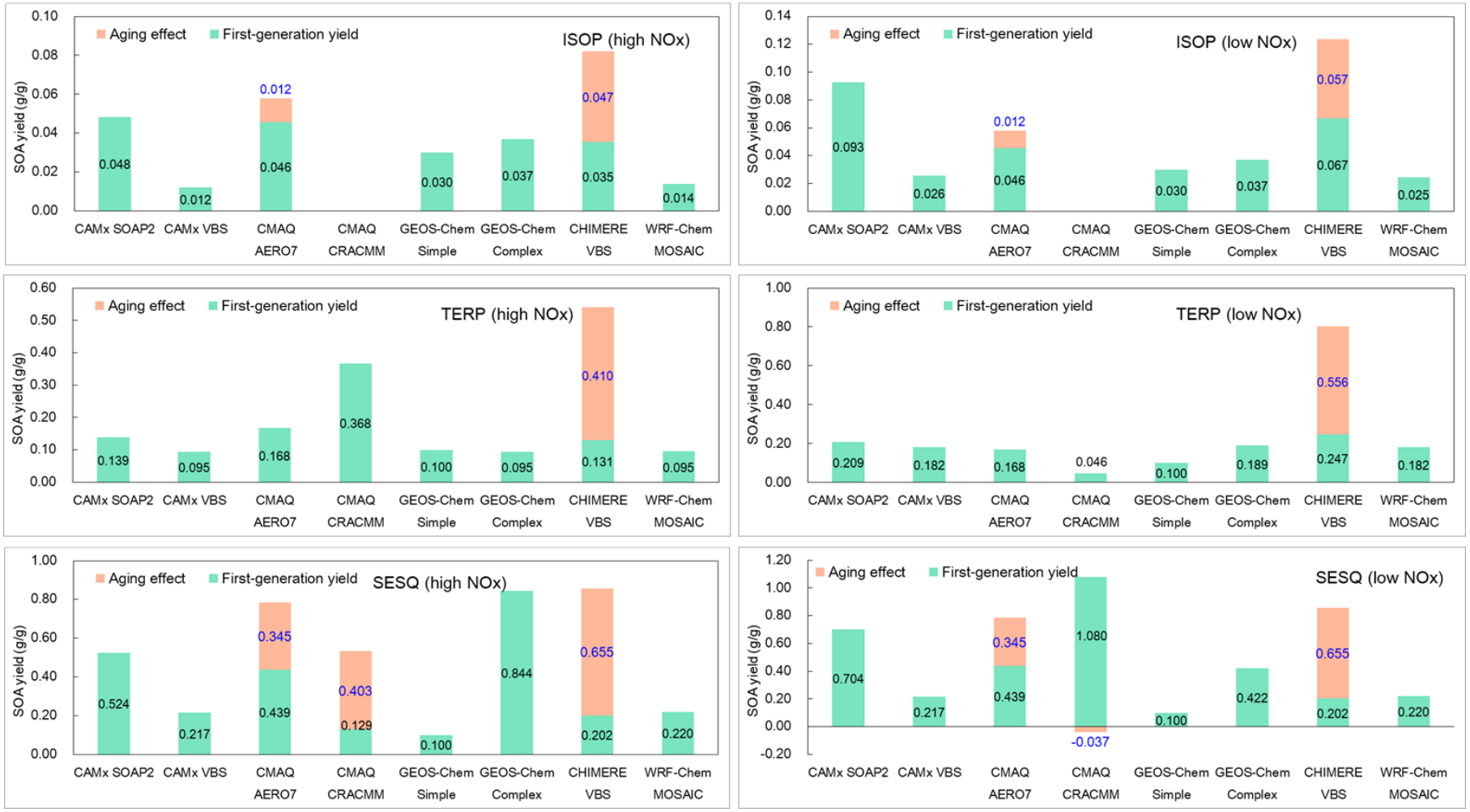

Figure 2-9. First-generation and aged SOA yields simulated by different models/schemes for isoprene (ISOP), monoterpenes (TERP), and sesquiterpenes (SESQ). For CHIMERE, results for SESQ are based on humulene. Aged SOA yields are calculated with a 24-hour exposure to OH concentration at 3 x 10^6 molecules/cm^3.

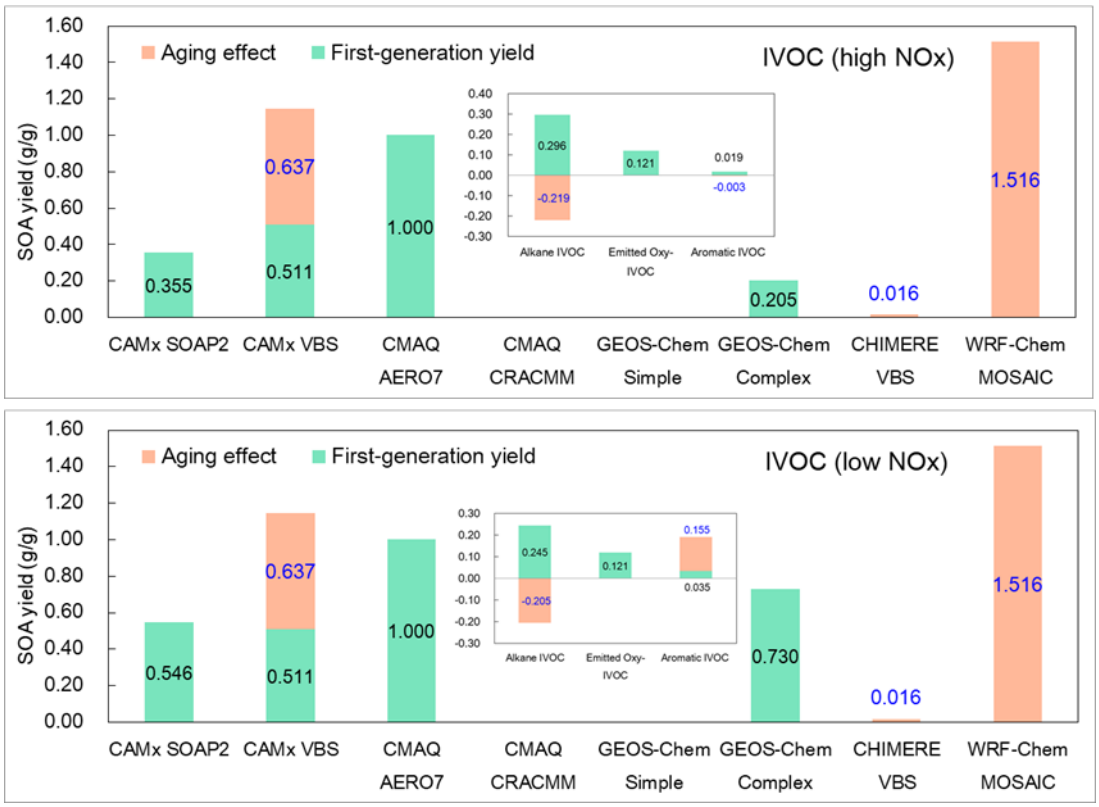

Figure 2-10. First-generation and aged SOA yields simulated by different models/schemes for IVOC. For CMAQ, results are presented for alkane IVOC, emitted oxygenated IVOC, and aromatic IVOC in the smaller plot. Aged SOA yields are calculated with a 24-hour exposure to OH concentration at 3 x 10^6 molecules/cm^3.

2.5.1 CAMx VBS

The CAMx VBS scheme incorporates a step-wise OH oxidation aging framework for ASOA and IV-SOA, utilizing an OH rate constant of 2×10^{-11} cm^3/molecule/s (Figure 2-2b). Fragmentation processes are not considered.

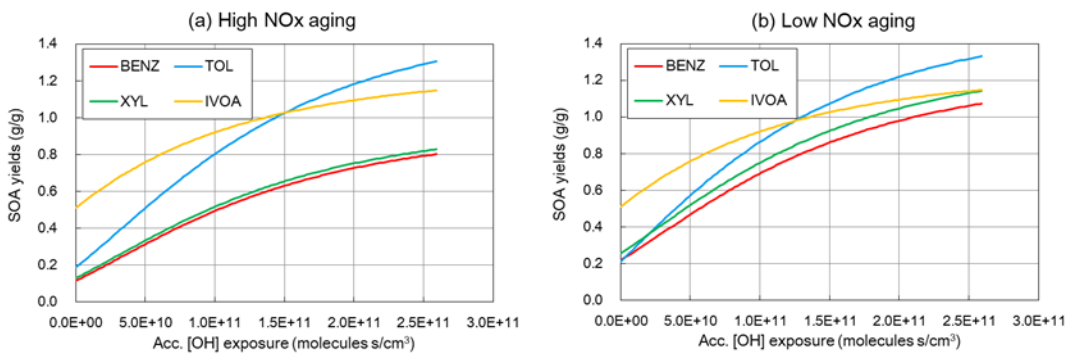

Figure 2-11 illustrates SOA mass yields as a function of accumulated OH exposure under high and low NOx conditions for various precursors. It is observed that the SOA yields increase with accumulated OH exposure, but the aging rate decelerates as the OH exposure increases. With an accumulated OH exposure of 2.59 x 10^{11} molecules s/cm^3, the SOA yield from BENZ, TOL, XYL, and IVOC increased by 592%, 590%, 535%, and 125%, respectively under high NOx conditions, compared to their initial yields. Similarly, these values were 388%, 531%, 344%, and 125% under

low NOx conditions, respectively. These findings highlight the significant impact of aging processes implemented in the CAMx VBS scheme.

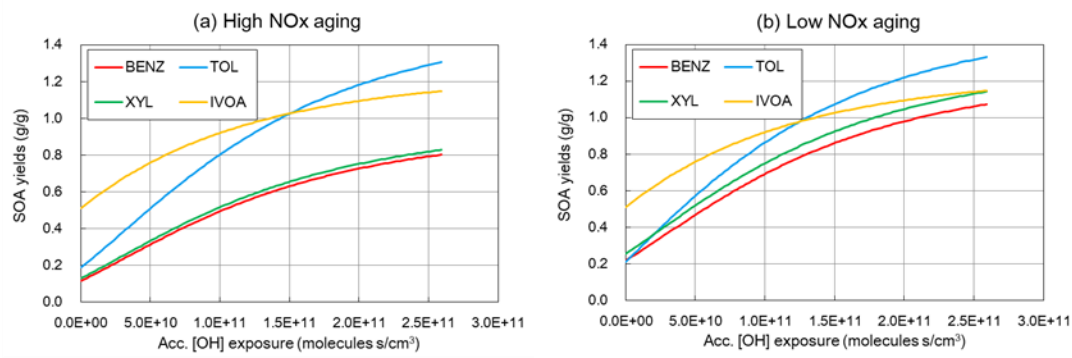

Figure 2-11. Aging of BENZ, TOL, XYL, and IVOA as a function of accumulated OH exposure under (a) high and (b) low NOx conditions in the CAMx VBS scheme.

2.5.2 CMAQ AERO7

The SOA aging process in the CMAQ AERO7 scheme involves particle-phase oligomerization and hydrolysis. Oligomerization, depicted in Figure 2-2d, applies to SOA formed from isoprene, sesquiterpenes, and aromatics (only under high-NOx conditions). On the other hand, aerosol hydrolysis affects SOA formed from monoterpene-derived organic nitrates, which are produced through the reaction of monoterpenes with NO_3 radical.

The oligomerization process has a lifetime of approximately 20 hr. Figure 2-12 shows the change of SOA yields as a function of oligomerization hour for different precursors. After 24 hours of oligomerization, there is a notable increase in SOA yields by 27%, 79%, and 46% to 57% for ISOP, SESQ, and aromatics, respectively. In contrast, the hydrolysis reaction has a shorter lifetime of around 3 hr. For monoterpene-derived organic nitrates, the SOA yield experiences a relative increase of 48% over 24 hours due to hydrolysis. Despite the hydrolysis rate being nearly ten times higher than the oligomerization rate, the resulting hydrolysis product has a lower molecular weight than the parent organic nitrates. This factor slows the overall SOA increase attributable to hydrolysis despite its faster reaction kinetics.

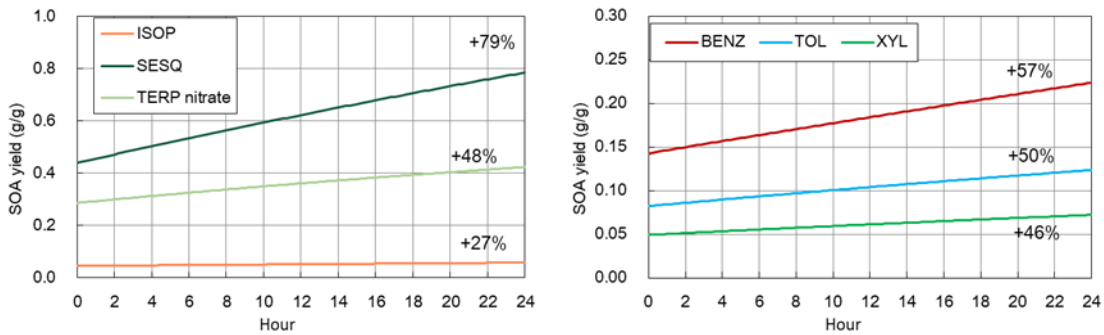

Figure 2-12. SOA yields from BVOC (left) and aromatics (right) due to oligomerization in the CMAQ AERO7 scheme.

2.5.3 CMAQ CRACMM

The aging processes in CMAQ CRACMM involve OH-oxidation reactions of the secondary oxygenated L/S/IVOCs. These reactions produce products with both higher and lower volatilities. As shown by Figure 2-13, the impact of aging on SOA yields differs depending on the precursor and NOx conditions. For instance, under high NOx conditions, the SOA yields from SESQ increased

by over 300% with an accumulated OH exposure of 2.59 x 10^{11} molecule·s/cm^3, while aromatics showed minimal effects. In contrast, SOA yields from XYL decreased by 44% under low NOx conditions with the same amount of OH exposure, whereas BENZ, TOL, and SESQ exhibited minor decreases (<10%).

In terms of IVOC (Figure 2-14), CMAQ CRACMM shows varied aging effects based on the type of IVOC. Emitted oxygenated IVOC do not exhibit aging effects since their oxidation products are considered non-volatile. SOA generated from alkane IVOC decreased by over 70% with an accumulated OH exposure of 2.59 x 10^{11} molecule·s/cm^3. On the other hand, SOA formed from aromatic IVOC exhibited negligible changes under high NOx conditions but decreased by 85% under low NOx conditions.

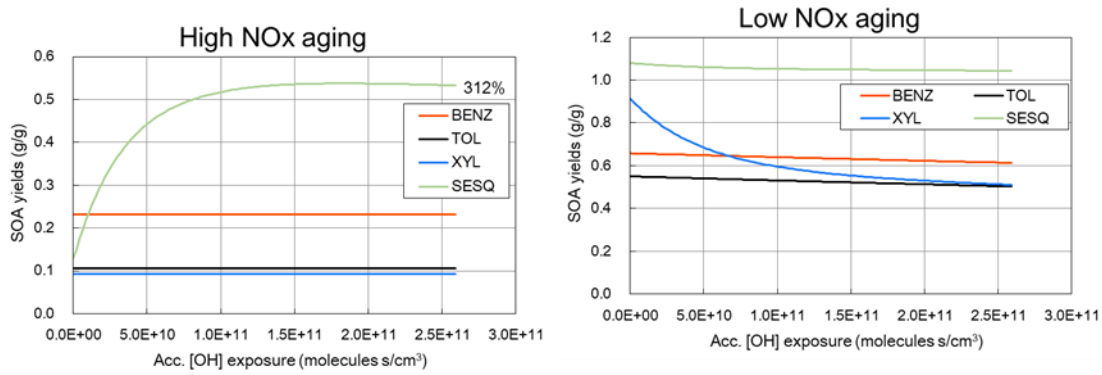

Figure 2-13. SOA aging for aromatics and SESQ as a function of OH exposure under high and low NOx conditions in the CMAQ CRACMM scheme. Results for xylene (XYL) are averages of XYM and XYE.

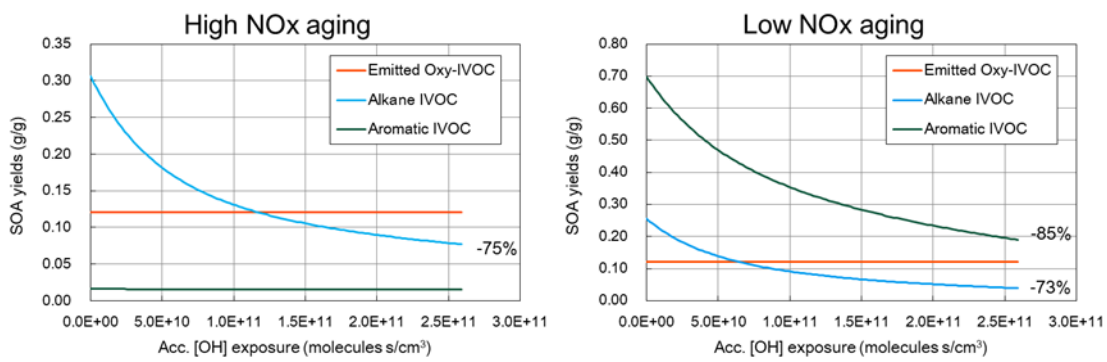

Figure 2-14. SOA aging for different IVOC as a function of OH exposure under high and low NOx conditions in the CMAQ CRACMM scheme.

2.5.4 CHIMERE VBS

The CHIMERE VBS scheme includes gas-phase functionalization and fragmentation and particle-phase oligomerization as its aging processes, as demonstrated by Eq. 9 to Eq. 15. Figure 2-15 presents the SOA aging effects within the CHIMERE VBS scheme. For BVOC, the aging effect is more pronounced for terpenes (TERP) and humulenes (HUMULE) than isoprene (ISOP). Under high NOx conditions, an accumulated OH exposure of 2.59 x 10^{11} molecule·s/cm^3 results in a substantial increase in SOA mass formed from ISOP, TERP, and HUMULE by 141%, 331%, and 341%, respectively. The aging effect is less pronounced under low NOx conditions, except for

HUMULE, which shows NOx-independency, yet the overall SOA yields are higher. Concerning aromatics, an OH exposure of 2.59 x 10^{11} molecule·s/cm^3 results in over 300% and 200% increase in SOA mass under high and low NOx conditions, respectively.

In the case of IVOC, aging with an OH exposure of 2.59 x 10^{11} molecule·s/cm^3 results in a substantial relative increase (almost 60 times) in SOA mass, as shown by Figure 2-16. Nevertheless, the SOA formed from IVOC remains relatively low around 0.01 g/g. This diminished IV-SOA yield can be attributed to the very low first-generation SOA yield from IVOC (~10^{-4} g/g) and the fact that starting from the third oxidation generation, 75% of the condensable gases undergo fragmentation towards more volatile products, while only 15% undergo functionalization as outlined in Eq. 15.

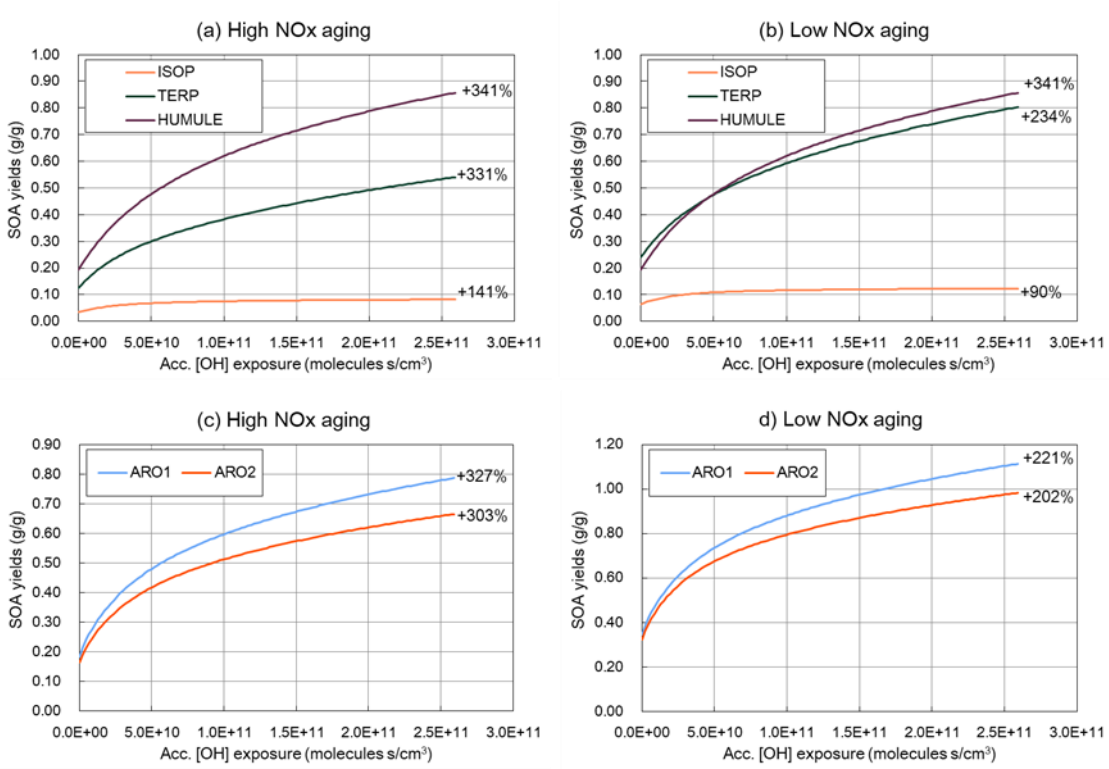

Figure 2-15. SOA aging for BVOC and aromatics as a function of OH exposure under (a & c) high and (b & d) low NOx conditions in the CHIMERE VBS scheme.

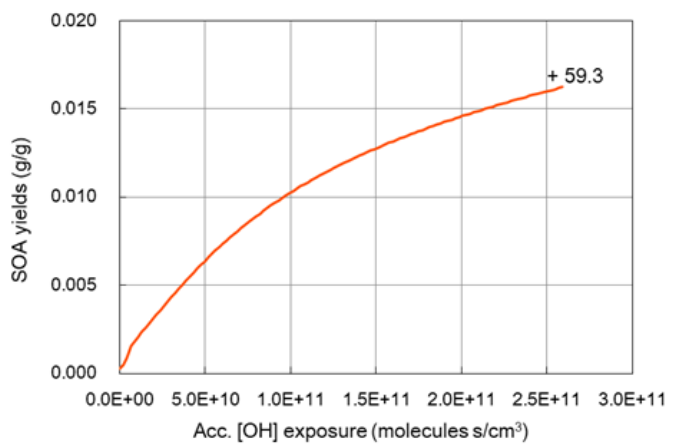

Figure 2-16. SOA aging for IVOC as a function of OH exposure in the CHIMERE VBS scheme.

2.5.5 WRF-Chem MOSAIC

In the WRF-Chem MOSAIC scheme, the aging effect for AVOC and BVOC is not accounted for. The SOA formation from IVOC is parameterized as stepwise OH-oxidation. For the non-oxygen component of condensable gases, a 15% mass increase is assumed for each generation (as per Eq. 16 & Eq. 18). The oxygen component of the condensable gases moves to lower volatility bins without a mass gain (as per Eq. 17 & Eq. 19). No fragmentation or particle-phase oligomerization is considered. Figure 2-17 illustrates the aging results for two scenarios: IVOC with hydrocarbon characteristics (0% oxygen at t=0, representing emissions from diesel sources) and IVOC with 50% oxygen (representing biomass burning emissions). In both instances, the non-fragmentation stepwise aging process in WRF-Chem leads to a huge increase in SOA yields. With an OH exposure of 2.59 x 10^{11} molecule·s/cm^3, the IV-SOA generated from hydrocarbon-like IVOC exceeds 1 g/g, suggesting significant aging effects.

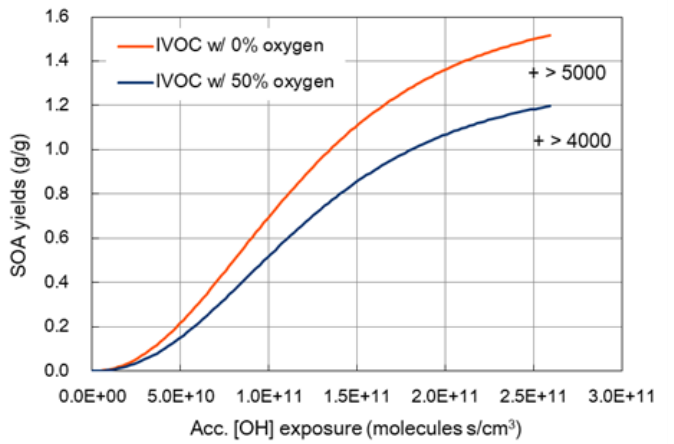

Figure 2-17. SOA aging for IVOC as a function of OH exposure in WRF-Chem MOSAIC scheme.

2.6 Effect of NOx on SOA yields

The impact of NOx on first-generation SOA yields can be seen from Table 2-12 by comparing the SOA yields for high-NOx and low-NOx conditions. There is no NOx-effect on SOA yields in the GEOS-Chem Simple scheme. For all other models/schemes the tendency is for larger SOA yields under low-NOx compared to high-NOx conditions, although there are exceptions. Several schemes have no NOx-effect for SOA from IVOC and/or sesquiterpenes. There are a few cases where the NOx-effect is reversed (i.e., high-NOx yield > low-NOx yield), namely BENZ in SOAP2, IVOC in CRACCM, TERP in CRACCM and SESQ in the GEOS-Chem Complex scheme.

The NOx-effect on the terpene SOA yield in CRACCM merits careful consideration because terpenes are an important SOA precursor in many woodland regions such as Eastern Texas including Houston. The effect of NOx on terpene SOA has been investigated by several experimental studies, as discussed by Sarrafzadeh et al. (2016) and Wildt et al. (2014), with a consistent finding that the SOA yield from terpenes is larger at low NOx than high NOx, i.e., opposite to CRACCM but consistent with the other schemes (except for GEOS-Chem Simple and AERO7 which have with no effect).

2.7 Conclusions and recommendations

2.7.1 Major findings

We reviewed eight SOA formation schemes implemented in five widely used CTMs, namely CAMx, CMAQ, GEOS-Chem, CHIMERE, and WRF-Chem. First-generation SOA yields at different OA concentrations as well as aged SOA yields under atmospheric relevant conditions simulated by each model/scheme were compared. The major findings from this work include:

- **SOA formation schemes:** Models are using diverse approaches to simulate SOA. VBS schemes are more common than two-product schemes but even within VBS schemes the implementation varies widely, especially the treatment of SOA aging processes.
- **SOA schemes are difficult to compare:** Differences in scheme formulation and the large numbers of parameters within each scheme make comparison difficult. Comparing SOA yield curves and SOA yields at a standard OA concentration are effective strategies.
- **First-generation SOA yields:** SOA yields vary widely across schemes. There are even differences between schemes in the ranking of precursors from highest to lowest SOA yield (Table 2-13). Some schemes predict that SOA yields increases with total OA whereas others do not.
- **Effect of NOx on SOA yields:** Schemes are inconsistent on whether NOx increases, decreases or has no effect on SOA yields. The NOx-effect on terpene SOA yield in CRACCM merits consideration because it is directionally opposite to most of the other models/schemes reviewed, and opposite to the experimental findings of Sarrafzadeh et al. (2016) and Wildt et al. (2014) and other experiments. This chemistry is SIP-relevant because terpenes are an important SOA precursor in many woodland regions, such as Eastern Texas including Houston, and NOx emission decreases feature in SIP strategies.

- **SOA aging treatment:** Not all models/schemes consider SOA aging processes. Those that do, represent aging through mechanisms such as OH-oxidation, oligomerization, and hydrolysis. The impact of aging on SOA yields differs among models, with some showing significant increases in SOA mass due to aging, while others exhibit minimal changes.
- **SOA formation from IVOC:** The handling of IVOC varies among models, with some like CMAQ CRACMM distinguishing between different types of IVOC (alkane, aromatic, and oxygenated) and applying specific aging processes to each. The aging of IVOC can lead to either an increase or decrease in SOA mass, depending on the model and the type of IVOC.
- **No objective basis for selecting one scheme over another:** Lack of consistency among the schemes reveals the absence of consensus even though schemes were based on laboratory data. Evaluating model simulations of SOA using ambient measurements is unlikely to resolve this difficulty because large uncertainties in the SOA schemes are confounded with large uncertainties in precursor emissions.
- **Implications for Air Quality Modeling**: The findings underscore the importance of understanding the limitations and strengths of different SOA schemes when applying them to air quality modeling. The choice of model/scheme can significantly influence the predicted SOA concentrations and their evolution over time, which in turn affects air quality forecasts, assessments and regulations.

In summary, this review provides a comprehensive comparison of SOA formation and aging processes in current CTMs, highlighting the variability in SOA yields and the need for careful consideration of model selection and application in the context of air quality studies.

2.7.2 Recommendations for CAMx SOA scheme updates

We found no compelling reason to change the structure of the CAMx SOAP2 scheme that TCEQ is using. More complex schemes contain more parameters (species, reactions, rate constants, condensable gas yields, etc.) that are difficult to specify with confidence. Therefore, adding complexity may be detrimental to an SOA scheme intended for establishing public health policy because there is risk of introducing model responses that are difficult to substantiate. The SOAP2 scheme can describe major attributes of SOA formation that are known with some confidence, including:

- SOA formation is temperature dependent.
- SOA formation depends on oxidant (OH, O_3, NO_3) concentrations that can be modeled using a gas-phase chemical mechanism such as CB7.
- SOA formation depends on total OA concentration although the shape of this relationship is uncertain and varies widely between models/schemes.
- SOA yields can depend on NOx concentration although the magnitude of this relationship remains uncertain.
- The effective yield of SOA in the atmosphere can evolve over time due to “aging” processes that include gas-phase chemical reactions, condensed-phase chemical reactions

and photolysis. SOAP2 includes condensed-phase chemical reaction (polymerization) and photolysis.

We do recommend however that SOA yield parameters for SOAP2 be updated, along with targeted updates to the SOAP2 structure. Due to the wide variation in SOA yields between models/schemes, several sets of updated yield parameters were proposed for testing in CAMx using box models for three Texas cities (Dallas/Fort-Worth, San Antonio, Tyler). Four schemes were tested:

- Existing SOAP2 yield parameters.
- SOA yield parameters for SOAP2 that emulate the AERO7 scheme in CMAQ.
- SOA yield parameters for SOAP2 that emulate the CRACMM scheme in CMAQ.
- SOA yield parameters for SOAP2 that are somewhat like the GEOS-Chem Simple scheme and similar to the scheme evaluated in Nault et al. (2021), i.e., yields of non-volatile SOA with values close to the multi-model means for low-NOx conditions, derived above.

The CMAQ AERO7 and CRACMM schemes were chosen for testing because they were developed by the US EPA to support air quality planning. The Simple-style scheme was chosen since its simplicity has practical advantages regarding implementation, model run-time, and ability to easily connect emissions to SOA formation. Implementation of the new SOA schemes into CAMx and results from box model tests are described in the following section.

3.0 BOX MODEL TESTS OF CAMX SOA UPDATES

3.1 Texas box model scenarios

CAMx box model runs are effectively 1-D simulations with emissions and meteorology that represent a limited area. Although box models are limited in their ability to represent spatial variations in concentrations, they have the advantage of simplicity and are useful to investigate atmospheric chemistry and test new chemical mechanisms. The implementation of CAMx SOA updates were tested using box model applications for three Texas locations: Dallas-Fort Worth (DFW), San Antonio (SAN), and Tyler (TYL) in Northeast Texas. The box model inputs and setup were developed from existing box model scenarios developed in a previous TCEQ project to compare chemical mechanisms for ozone (Ramboll, 2023). Since surface POA emissions were not included in the original model input, they were added by scaling to CO emissions using a scaling factor of 0.2. POA emissions are important because POA enhances SOA. These emissions result in average daily POA concentrations of 1.14 μg/m^3 at Dallas-Fort Worth, 0.42 μg/m^3 at San Antonio, and 0.21 μg/m^3 at Tyler. TCEQ is currently developing emissions with PM which can be used in the box model scenarios when available.

The modeling domains for the CAMx box model used in this study are each 3 x 3 x 2 grid cells (in the x, y, and z dimensions). The center grid cells of each domain, i.e. (2,2,1) and (2,2,2), form a 1-D column with layer 1 representing the planetary boundary layer (PBL) and layer 2 representing a residual layer between the PBL and the CAMx top. The PBL depth varies in time, whereas the top of layer 2 is constant in time at 3,000 m. Horizontal wind speeds in layer 1 are set to zero, preventing horizontal exchange between grid cells and ensuring boundary conditions (BCs) in neighboring cells are not used to compute concentrations. In layer 2, there is a constant horizontal wind speed to purge the layer with a 12-hour lifetime to limit the accumulation of pollutants over time.

Additional details on the box model scenarios and development of model input are described in Ramboll (2023).

3.2 Updated SOA schemes for CAMx

Based on the literature review presented in Section 2.0, three new SOA schemes (i.e., AERO7, CRACMM, SIMPLE) were implemented into CAMx and tested along with the existing SOAP2 scheme in box model scenarios. While the new schemes retain the current SOAP2 structure, SOA yields were changed. Development of the new schemes are described below.

3.2.1 SOAP2 scheme in CAMx

The existing SOAP2 scheme was unchanged in the box model testing. Details about the scheme, including SOA yields, are provided in Section 2.3.1.1.

3.2.2 AERO7 and CRACMM based schemes for CAMx

The analysis of SOA yields as a function of ambient OA concentration (C_{OA}) (performed in Section 2.4) was leveraged to develop SOA schemes for CAMx that are similar to CMAQ's AERO7 and

CRACMM. Curves were fit to the AERO7 and CRACMM data (Figure 2-4 through Figure 2-7) for each SOA precursor using the SOAP2 C* values. The molar-based SOA yields in Table 3-1 through Table 3-4 provide good fits to the AERO7 and CRACMM data and are used in the new CAMx SOA schemes. Figure 3-1 shows an example fit for monoterpenes (TERP). The R^2 values for each fit range from 0.965 to 1.000 and the relative bias ranges from -1.6% to 3.3%. Since CRACMM has different chemical pathways for isoprene compared to CAMx, it was not possible to fit yield data. The values in
Table 3-4 are therefore from the SIMPLE scheme described below.

The NOx effect on the monoterpene SOA yield in the CRACMM based scheme is unusual since the yield is significantly higher under high NOx conditions compared to low NOx. For all other species and schemes, high NOx yields are lower or the same as the low NOx yields. This difference is highlighted in Figure 3-1. The CRACMM trend is also opposite of results from several experimental studies, as discussed by Sarrafzadeh et al. (2016) and Wildt et al. (2014). The implications of this are discussed in context of the box model results in the following sections.

Table 3-1. SOA molar-based yields from anthropogenic precursors under high (top) and low (bottom) NOx conditions for implementation of AERO7 based scheme into CAMx SOAP2

C* [μg/m^3] @ 300K	0	0.31	14
CG/SOA MW [g/mol]	220	150	160
ΔH_{vap} [kJ/mol]	-	18	18
Benzene	0.131	0.00	0.00
	0.004	0.00	0.187
Toluene	0.126	0.00	0.00
	0.00	0.012	0.092
Xylene	0.174	0.00	0.00
	0.005	0.00	0.064
IVOC	1.00	0.00	0.00
	1.00	0.00	0.00

Table 3-2. SOA molar-based yields from biogenic precursors under high (top) and low (bottom) NOx conditions for implementation of AERO7 based scheme into CAMx SOAP2

C* [μg/m^3] @ 300K	0	0.45	26
CG/SOA MW [g/mol]	220	180	180
ΔH_{vap} [kJ/mol]	-	85	65
Isoprene	0.00	0.008	0.0038
	0.00	0.008	0.0038
Monoterpene	0.031	0.038	0.166
	0.031	0.038	0.166
Sesquiterpene	0.00	0.068	1.417
	0.00	0.068	1.417

Table 3-3. SOA molar-based yields from anthropogenic precursors under high (top) and low (bottom) NOx conditions for implementation of CRACMM based scheme into CAMx SOAP2

C* [μg/m³] @ 300K	0	0.31	14
CG/SOA MW [g/mol]	220	150	160
ΔH_{vap} [kJ/mol]	-	89	81
Benzene	0.142	0.141	0.00
	0.082	0.001	0.00
Toluene	0.126	0.160	0.00
	0.044	0.00	0.00
Xylene	0.005	0.304	0.778
	0.043	0.002	0.00
IVOC	0.00	0.117	0.583
	0.00	0.190	0.583

Table 3-4. SOA molar-based yields from biogenic precursors under high (top) and low (bottom) NOx conditions for implementation of CRACMM based scheme into CAMx SOAP2

C* [μg/m³] @ 300K	0	0.45	26
CG/SOA MW [g/mol]	220	180	180
ΔH_{vap} [kJ/mol]	-	85	81
Isoprene	0.01	0.00	0.00
	0.01	0.00	0.00
Monoterpene	0.028	0.00	0.00
	0.226	0.00	0.00
Sesquiterpene	0.009	0.963	0.873
	0.00	0.034	0.351

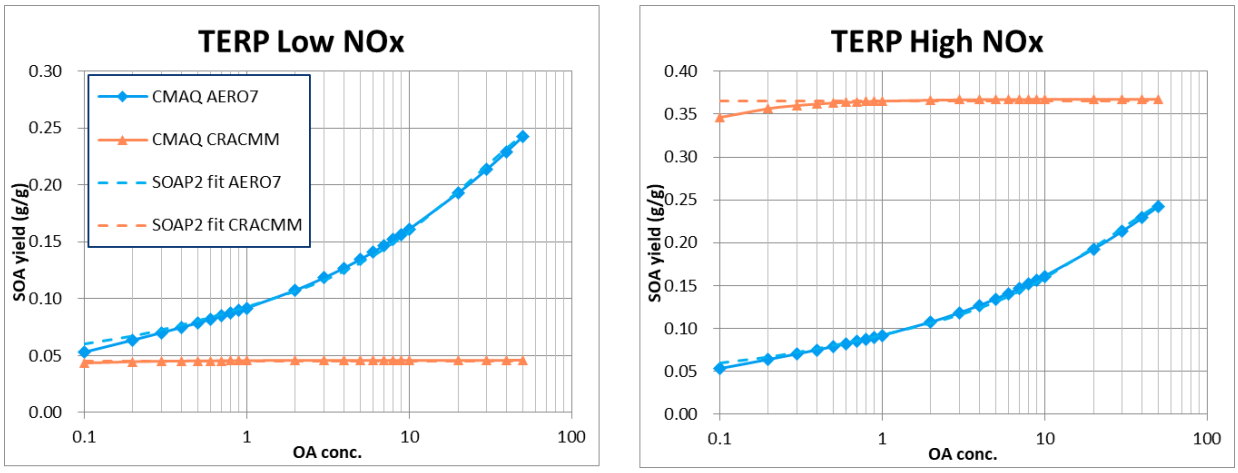

Figure 3-1. SOA yields for terpenes under low and high NOx conditions for the AERO7 and CRACMM schemes (solid lines), and the corresponding fit (dashed lines) for the new schemes implemented in CAMx SOAP2.

3.2.3 SIMPLE scheme for CAMx

The SIMPLE scheme assumes all SOA formed is non-volatile. This is similar to the GEOS-Chem SIMPLE scheme and the SOA scheme evaluated by Nault et al. (2021). The advantages to this scheme are that it is straightforward to implement, particularly with CAMx's source apportionment probing tools, and behaves more predictably and without nonlinearities present in other schemes. The SOA yields for the CAMx SIMPLE scheme are provided in Table 3-5 and Table 3-6.

The SOA yields for biogenic precursors are based on the literature review described in Section 2.0. The average SOA yield for each precursor species was calculated for an OA concentration (C_{OA}) of 10 µg/m^3 across different models (Table 2-12). 10 µg/m^3 is a relevant C_{OA} to ambient air quality and often used as a reference for comparison. The high NOx SOA yields for isoprene, monoterpenes, and sesquiterpenes are the average yields from the following models/schemes: CAMx VBS, CMAQ AERO7, CMAQ CRACMM, GEOS-Chem Complex, CHIMERE VBS, and WRF-Chem MOSAIC. CAMx SOAP2 yields were excluded from the average since SOA aging is assumed in the yield values. Under low NOx conditions, the multi-model average SOA yields for the biogenic species are 25-55% larger than the high NOx yields. Considering this and the work by Sarrafzadeh et al. (2016) and Wildt et al. (2014), the low NOx yields in the new SIMPLE scheme were set at 30% larger than the high NOx yields. This ensures a similar SOA behavior for all biogenic precursors at different NOx levels.

The SOA yields for anthropogenic precursors are based on work by Seltzer et al. (2021). High NOx yields for benzene, toluene, and xylene are provided by Seltzer et al. (2021) and the IVOC yield is calculated by averaging the yields of the 15-carbon species (including alkanes and PAHs) since IVOC is a 15-carbon species in CAMx. The yields for toluene and xylene are comparable to the multi-model average from Ramboll's literature review, whereas the yields for benzene and IVOC are higher than the multi-model average. Since benzene, toluene, and xylene are all aromatic species with similar chemistry, they should behave similarly under varying NOx conditions. The low NOx yields are therefore assumed to be two times higher than the high NOx yields for the aromatics. For IVOC, low NOx yields are assumed to be 30% higher than the high NOx yields. Both scaling factors are consistent with the literature review results.

Table 3-5. SOA molar-based yields from anthropogenic precursors under high (top) and low (bottom) NOx conditions for implementation of the SIMPLE scheme into CAMx SOAP2

C* [µg/m^3] @ 300K	0	0.31	14
CG/SOA MW [g/mol]	220	150	160
ΔH_{vap} [kJ/mol]	-	-	-
Benzene	0.20	0.00	0.00
	0.10	0.00	0.00
Toluene	0.12	0.00	0.00
	0.06	0.00	0.00
Xylene	0.09	0.00	0.00
	0.04	0.00	0.00
IVOC	1.00	0.00	0.00
	1.00	0.00	0.00

Table 3-6.SOA molar-based yields from biogenic precursors under high (top) and low (bottom) NOx conditions for implementation of the SIMPLE based scheme into CAMx SOAP2

C* [μg/m^3] @ 300K	0	0.45	26
CG/SOA MW [g/mol]	220	180	180
ΔH_{vap} [kJ/mol]	-	-	-
Isoprene	0.01	0.00	0.00
	0.01	0.00	0.00
Monoterpene	0.10	0.00	0.00
	0.07	0.00	0.00
Sesquiterpene	0.40	0.00	0.00
	0.32	0.00	0.00

Since the SIMPLE scheme only forms non-volatile SOA from each precursor species, it is possible to calculate the emission-weighted SOA potential of precursors. This is done by multiplying the average daily emissions by the molar SOA yield. Results for each city, using average daily emissions over the box modelling periods, are shown in Figure 3-2 through Figure 3-4. The importance of SOA yield values is evident when comparing the SOA potential to the emissions. Isoprene emissions are dominant at each location, however the relative contribution to the SOA potential is much smaller due to the relatively low SOA yield. The opposite trend is seen for IVOC, with a much larger contribution to SOA potential compared the emissions.

At DFW and SAN, IVOC produces the majority (over 70%) of total SOA under both high and low NOx conditions, due to the relatively high emissions and high SOA yield. Toluene is the next most important SOA precursor, followed by isoprene. At TYL, the biogenic versus anthropogenic emissions are much higher than at the other two locations which is evident in Figure 3-4. Isoprene is the dominant SOA precursor, contributing about 35% to the total SOA potential. IVOC (25-32% of SOA potential) and benzene (20% of SOA potential) are also important precursors for SOA formation at TYL. More SOA is produced under low NOx conditions at each of the locations due to the increased SOA yields.

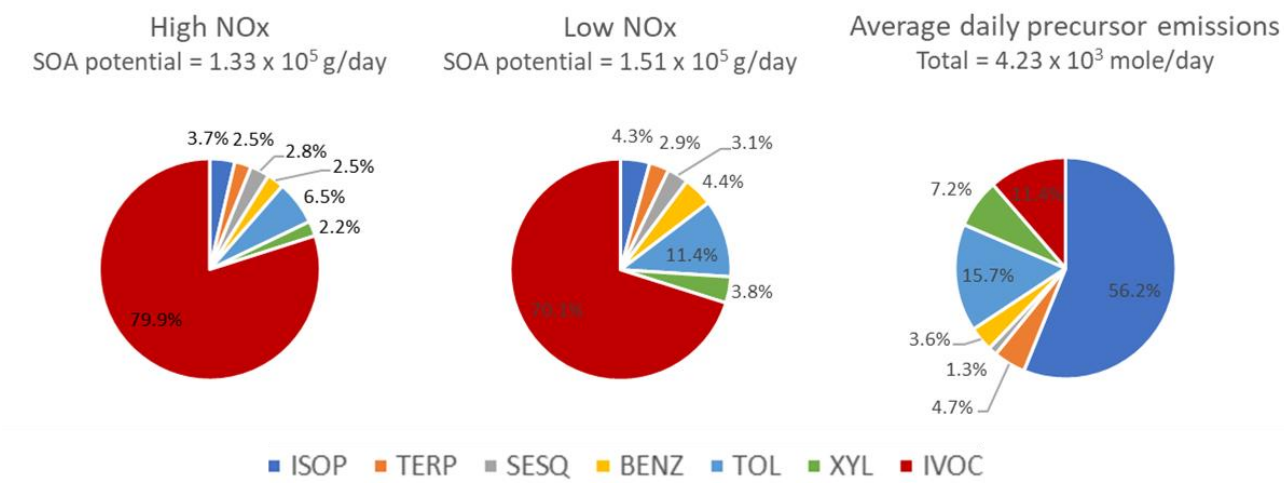

Figure 3-2. Emission-weighted SOA potential of precursor species under high (left) and low (middle) NOx conditions at DFW, along with the contribution of precursors to the average daily emissions (right).

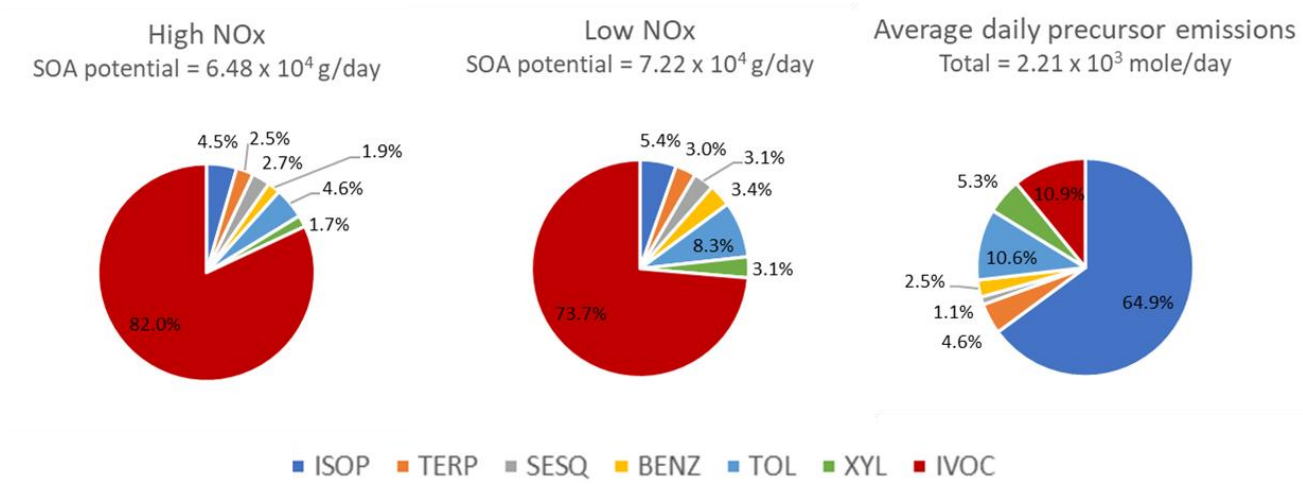

Figure 3-3. Emission-weighted SOA potential of precursor species under high (left) and low (middle) NOx conditions at SAN, along with the contribution of precursors to the average daily emissions (right).

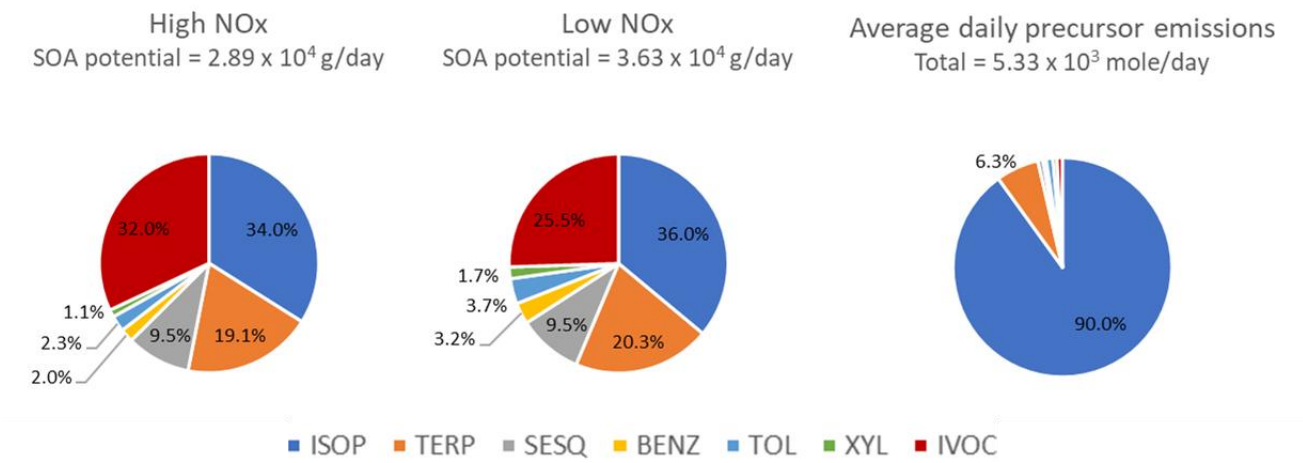

Figure 3-4. Emission-weighted SOA potential of precursor species under high (left) and low (middle) NOx conditions at TYL, along with the contribution of precursors to the average daily emissions (right).

3.3 Box model results

3.3.1 Base case emissions scenario

Base case simulations were performed to compare chemical species concentrations at each location between four different SOA schemes: SOAP2, AERO7, CRACMM, and SIMPLE. Figure 3-5 shows the diurnal profiles of hourly average concentrations for total SOA, which is the sum of the 6 SOA species in CAMx (SOA1, SOA2, SOA3, SOA4, SOPA, SOPB). Table 3-7 presents average concentrations of individual SOA species and total SOA for each location and SOA scheme. The averages are calculated for days 2 through 5 of the model run since the first day is considered model spin-up.

SOA concentrations are highest at DFW, followed by TYL and then SAN. Each location and scheme shows a diurnal profile of SOA increasing throughout the day and overnight and a sharp decline in the early morning around 6:00 am when the PBL depth starts to increase. DFW and SAN show similar trends between the SOA schemes, with the highest modeled concentrations from SIMPLE and AERO7 and the lowest from CRACMM. At TYL, there is a smaller spread among the different schemes compared to DFW and SAN. SOAP2 and CRACMM have the highest concentrations overnight, which is opposite of the other locations, and SIMPLE and CRACMM are the highest during the day. TYL also shows differences in the maximum and minimum average SOA concentrations, as seen in Table 3-7. At DFW and SAN, SIMPLE and CRACMM respectively predict the highest and lowest total SOA concentrations, while at TYL, CRACMM has the highest average concentration and AERO7 has the lowest.

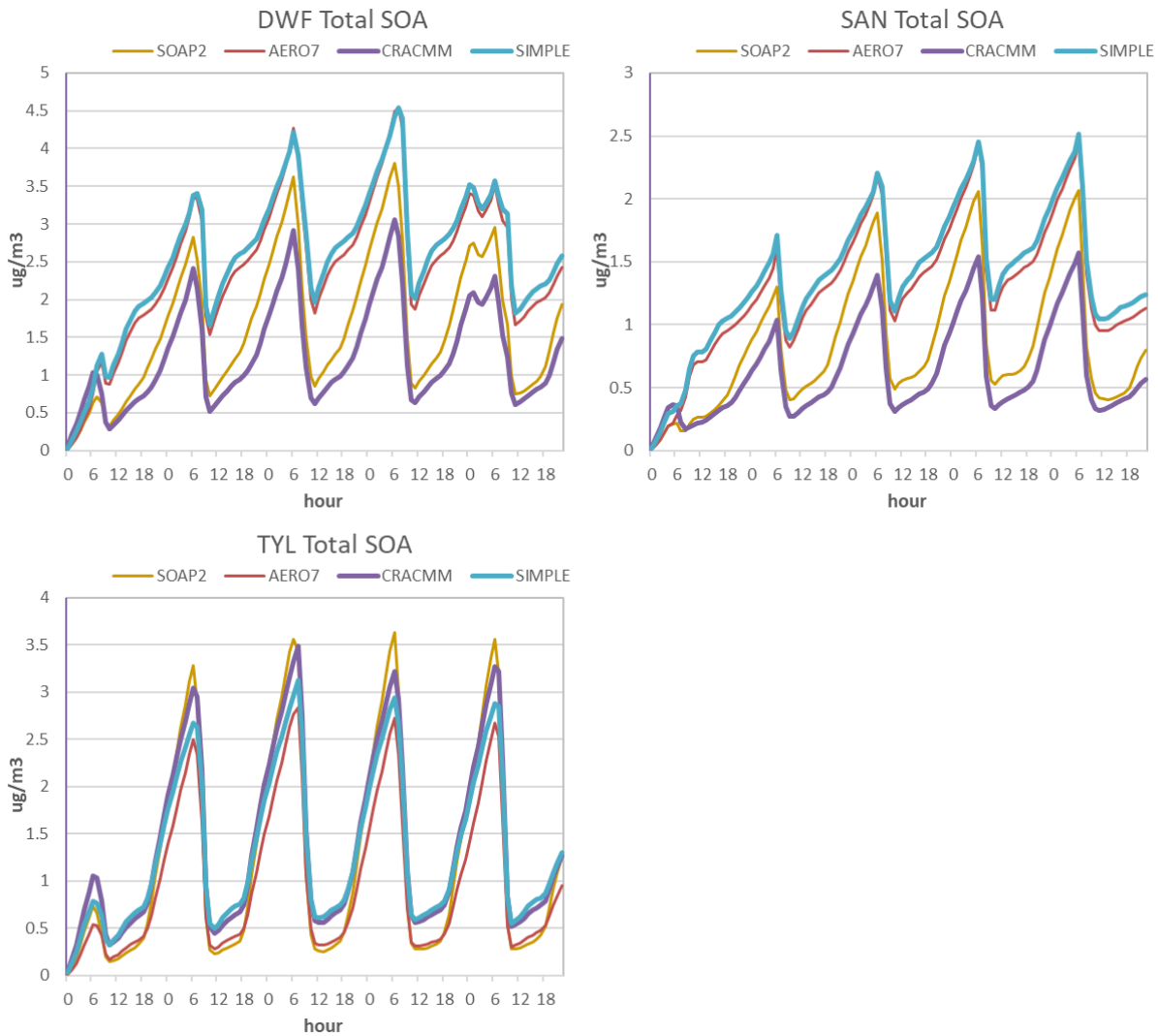

Figure 3-5. Diurnal profiles of total SOA (µg/m^3) from the 5-day box model base simulations at DFW, SAN, and TYL.

Table 3-7. Secondary organic aerosol (SOA) concentrations (μg/m³) averaged over days 2 through 5 of base model simulations for each SOA scheme.

	SOAP2	AERO7	CRACMM	SIMPLE
DFW				
SOA1	0.10	0.04	**0.14**	0.00
SOA2	**0.79**	0.01	0.36	0.00
SOA3	0.08	**0.12**	0.00	0.00
SOA4	**0.21**	0.18	0.00	0.00
SOPA	0.53	2.28	0.28	**2.44**
SOPB	0.17	*0.12*	**0.65**	0.45
Total SOA	1.89	2.75	1.43	**2.88**
SAN				
SOA1	0.05	0.01	**0.06**	0.00
SOA2	**0.40**	0.01	0.18	0.00
SOA3	0.04	**0.05**	0.00	0.00
SOA4	**0.12**	0.10	0.00	0.00
SOPA	0.29	1.25	0.13	**1.31**
SOPB	0.09	0.06	**0.33**	0.25
Total SOA	0.98	1.47	0.70	**1.56**
TYL				
SOA1	**0.02**	0.00	**0.02**	0.00
SOA2	**0.12**	0.00	0.07	0.00
SOA3	**0.18**	0.17	0.00	0.00
SOA4	**0.54**	0.39	0.00	0.00
SOPA	0.10	0.28	0.07	**0.30**
SOPB	0.47	0.31	**1.40**	1.19
Total SOA	1.43	1.16	**1.56**	1.49

Notes: Maximum values are bolded and minimum values are underlined. There is no formation of SOA1-4 in the SIMPLE scheme, so it is excluded from the max/min determination for these species. Total SOA is the sum of the 6 individual SOA species. The first day of each simulation is considered model spin-up so is excluded from the average calculation.

3.3.2 Scaled emissions scenario

The response of SOA concentrations to varying anthropogenic VOC and NOx emissions was investigated by performing a matrix of 100 box simulations for each location and SOA scheme. This provides a comparison of the SOA schemes for both a range of atmospheric concentrations and a range of VOC/NOx ratios. The matrix simulations were based on weekday anthropogenic emission rates for all dates. The biogenic emissions were not scaled and varied by date, similar to the base runs. The scaling factors applied to the base run anthropogenic VOC emissions range from 0.1 to 1.0 in increments of 0.1, and the scaling factors applied to the anthropogenic NOx emissions range from 0 to 9 in increments of 1. An additional model simulation with NOx emissions

decreased by 50% was also performed to study how SOA changes as NOx is decreased, which is important since air quality plans will likely aim to reduce NOx emissions.

SOA response surface plots for 24-hour average SOA were constructed using results from the matrix simulations and are shown in Figure 3-6 through Figure 3-8. For reference, ozone response surfaces are provided in Figure 3-9 to aid in understanding which parts of the response surface are considered NOx- or VOC-limited for ozone. The response surfaces for each location were similar in shape for each simulation day so only a single day is shown in the figures. Note that the concentration scale is different for each scheme.

At DFW, the total SOA concentration decreases as the NOx emissions are increased compared to the base emissions (NOx scaling factors 2 through 9) for all SOA schemes except CRACMM. CRACMM predicts nearly no impact or a slight increase to SOA as NOx increases from the low to mid scaling factors. A decrease in SOA does not occur until the NOx emissions are increased by about a factor of 7 or greater. CRACMM also predicts the lowest SOA concentrations across all scaling factors. AERO7 and SIMPLE are very similar in both shape and magnitude. For each scheme, SOA concentrations decrease as the VOC emissions decrease.

The response surface plots for SAN show similar trends to DFW, but the decrease in SOA as NOx increases is less prominent, especially in the CRACMM scheme where SOA levels are nearly unaffected by NOx factors greater than 1. At TYL, the response surface plots are similar for AERO7 and SIMPLE and SOA remains nearly constant at NOx scales greater than 1. SOAP2 also shows a small impact on SOA as NOx varies. CRACMM shows a much bigger response to NOx changes, with SOA increasing as NOx increases. SOA concentrations are minimally affected by varying VOC in all schemes.

The ozone response surface plots for daily maximum 1-h (MDA1) O_3 are provided in Figure 3-9 for each location. Since the SOA scheme has only a minor impact on O_3, only the SOAP2 results are shown. The base case simulations (VOC and NOx scaling factors of 1) are in a NOx-limited regime where O_3 is much more responsive to NOx emission reductions than anthropogenic VOC emission reductions. When starting from the base case, O_3 concentrations change significantly as NOx varies, whereas O_3 is nearly unaffected by varying VOC. TYL was still under NOx-limited conditions at a NOx scaling factor of 9.0, which is evident by the fact that O_3 does not decrease with increasing NOx factor. At each location, the O_3 response surface plots from the different SOA schemes are nearly identical.

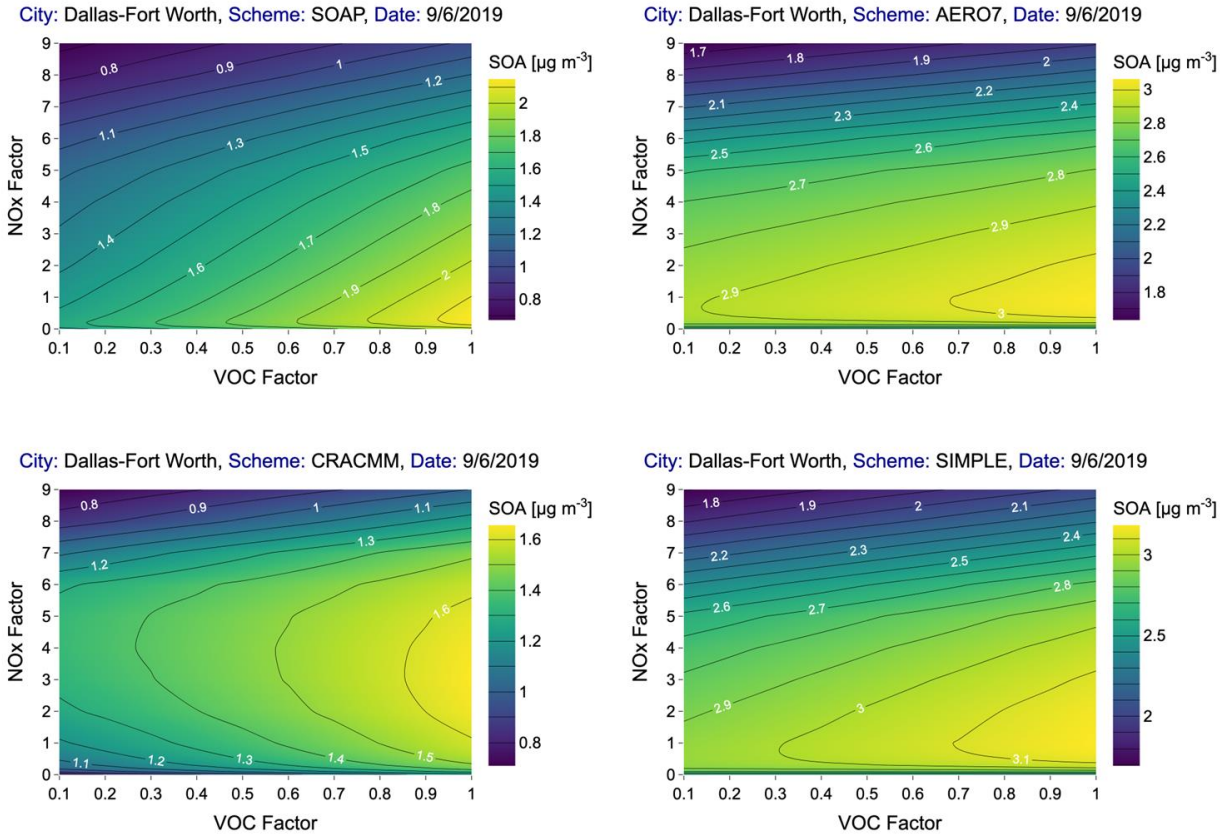

Figure 3-6. SOA response surface (24-hr average, µg/m³) to varying anthropogenic NOx and VOC emissions for DFW for four different SOA schemes. NOx and VOC scaling factors of 1 are the base case simulation. Note that the concentration scale is different for each scheme.

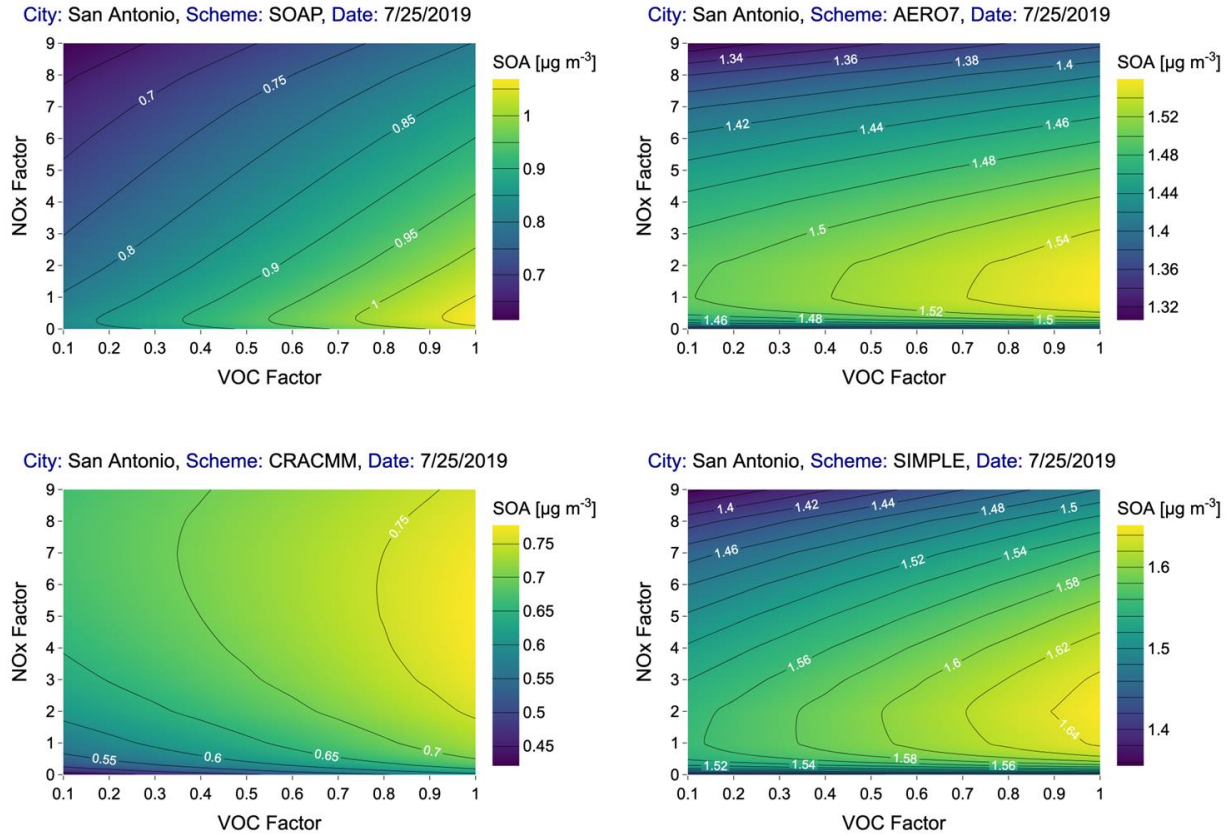

Figure 3-7. SOA response surface (24-hr average, μg/m³) to varying anthropogenic NOx and VOC emissions for SAN for four different SOA schemes. NOx and VOC scaling factors of 1 are the base case simulation. Note that the concentration scale is different for each scheme.

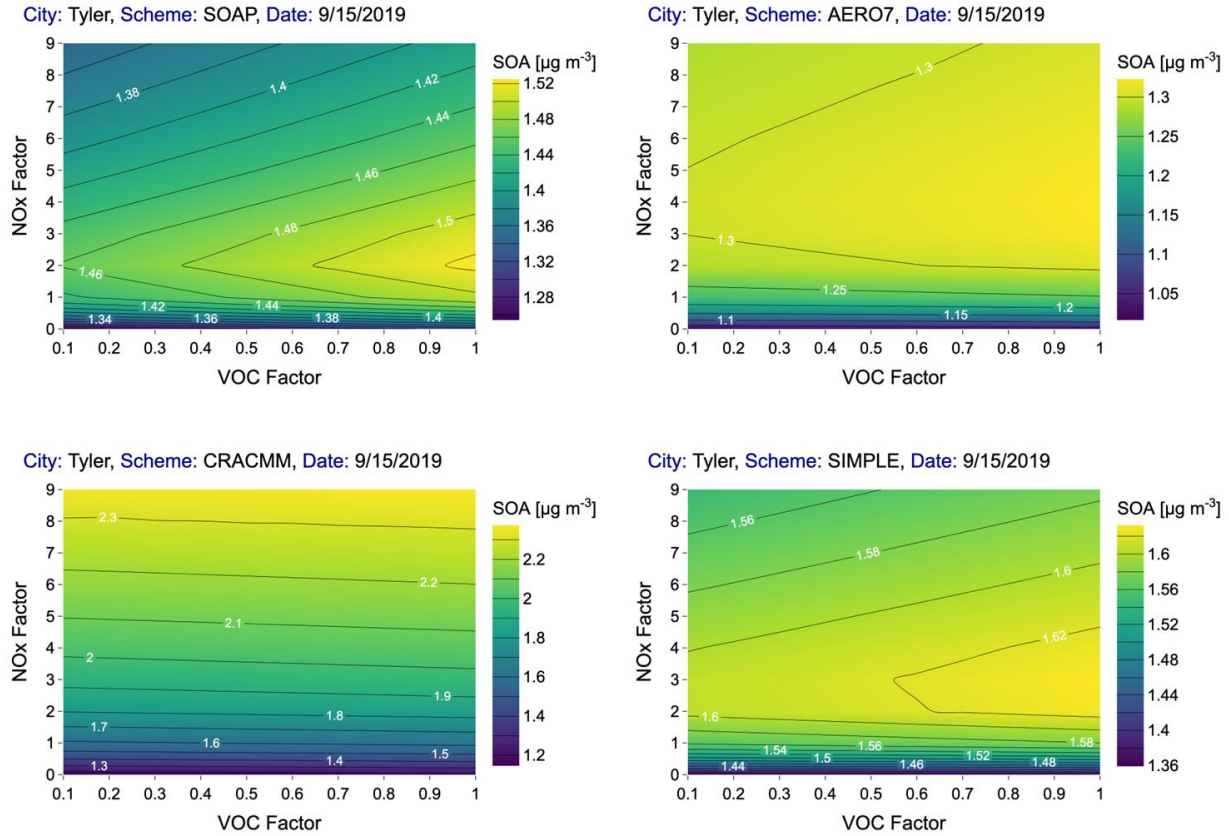

Figure 3-8. SOA response surface (24-hr average, µg/m³) to varying anthropogenic NOx and VOC emissions for TYL for four different SOA schemes. NOx and VOC scaling factors of 1 are the base case simulation. Note that the concentration scale is different for each scheme.

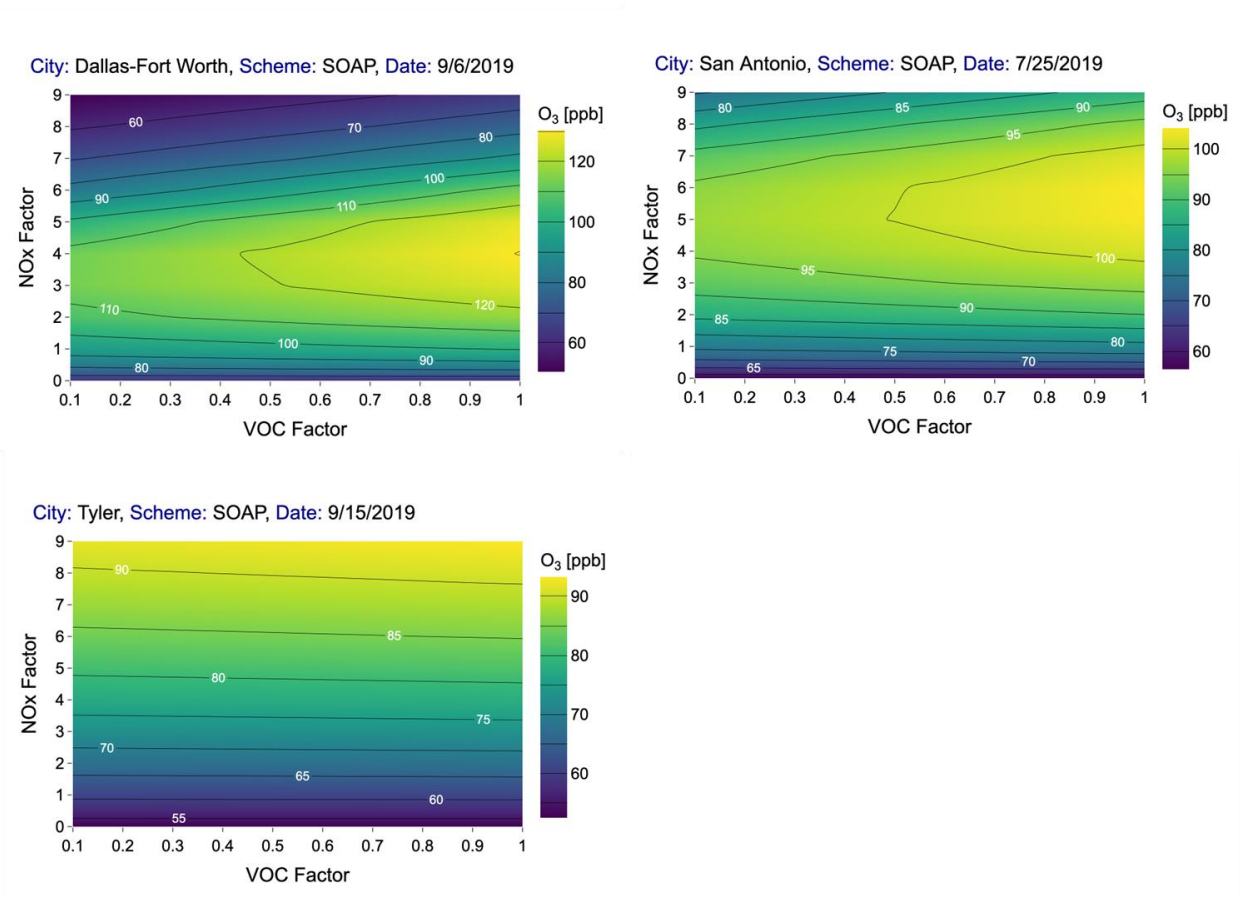

Figure 3-9. Ozone response surface (MDA1, ppb) to varying anthropogenic NOx and VOC emissions for DFW, SAN, and TYL for the SOAP2 simulation. NOx and VOC scaling factors of 1 are the base case simulation. Note that the concentration scale is different for each scheme.

Understanding how SOA responds to NOx emission reductions from the base case is relevant to near-term air quality planning because existing strategies are expected to reduce NOx emissions, e.g., cleaner vehicles. Model simulations were performed with NOx emissions reduced by 50% and the impact of this reduction on the total SOA, total anthropogenic SOA (ASOA), and total biogenic SOA (BSOA) concentrations is shown in Table 3-8. Concentrations presented are averages over days 2 through 5 of each simulation. Shaded cells in the table highlight cases where the NOx reduction causes a decrease in SOA concentrations.

For all model scenarios, reducing NOx causes an increase in ASOA concentrations, with SOAP2 predicting the largest increase. The SIMPLE scheme predicts the smallest increase in ASOA at DFW and SAN and CRACMM predicts the smallest increase at TYL.

At DFW and SAN, reducing NOx also leads to an increase in BSOA concentrations for all SOA schemes except CRACMM. Similar to ASOA, SOAP2 predicts the largest increase in BSOA. The CRACMM results are due to the monoterpene SOA yields which respond to NOx differently than other schemes and from experimental results, decreasing rather than increasing under low NOx

conditions. The large decrease in BSOA at DFW and SAN for the CRACMM simulations leads to a decrease in total SOA, which is again opposite from the other schemes.

At TYL, each SOA scheme predicts a decrease in BSOA and total SOA, with the largest decreases in the CRACMM simulation. Compared to DFW and SAN, TYL has higher biogenic versus anthropogenic emissions which is evident in the higher concentrations of BSOA. The differences in the response of the SOA schemes to NOx reduction at TYL versus DFW and SAN are likely due to differences in biogenic chemistry at various NOx/VOC ratios.

Table 3-8. Average concentrations (μg/m³) of secondary organic aerosol (SOA) species over days 2 through 5 for the base and reduced NOx model simulations.

	SOAP2			AERO7			CRACMM			SIMPLE		
	Base	50% NOx	Diff (%)	Base	50% NOx	Diff (%)	Base	50% NOx	Diff (%)	Base	50% NOx	Diff (%)
DFW												
ASOA	1.34	1.48	9.6%	2.34	2.38	1.9%	0.78	0.81	3.5%	2.44	2.45	0.6%
BSOA	0.42	0.48	12.2%	0.41	0.42	0.4%	0.65	0.59	-10.7%	0.45	0.46	2.4%
Total SOA	1.76	1.96	10.3%	2.75	2.80	1.6%	1.43	1.40	-2.5%	2.88	2.91	0.9%
SAN												
ASOA	0.73	0.75	3.7%	1.26	1.29	2.1%	0.37	0.38	2.3%	1.31	1.33	1.0%
BSOA	0.25	0.26	3.7%	0.21	0.21	0.3%	0.33	0.30	-10.0%	0.25	0.25	1.8%
Total SOA	0.98	1.02	3.7%	1.47	1.50	1.8%	0.70	0.68	-3.2%	1.56	1.58	1.1%
TYL												
ASOA	0.24	0.25	4.4%	0.28	0.31	9.9%	0.16	0.17	1.0%	0.30	0.32	8.5%
BSOA	1.19	1.14	-4.1%	0.87	0.82	-6.2%	1.40	1.24	-12.6%	1.19	1.14	-4.4%
Total SOA	1.43	1.40	-2.5%	1.16	1.14	-1.8%	1.56	1.41	-11.0%	1.49	1.46	-1.5%

Notes: Anthropogenic SOA (ASOA) is the sum of SOA1, SOA2, and SOPA; Biogenic SOA (BSOA) is the sum of SOA3, SOA4, and SOPB; Total SOA is the sum of all 6 SOA species. Shading indicates a decrease in SOA concentrations in the reduced NOx model runs compared to the base runs.

3.4 Recommendations for 3-D CAMx testing

Three SOA schemes were implemented into CAMx and tested alongside the existing SOAP2 scheme using box model simulations for three Texas locations. The SOAP2, AERO7, and SIMPLE schemes behaved similarly to variations in VOC and NOx emissions. AERO7 and SIMPLE also predicted similar SOA concentrations in each of the model simulations. The response of SOA to varying NOx was noticeably different in the CRACMM runs compared to the other schemes as was seen in the surface response plots. In particular, CRACMM predicted a decrease in SOA from biogenic precursors at each location when NOx was reduced by 50%, which led to a decrease in the total SOA concentrations. Since this behavior was unique to CRACMM in the box model tests, we do not recommend implementing this scheme in CAMx. Note that although the schemes referred to here as AERO7 and CRACMM differ from the original implementations in CMAQ, we expect the CAMx implemented versions tested here to have similar responses to emission changes as the original CMAQ schemes. We instead proceeded with 3-D testing of the SIMPLE and AERO7 schemes in CONUS 12 km simulations based on the EPA 2016 platform which is described in the following section. The new AERO7 scheme implemented in CAMx was renamed “COMPLEX” since it differs from AERO7 in CMAQ.

4.0 CAMX 3-D SIMULATIONS WITH SOA UPDATES

4.1 CAMx modeling platform

Following box model testing, two of the new SOA schemes were recommended for 3-D testing in simulations covering the continental US (CONUS) with 12 km grid resolution. The new schemes retain the existing structure of the current CAMx scheme, SOAP2, but update the SOA yield parameters. The first scheme, referred to as "SIMPLE", assumes all SOA formed is non-volatile. This scheme is similar to that used by Nault et al. (2021) who evaluated model predicted anthropogenic SOA concentrations against atmospheric measurements and found that a simple non-volatile SOA scheme performed better in many cases than more complicated volatility basis set (VBS) SOA schemes. The second recommended scheme, referred to as "COMPLEX", emulates the AERO7 scheme in the EPA's Community Multiscale Air Quality (CMAQ; Appel et al., 2021) model. More details on the development of the SIMPLE and COMPLEX schemes are provided in the previous section. These schemes were tested alongside the existing SOAP2 scheme in 3-D CAMx simulations.

CAMx v7.2 (Ramboll, 2022) was used to model the month of July, 2016 following a 10-day spin-up period. The three model scenarios (SOAP2, SIMPLE and COMPLEX) were run using input data from EPA's 2016v3 modeling platform (EPA, 2023) and the CAMx options shown in Table 4-1. The CB7r1 chemical mechanism (Ramboll, 2023) was used in these runs, consistent with the previous box modeling. All terpenes, including α-pinene, were assigned to model species TERP in the 2016v3 platform emission files, which means that the CB7r1 model species APIN was effectively unused in these simulations.

Table 4-1. CAMx modeling setup in 2016v3 Modeling Platform.

Science Process	Option
Advection Solver	PPM
Vertical Advection solver	PPM
Chemistry Solver	EBI
Dry Deposition	Zhang03
Bi-directional Ammonia Treatment	False
Wet Deposition	True
Vertical Diffusion	ACM2
Inline Iodine Emissions	False
Chemical Mechanism	CB7r1
Stratospheric Ozone Profile	False
Super Stepping	True

4.2 Model performance evaluation (MPE)

The 2016 CAMx modeled data were evaluated against observational organic carbon (OC) data for the month of July, 2016 from the rural Interagency Monitoring of Protected Visual Environments (IMPROVE) and the urban Chemical Speciation Network (CSN) monitoring networks. Total $PM_{2.5}$ mass was also evaluated using data from CSN, IMPROVE, and the Air Quality System (AQS). The

analysis was conducted using the Atmospheric Model Evaluation Tool (AMET) version 1.4 (Appel et al. 2011; UNC 2008). The monitoring data used in the evaluation were obtained from AMET's processed multi-year data repository. Statistical measures used in the analysis included normalized mean bias (NMB), normalized mean error (NME), fractional bias (FB), fractional error (FE), and correlation coefficient (r). Table 4-2 provides the equations of each metric, where P and O are the predicted and observed concentrations, respectively, along with NMB and NME performance criteria proposed by Emery et al. (2016) for OC.

Table 4-2. Model statistical performance metrics and criteria.

Statistical Measure	**Mathematical expression**	**OC Performance criteria**
Normalized Mean Bias (NMB) (%)	$NMB = \frac{\sum_N (P - O)}{\sum_N O}$	<±50%
Normalized Mean Error (NME) (%)	$NME = \frac{\sum_N \lvert (P - O) \rvert}{\sum_N O}$	<65%
Fractional Bias (FB) (%)	$FB = \frac{2}{N} \sum_N \frac{(P - O)}{(P + O)}$	
Fractional Error (FE) (%)	$FE = \frac{2}{N} \sum_N \frac{(P - O)}{(P + O)}$	
Correlation coefficient (r)	$r = \frac{\sum_N [(P - \bar{P}) \times (O - \bar{O})]}{\sqrt{\sum_N (P - \bar{P})^2 \times \sum_N (O - \bar{O})^2}}$	

Table 4-3 lists the domain-wide July, 2016 monthly statistics for OC for the three scenarios at CSN and IMPROVE monitors. CAMx OA concentrations, including POA and the six SOA species (SOA1, SOA2, SOA3, SOA4, SOPA, SOPB), were converted to OC and summed to total OC using Eq. 20.

$$OC = POA + \frac{SOA1}{2} + \frac{SOA2}{2} + \frac{SOA3}{1.7} + \frac{SOA4}{1.7} + \frac{SOPA}{2.1} + \frac{SOPB}{2.1} \qquad \text{Eq. 20}$$

All three scenarios show similar performance, with NMB ranging from approximately 25 to 30% for CSN sites and -17 to -8% for IMPROVE sites. NME ranges from 50 to 52% for CSN and 60 to 62% for IMPROVE. SIMPLE predicted slightly higher OC concentrations compared to SOAP2 and COMPLEX, which is closer to IMPROVE observations (lower bias/error) but farther from CSN observations (higher bias/error).

Table 4-3. Domain wide model performance for organic carbon (OC) at CSN and IMPROVE monitors for July, 2016.

Scenario	No. of Obs	Mean Obs (μg/m³)	Mean Model (μg/m³)	NMB (%)	NME (%)	FB (%)	FE (%)	RMSE (μg/m³)	r
CSN									
SOAP2	1002	1.86	2.34	25.8	52.8	13.4	44.9	1.39	0.48
COMPLEX	1002	1.86	2.32	24.9	50.8	12.7	43.4	1.38	0.50
SIMPLE	1002	1.86	2.42	30.4	52.8	18.4	43.9	1.40	0.50
IMPROVE									
SOAP2	1406	1.06	0.96	-9.63	62.2	-23.1	57.7	2.98	0.12
COMPLEX	1406	1.06	0.88	-17.1	61.0	-31.9	60.9	2.97	0.13
SIMPLE	1406	1.06	0.98	-8.04	59.9	-18.1	54.2	2.96	0.13

Figure 4-1 shows the scatter plots of all three scenarios for CSN (top panel) and IMPROVE (bottom panel). Overall, all three scenarios show similar scatter around the 1:1 line, with under prediction (negative NMB) at IMPROVE sites and over prediction (positive NMB) at CSN sites. At CSN sites, both COMPLEX and SIMPLE slightly increased the over prediction at a few sites for the upper range of OC values (8-10 μg/m^3). However, at IMPROVE sites, SIMPLE reduced the under prediction and COMPLEX increased the under prediction compared to SOAP2.

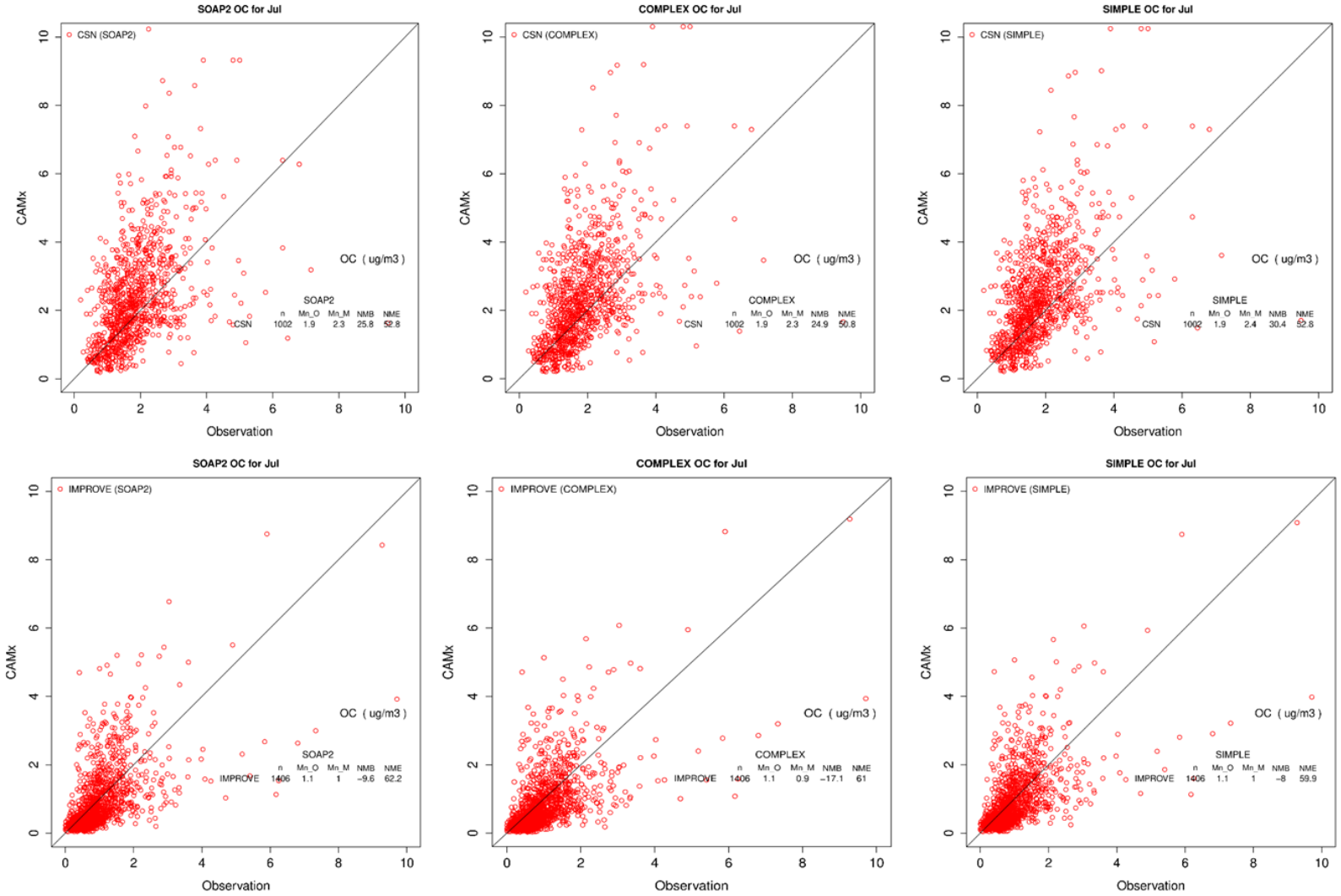

Figure 4-1. Scatter plots of observed vs modeled organic carbon (OC) for SOAP2 (left), COMPLEX (middle) and SIMPLE (right) at CSN (top) and IMPROVE (bottom) sites.

Figure 4-2 and Figure 4-3 display spatial maps of site-specific July, 2016 average NMB for OC across the 12 km CONUS domain at CSN and IMPROVE sites, respectively. Sites that are colored in grey are within the ±50% OC performance criteria. All three scenarios show a similar NMB trend spatially, with some under predictions across the western US sites, more neutral performance in the central US, and over predictions in the eastern US. At a few western IMPROVE sites, COMPLEX increased the under prediction and SIMPLE reduced the under prediction when compared to SOAP2. In the Texas region, SIMPLE and COMPLEX had similar performance to SOAP2 at the two CSN sites in the eastern part of the state and the under predication was mitigated at the site within El Paso. SIMPLE reduced the under prediction slightly at the two western Texas IMPROVE sites.

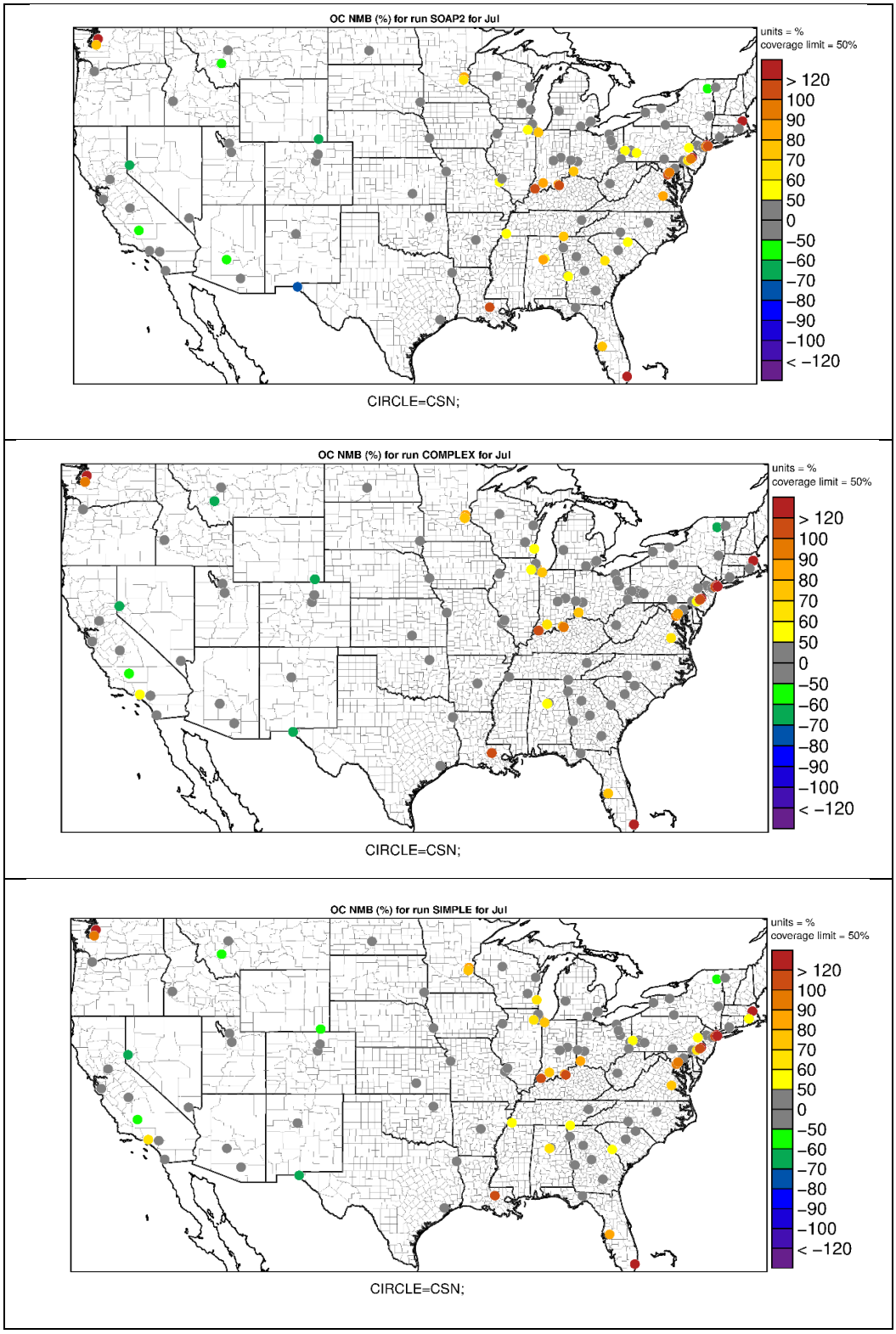

Figure 4-2. Spatial plot showing the normalized mean bias (NMB) metric at CSN sites for OC across the 12 km CONUS2 domain for July, 2016 for SOAP2 (top), COMPLEX (middle), and SIMPLE (bottom).

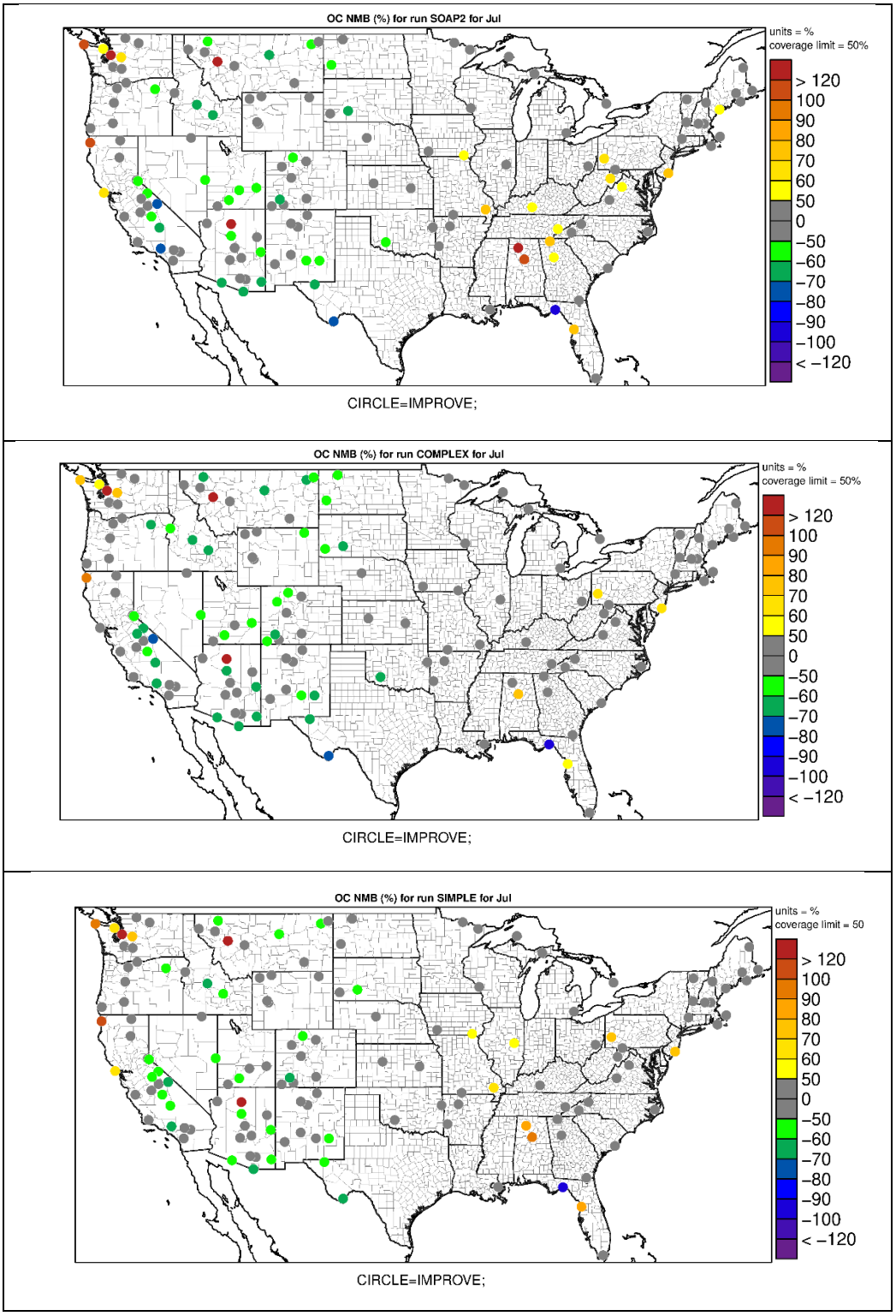

Figure 4-3. Spatial plot showing the normalized mean bias (NMB) metric at IMPROVE sites for OC across the 12 km CONUS domain for July, 2016 for SOAP2 (top), COMPLEX (middle), and SIMPLE (bottom).

Figure 4-4 presents time series of observed and simulated OC for July, 2016 at three representative monitoring sites in Texas. Overall, the three modeling scenarios behaved similarly. All three model scenarios underpredicted OC at the Big Bend IMPROVE site but captured the general trend well. At the CSN sites at Deer Park (482011039) and Karnak (482030002), the modeled OC was similar to observations in the first half of the month but higher in the later part of July. As mentioned before, SIMPLE generally shows slightly higher concentrations than COMPLEX and SOAP2, reducing some of the OC under prediction at the IMPROVE site but increasing the over prediction at the Karnak CSN site in the later part of July.

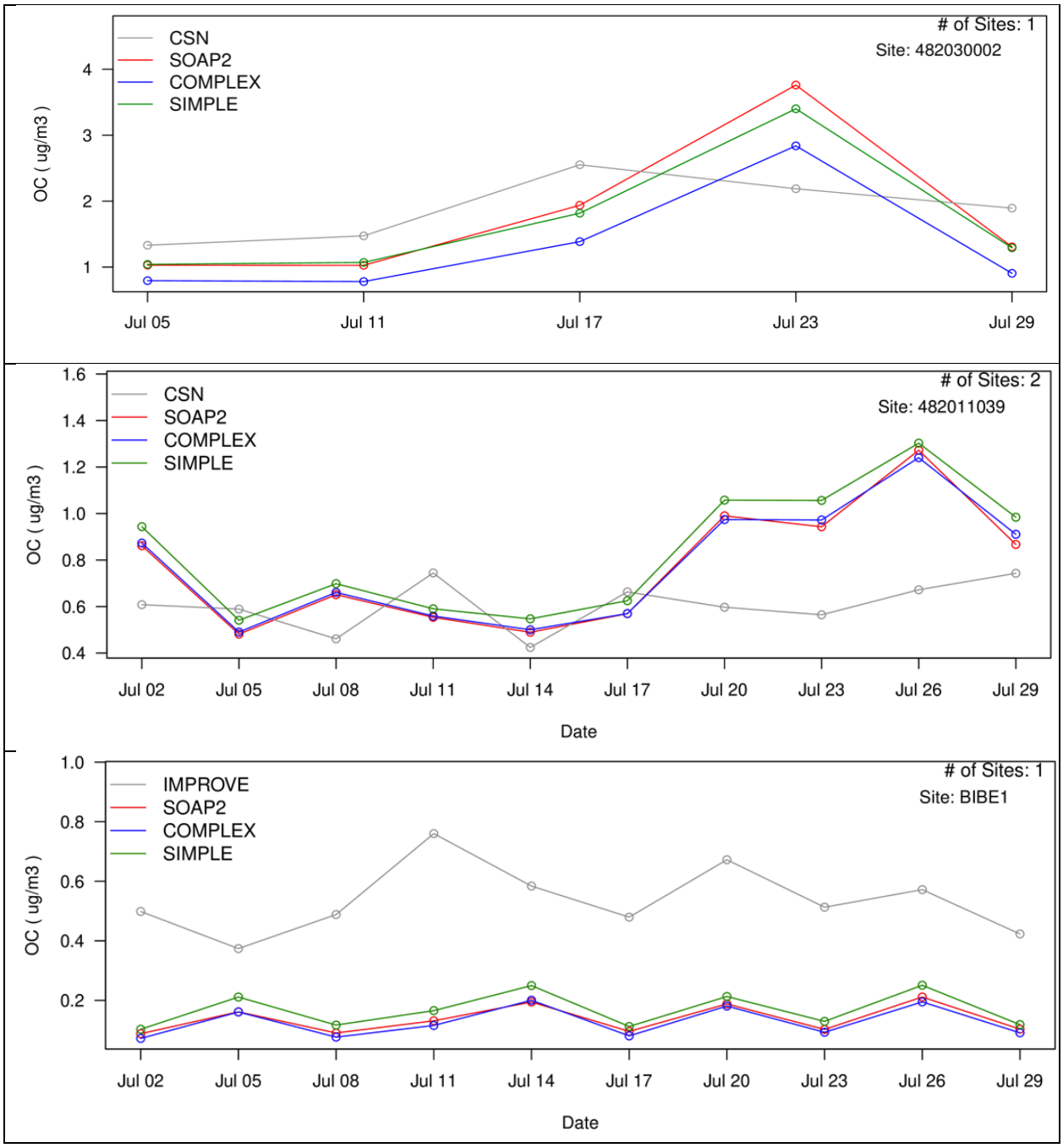

Figure 4-4. Timeseries of all three model scenarios at CSN sites (482030002 – Karnack and 482011039 – Deer Park) and IMPROVE site (BIBE-Big Bend) in Texas.

Table 4-4 lists the domain-wide July, 2016 monthly statistics of total $PM_{2.5}$ mass for the three scenarios at AQS, CSN and IMPROVE monitors. SIMPLE shows slightly lower NMB and NME (~1-4% lower) than SOAP2. COMPLEX shows similar NMB and slightly higher NME (~1-2 % higher) than SOAP2. Overall, the differences between all three scenarios are relatively small.

Table 4-4. Domain wide model performance for total $PM_{2.5}$ at AQS, CSN and IMPROVE monitors for July, 2016.

Scenario	No. of Obs	Mean Obs (µg/m³)	Mean Model (µg/m³)	NMB (%)	NME (%)	FB (%)	FE (%)	RMSE (µg/m³)	r
AQS									
SOAP2	32450	7.90	6.52	-17.4	46.7	-23.6	52.3	7.72	0.22
COMPLEX	32450	7.90	6.43	-18.5	46.9	-25.1	52.9	7.78	0.22
SIMPLE	32450	7.90	6.79	-14.1	45.9	-19.4	50.2	7.73	0.23
CSN									
SOAP2	5426	8.91	8.36	-6.24	41.0	-8.76	43.0	5.72	0.32
COMPLEX	5426	8.91	8.31	-6.80	40.9	-9.41	42.9	5.72	0.33
SIMPLE	5426	8.91	8.70	-2.38	40.7	-4.45	41.5	5.71	0.33
IMPROVE									
SOAP2	1381	5.06	3.16	-37.5	55.2	-56.8	70.9	5.46	0.26
COMPLEX	1381	5.06	3.03	-40.2	56.4	-60.5	73.6	5.52	0.25
SIMPLE	1381	5.06	3.29	-35.1	53.6	-52.5	67.3	5.42	0.26

Figure 4-5 displays spatial maps of site-specific July, 2016 monthly NMB patterns for $PM_{2.5}$ across the 12US2 CONUS domain at AQS sites (which combines CSN and IMPROVE and adds Federal Reference and Equivalent Method $PM_{2.5}$ monitors). All three scenarios show similar NMB trends spatially, with significant under prediction (blue) across much of the western US and Texas, under prediction in central/southeastern US (green), over prediction in northeastern US (yellow), and better model performance (grey) in eastern US.

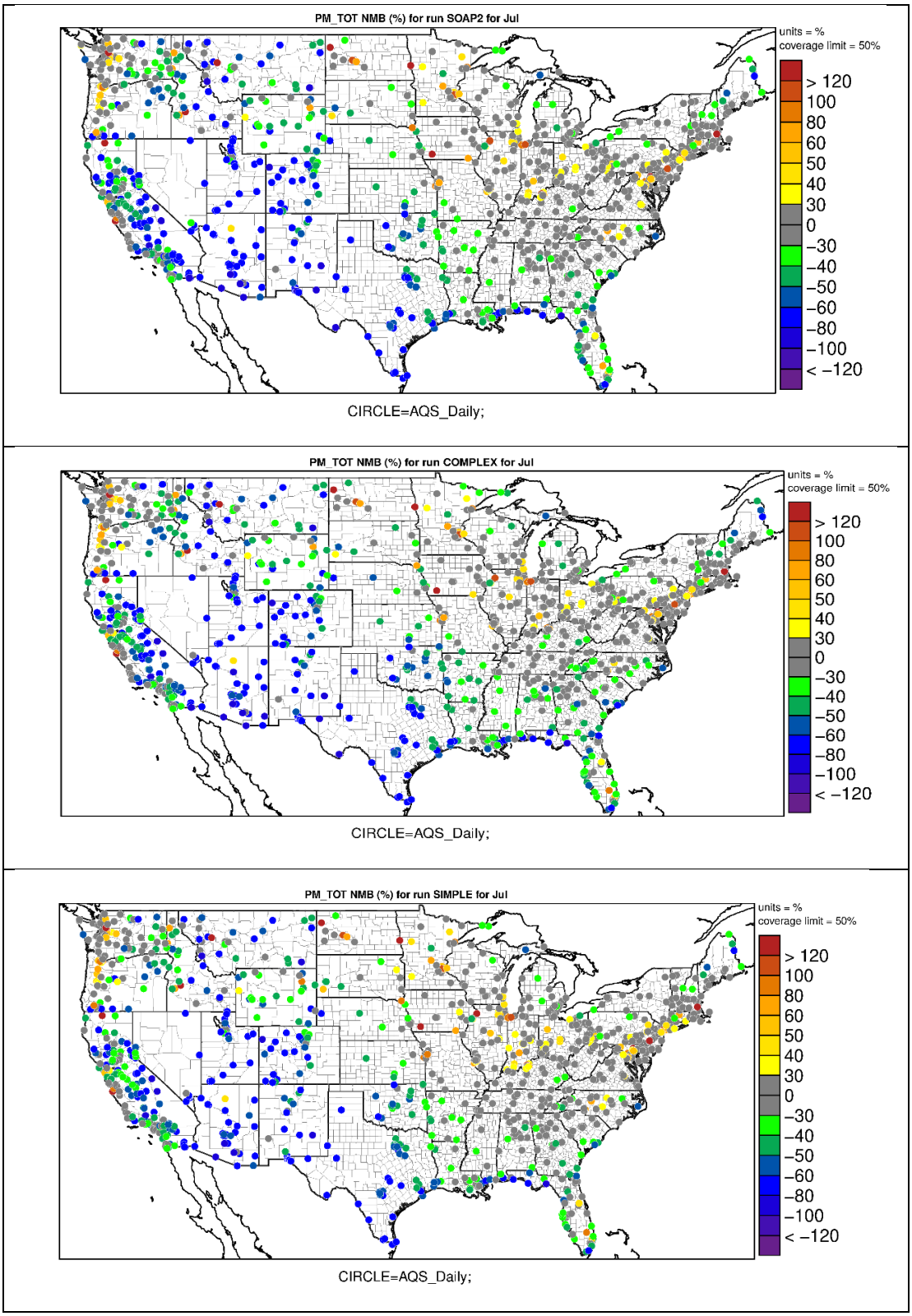

Figure 4-5. Spatial plot showing the normalized mean bias (NMB) metric at AQS sites for total $PM_{2.5}$ across the 12 km CONUS domain for July, 2016 for SOAP2 (top), COMPLEX (middle), and SIMPLE (bottom).

5.0 SUMMARY AND RECOMMENDATIONS

Updated SOA schemes were recommended for implementation in CAMx following a literature review of the state of science on SOA formation. Eight SOA formation schemes implemented in five widely used CTMs, namely CAMx, CMAQ, GEOS-Chem, CHIMERE, and WRF-Chem were reviewed. First-generation SOA yields as well as aged SOA yields from each scheme were compared. Treatment of SOA formation (including SOA yields, effect of NOx, aging processes, and IVOC speciation) varies widely across models. This variability highlights that the choice of model/scheme can significantly influence the predicted SOA concentrations and their evolution over time, which in turn affects air quality forecasts, assessments and regulations.

Because of the lack of consistency among schemes, there was no objective basis to choose one over another when considering CAMx updates. There was also no compelling reason to change the structure of the CAMx SOAP2 scheme that TCEQ is currently using. More complex schemes contain more parameters (species, reactions, rate constants, condensable gas yields, etc.) that are difficult to specify with confidence. Therefore, adding complexity may be detrimental to an SOA scheme intended for establishing public health policy because there is risk of introducing model responses that are difficult to substantiate. However, more recent published data on SOA yields is available so there is a benefit to updating the yields in CAMx.

Four sets of updated yield parameters were tested in CAMx using box models for three Texas cities (Dallas/Fort-Worth, San Antonio, Tyler):

- Existing SOAP2 yield parameters.
- SOA yield parameters for SOAP2 that emulate the AERO7 scheme in CMAQ.
- SOA yield parameters for SOAP2 that emulate the CRACMM scheme in CMAQ.
- SOA yield parameters for SOAP2 that are somewhat like the GEOS-Chem Simple scheme and similar to the scheme evaluated in Nault et al. (2021), i.e., yields of non-volatile SOA with values close to the multi-model means for low-NOx conditions, derived above.

AERO7 and SIMPLE predicted similar SOA concentrations in each of the box model simulations and SOAP2, AERO7, and SIMPLE responded similarly to variations in VOC and NOx emissions. CRACMM, on the other hand, was the only scheme to predict a decrease in total SOA when NOx was reduced by 50%. This is due to the unique treatment of the monoterpene SOA yield in CRACMM which decreases under low NOx conditions compared to high NOx. The other schemes reviewed in this work, along with experimental results, suggest that the change in yield should be opposite, i.e., higher under low NOx conditions. Because of this unique behavior, further testing of the CRACMM-based scheme was not performed.

The AERO7 and SIMPLE schemes were tested in 3-D CAMx simulations alongside SOAP2 for the month of July, 2016 and model results were evaluated against observational data. The AERO7 scheme implemented in CAMx was renamed as “COMPLEX” since it differs from AERO7 in CMAQ. The model scenarios covered the continental US (CONUS) with 12 km grid resolution and were run using input data from EPA’s 2016v3 modeling platform (EPA, 2023).

An operational evaluation using statistical and graphical analysis was conducted to understand the performance of the two updated SOA schemes (SIMPLE and COMPLEX) and the existing scheme (SOAP2) in CAMx. Organic carbon (OC) and $PM_{2.5}$ data from AQS, CSN, and IMPROVE monitoring sites were compared to modelled data for this analysis. Overall, all the schemes performed similarly, with similar bias and error compared to observations. The spatial trends of the statistical metrics across the

CONUS, along with the monthly time series of OC concentrations, were also similar between the three model runs.

While the model performance analysis provides an important comparison of the different SOA schemes, it is difficult to recommend one scheme over the other based solely on these results due to uncertainties in model emissions that impact predicted SOA concentrations. In particular, there are large differences in biogenic emissions inventories used in models (i.e., BEIS versus MEGAN) and the magnitude and speciation of IVOC emissions are uncertain. The IVOC speciation directly influences SOA yield values and contributes to yield uncertainties. Both biogenic VOCs (isoprene, terpene, sesquiterpene) and IVOC are major contributors to SOA formation, as seen in the emission-weighted SOA potential plots for Dallas-Fort Worth (Figure 3-2), San Antonio (Figure 3-3) and Tyler in Northeast Texas (Figure 3-4).

Overall, the schemes performed similarly and differences in performance between them are smaller than uncertainties in model input data such as the biogenic and anthropogenic emission inventories. The SOA yields used in the updated SIMPLE and COMPLEX schemes are based on more recent published studies and are therefore recommended over SOAP2. Similar to the conclusions from Nault et al. (2021), our analysis did not see meaningful differences in results between the more complicated COMPLEX scheme and the SIMPLE scheme. Both schemes are subject to large uncertainties reported in SOA yields. In addition to its reasonable performance, the SIMPLE scheme has practical advantages, including the ability to calculate emission-weighted SOA potential (as in Figure 3-2 through Figure 3-4) and the potential for efficiency gains with CAMx's source apportionment probing tools by reducing the number of tracer species. The required SOA tracers in CAMx's Particulate Source Apportionment Technology (PSAT) probing tool would be reduced from 17 with the COMPLEX scheme to 9 with the SIMPLE scheme, allowing for more detailed and/or rapid analysis using SIMPLE. PSAT is a powerful tool for understanding source contributions to $PM_{2.5}$ and future work to update PSAT for the SIMPLE scheme would benefit TCEQ's PM modeling and SIP strategies.

In addition to the SOA yield updates evaluated and recommended in this project, structural updates to CAMx's SOA scheme are also suggested, including:

- Expanding the terpene SOA scheme to differentiate α-pinene from other terpenes in alignment with CB7 species APIN and TERP, respectively (and other oxidant mechanisms).
- Making the SOA yields from NO3 + terpene reactions different from OH/O3 + terpene reactions. Additional literature supports this update.
- Making the SOA yields from NO3 + α-pinene reaction near zero which is supported by laboratory data and makes α-pinene different from other terpenes. Additional literature review supports this update.
- If feasible via minor modifications, improving the SOAP2 treatment of SOA-photolysis to recognize that a large fraction of SOA does not photolyze (the "recalcitrant" fraction; O'Brien and Kroll, 2019) while the remaining fraction does photolyze more rapidly than assumed by SOAP2. Additional literature review is ongoing to support this update.

Work to implement the first three points has been done but thorough testing of these updates has not yet been performed. We recommend evaluating the impact of the updates in a similar manner as the SOA yield updates presented in this project, including box model tests and 3-D simulations with model performance evaluation.

6.0 REFERENCES

Appel, K.W., Gilliam, R.C., Davis, N., Zubrow, A., and Howard, S.C. (2011). Overview of the Atmospheric Model Evaluation Tool (AMET) v1.1 for evaluating meteorological and air quality models, *Environ. Modell. Softw.,26*, 4, 434-443.

Appel, K. W., Bash, J. O., Fahey, K. M., Foley, K. M., Gilliam, R. C., Hogrefe, C., ... & Wong, D. C. (2021). The Community Multiscale Air Quality (CMAQ) model versions 5.3 and 5.3. 1: system updates and evaluation. *Geoscientific Model Development*, *14*(5), 2867-2897.

Ahmadov, R., McKeen, S. A., Robinson, A. L., Bahreini, R., Middlebrook, A. M., De Gouw, J. A., ... & Trainer, M. (2012). A volatility basis set model for summertime secondary organic aerosols over the eastern United States in 2006. *Journal of Geophysical Research: Atmospheres*, *117*(D6).

Beekmann, M., & Vautard, R. (2010). A modelling study of photochemical regimes over Europe: robustness and variability. *Atmospheric Chemistry and Physics*, *10*(20), 10067-10084.

CHIMERE Users Guide (2023). https://www.lmd.polytechnique.fr/chimere/

Cholakian, A., Beekmann, M., Colette, A., Coll, I., Siour, G., Sciare, J., ... & Dulac, F. (2018). Simulation of fine organic aerosols in the western Mediterranean area during the ChArMEx 2013 summer campaign. *Atmospheric chemistry and physics*, *18*(10), 7287-7312.

Couvidat, F., Bessagnet, B., Garcia-Vivanco, M., Real, E., Menut, L., & Colette, A. (2018). Development of an inorganic and organic aerosol model (CHIMERE 2017 β v1. 0): Seasonal and spatial evaluation over Europe. *Geoscientific Model Development*, *11*(1), 165-194.

Emery, C.E., Z. Liu, A.G. Russell, M.T. Odman, G. Yarwood, and N. Kumar. (2016). Recommendations on statistics and benchmarks to assess photochemical model performance. *Journal of the Air and Waste Management Assoc., 67/5*, DOI: 10.1080/10962247.2016.1265027.

Environmental Protection Agency (EPA) (2023). Technical Support Document (TSD): Preparation of Emission Inventories for the 2016v3 North American Emissions Modeling Platform. Retrieved from https://www.epa.gov/air-emissions-modeling/2016v3-platform

Donahue, N. M., Robinson, A. L., Stanier, C. O., & Pandis, S. N. (2006). Coupled partitioning, dilution, and chemical aging of semivolatile organics. *Environmental science & technology*, *40*(8), 2635-2643.

Donahue, N. M., Epstein, S. A., Pandis, S. N., & Robinson, A. L. (2011). A two-dimensional volatility basis set: 1. organic-aerosol mixing thermodynamics. *Atmospheric Chemistry and Physics*, *11*(7), 3303-3318.

Honoré, C., Rouil, L., Vautard, R., Beekmann, M., Bessagnet, B., Dufour, A., ... & Poisson, N. (2008). Predictability of European air quality: Assessment of 3 years of operational forecasts and analyses by the PREV'AIR system. *Journal of Geophysical Research: Atmospheres*, *113*(D4).

Hodzic, A., Jimenez, J. L., Madronich, S., Aiken, A. C., Bessagnet, B., Curci, G., ... & Ulbrich, I. M. (2009). Modeling organic aerosols during MILAGRO: application of the CHIMERE model and importance of biogenic secondary organic aerosols. *Atmos. Chem. Phys. Discuss*, *9*, 12207-12281.

Hodzic, A., Jimenez, J. L., Madronich, S., Canagaratna, M. R., DeCarlo, P. F., Kleinman, L., & Fast, J. (2010). Modeling organic aerosols in a megacity: potential contribution of semi-volatile and intermediate volatility primary organic compounds to secondary organic aerosol formation. *Atmospheric Chemistry and Physics*, *10*(12), 5491-5514.

Hodzic, A. and Jimenez, J. L. (2011). Modeling anthropogenically controlled secondary organic aerosols in a megacity: a simplified framework for global and climate models. *Geoscientific Model Development*, *4*, 901-917. https://gmd.copernicus.org/articles/4/901/2011/

Huang, L., Liu, H., Yarwood, G., Wilson, G., Tao, J., Han, Z., ... & Li, L. (2023). Modeling of secondary organic aerosols (SOA) based on two commonly used air quality models in China: Consistent S/IVOCs contribution but large differences in SOA aging. *Science of The Total Environment*, *903*, 166162.

Koo, B., Knipping, E., & Yarwood, G. (2014). 1.5-Dimensional volatility basis set approach for modeling organic aerosol in CAMx and CMAQ. *Atmospheric Environment*, *95*, 158-164.

Ma, P.K., Zhao, Y., Robinson, A.L., Worton, D.R., Goldstein, A.H., Ortega, A.M., Jimenez, J.L., Zotter, P., Prévôt, A.S., Szidat, S. and Hayes, P.L., 2017. Evaluating the impact of new observational constraints on PS/IVOC emissions, multi-generation oxidation, and chamber wall losses on SOA modeling for Los Angeles, CA. *Atmospheric chemistry and physics*, 17(15), pp.9237-9259.

Marais, E. A., Jacob, D. J., Jimenez, J. L., Campuzano-Jost, P., Day, D. A., Hu, W., ... & McNeill, V. F. (2016). Aqueous-phase mechanism for secondary organic aerosol formation from isoprene: application to the southeast United States and co-benefit of SO 2 emission controls. *Atmospheric Chemistry and Physics*, *16*(3), 1603-1618.

Murphy, B. N., Sonntag, D., Seltzer, K. M., Pye, H. O., Allen, C., Murray, E., ... & Robinson, A. L. (2023). Reactive organic carbon air emissions from mobile sources in the United States. *Atmospheric Chemistry and Physics*, *23*(20), 13469-13483.

Murphy, B. N., Woody, M. C., Jimenez, J. L., Carlton, A. M. G., Hayes, P. L., Liu, S., ... & Pye, H. O. (2017). Semivolatile POA and parameterized total combustion SOA in CMAQv5.2: impacts on source strength and partitioning. *Atmospheric chemistry and physics*, *17*(18), 11107-11133.

Murphy, B., W. Appel, J. Bash, K. Fahey, B. Henderson, Bill Hutzell, D. Kang, D. Luecken, R. Mathur, S. Napelenok, Chris Nolte, H. Pye, Jon Pleim, M. Qin, L. Ran, S. Roselle, G. Sarwar, D. Schwede, Q. Shu, AND T. Spero. Scientific and Structural Developments in CMAQv5.3. 2018 CMAS Conference, Chapel Hill, North Carolina, October 22 - 24, 2018.

Nault, B. A., Campuzano-Jost, P., Day, D. A., Jo, D. S., Schroder, J. C., Allen, H. M., ... & Jimenez, J. L. (2021). Chemical transport models often underestimate inorganic aerosol acidity in remote regions of the atmosphere. *Communications Earth & Environment*, *2*(1), 93.

O'Brien, R.E. and Kroll, J.H. (2019). Photolytic aging of secondary organic aerosol: Evidence for a substantial photo-recalcitrant fraction. *The journal of physical chemistry letters*, *10*(14), pp.4003-4009.

Pai, S. J., Heald, C. L., Pierce, J. R., Farina, S. C., Marais, E. A., Jimenez, J. L., ... & Vu, K. (2020). An evaluation of global organic aerosol schemes using airborne observations. *Atmospheric Chemistry and Physics*, *20*(5), 2637-2665.

Pankow, J. F. (1994). An absorption model of the gas/aerosol partitioning involved in the formation of secondary organic aerosol. *Atmospheric Environment*, *28*(2), 189-193.

Pye, H. O. T., Chan, A. W. H., Barkley, M. P., & Seinfeld, J. H. (2010). Global modeling of organic aerosol: the importance of reactive nitrogen (NOx and NO_3). *Atmospheric Chemistry and Physics*, *10*(22), 11261-11276.

Pye, H.O., D'Ambro, E.L., Lee, B.H., Schobesberger, S., Takeuchi, M., Zhao, Y., Lopez-Hilfiker, F., Liu, J., Shilling, J.E., Xing, J. and Mathur, R. (2019). Anthropogenic enhancements to production of highly oxygenated molecules from autoxidation. *Proceedings of the National Academy of Sciences*, *116*(14), pp.6641-6646.

Pye, H. O., Place, B. K., Murphy, B. N., Seltzer, K. M., D'Ambro, E. L., Allen, C., ... & Stockwell, W. R. (2023). Linking gas, particulate, and toxic endpoints to air emissions in the Community Regional Atmospheric Chemistry Multiphase Mechanism (CRACMM). *Atmospheric Chemistry and Physics*, *23*(9), 5043-5099.

Ramboll (2022). CAMx User's Guide, Version 7.20. Retrieved from https://www.camx.com/download/source/

Ramboll (2023). Comparing ozone precursor responses and volatile organic compound (VOC) reactivity of Cabon Bond version 7 revision 1 (CB7r1) to other mechanisms. Report prepared for TCEQ Work Order 582-23-42327-033, June 2023.

Robinson, A. L., Donahue, N. M., Shrivastava, M. K., Weitkamp, E. A., Sage, A. M., Grieshop, A. P., ... & Pandis, S. N. (2007). Rethinking organic aerosols: Semivolatile emissions and photochemical aging. *Science*, *315*(5816), 1259-1262.

Robinson, A.L., Donahue, N.M., Shrivastava, M.K., Weitkamp, E.A., Sage, A.M., Grieshop, A.P., Lane, T.E., Pierce, J.R. and Pandis, S.N., 2007. Rethinking organic aerosols: Semivolatile emissions and photochemical aging. *Science*, *315*(5816), pp.1259-1262.

Sarrafzadeh, M., Wildt, J., Pullinen, I., Springer, M., Kleist, E., Tillmann, R., Schmitt, S.H., Wu, C., Mentel, T.F., Zhao, D. and Hastie, D.R. (2016). Impact of NO x and OH on secondary organic aerosol formation from β-pinene photooxidation. *Atmospheric chemistry and physics*, *16*(17), pp.11237-11248.

Sciare, J., d'Argouges, O., Zhang, Q. J., Sarda-Estève, R., Gaimoz, C., Gros, V., ... & Sanchez, O. (2010). Comparison between simulated and observed chemical composition of fine aerosols in Paris (France) during springtime: contribution of regional versus continental emissions. *Atmospheric Chemistry and Physics*, *10*(24), 11987-12004.

Schell, B., Ackermann, I. J., Hass, H., Binkowski, F. S., & Ebel, A. (2001). Modeling the formation of secondary organic aerosol within a comprehensive air quality model system. *Journal of Geophysical Research: Atmospheres*, *106*(D22), 28275-28293.

Seltzer, K., Pennington, E., Rao, V., Murphy, B., Strum, M., Isaacs, K., and Pye, H. (2021). Reactive organic carbon emissions from volatile organic products. *Atmospheric chemistry and physics, 21,* pp.5079-5100.

Shrivastava, M., Easter, R. C., Liu, X., Zelenyuk, A., Singh, B., Zhang, K., ... & Tiitta, P. (2015). Global transformation and fate of SOA: Implications of low-volatility SOA and gas-phase fragmentation reactions. *Journal of Geophysical Research: Atmospheres*, *120*(9), 4169-4195.

Shrivastava, M., Fast, J., Easter, R., Gustafson Jr, W. I., Zaveri, R. A., Jimenez, J. L., ... & Hodzic, A. (2011). Modeling organic aerosols in a megacity: comparison of simple and complex representations of the volatility basis set approach. *Atmospheric Chemistry and Physics*, *11*(13), 6639-6662.

Strader, R., Lurmann, F., & Pandis, S. N. (1999). Evaluation of secondary organic aerosol formation in winter. *Atmospheric Environment*, *33*(29), 4849-4863.

University of North Carolina (UNC). (2008). Atmospheric Model Evaluation Tool (AMET) User's Guide. Prepared for the U.S. EPA, Office of Research and Development, Research Triangle Park, North Carolina. Prepared by the Institute for the Environment, University of North Carolina at Chapel Hill.

Wildt, J., Mentel, T.F., Kiendler-Scharr, A., Hoffmann, T., Andres, S., Ehn, M., Kleist, E., Müsgen, P., Rohrer, F., Rudich, Y. and Springer, M. (2014). Suppression of new particle formation from monoterpene oxidation by NOx. *Atmospheric chemistry and physics*, *14*(6), pp.2789-2804.

WRF-Chem version 4.4 Users Guide. (2022). https://ruc.noaa.gov/wrf/wrf-chem/Users_guide.pdf

Zawadowicz, M. A., Lee, B. H., Shrivastava, M., Zelenyuk, A., Zaveri, R. A., Flynn, C., ... & Shilling, J. E. (2020). Photolysis controls atmospheric budgets of biogenic secondary organic aerosol. Environmental Science & Technology, 54(7), 3861-3870.

Zhang, Q., Laurent, B., Velay-Lasry, F., Ngo, R., Derognat, C., Marticorena, B., & Albergel, A. (2012). An air quality forecasting system in Beijing-Application to the study of dust storm events in China in May 2008. *Journal of Environmental Sciences*, *24*(1), 102-111.

Zhang, Q. J., Beekmann, M., Drewnick, F., Freutel, F., Schneider, J., Crippa, M., ... & Perrussel, O. (2013). Formation of organic aerosol in the Paris region during the MEGAPOLI summer campaign: evaluation of the volatility-basis-set approach within the CHIMERE model. *Atmospheric Chemistry and Physics*, *13*(11), 5767-5790.

Zhao, Y., Hennigan, C. J., May, A. A., Tkacik, D. S., de Gouw, J. A., Gilman, J. B., ... & Robinson, A. L. (2014). Intermediate-volatility organic compounds: a large source of secondary organic aerosol. *Environmental Science & Technology*, *48*(23), 13743-13750.